UNIVERSITÉ MONTPELLIER II
SCIENCES ET TECHNIQUES DU LANGUEDOC

THÈSE

pour obtenir le grade de

DOCTEUR DE L'UNIVERSITÉ MONTPELLIER II

Discipline : Biologie des Organismes

École Doctorale : SIBAGHE - Systèmes intégrés en Biologie, Agronomie, Géosciences, Hydrosciences et Environnement

présentée et soutenue publiquement par

Lu FENG

le 17 novembre 2011

Connexion entre modèles dynamiques de communautés végétales et modèles architecture-fonction – cas du modèle GreenLab

Connection between plant community dynamics models and architectural-functional plant models – the GreenLab case

Jury

M. Jean-Claude MAILHOL, Directeur de recherche, Cemagref	**Président**
M. Daniel AUCLAIR, Directeur de recherche, INRA	**Directeur de Thèse**
M. Philippe DE REFFYE, Directeur de recherche, CIRAD	**Directeur de Thèse**
M. Paul-Henry COURNEDE, Professeur, École Centrale Paris	**Rapporteur**
M. Yan GUO, Professeur, China Agricultural University	**Rapporteur**
M^{me}. Catherine COLLET, Chargée de recherche, INRA	**Examinateur**

UNIVERSITÉ MONTPELLIER II
SCIENCES ET TECHNIQUES DU LANGUEDOC

THÈSE

pour obtenir le grade de

DOCTEUR DE L'UNIVERSITÉ MONTPELLIER II

Discipline : Biologie des Organismes

École Doctorale : SIBAGHE - Systèmes intégrés en Biologie, Agronomie, Géosciences, Hydrosciences et Environnement

présentée et soutenue publiquement par

Lu FENG

le 17 novembre 2011

Connexion entre modèles dynamiques de communautés végétales et modèles architecture-fonction – cas du modèle GreenLab

Connection between plant community dynamics models and architectural-functional plant models – the GreenLab case

Jury

M. Jean-Claude MAILHOL, Directeur de recherche, Cemagref	**Président**
M. Daniel AUCLAIR, Directeur de recherche, INRA	**Directeur de Thèse**
M. Philippe DE REFFYE, Directeur de recherche, CIRAD	**Directeur de Thèse**
M. Paul-Henry COURNEDE, Professeur, École Centrale Paris	**Rapporteur**
M. Yan GUO, Professeur, China Agricultural University	**Rapporteur**
M^{me}. Catherine COLLET, Chargée de recherche, INRA	**Examinateur**

Acknowledgements

This study was conducted at UMR-AMAP, CIRAD. I undertook this thesis with the help of many people to whom I now wish to express my heartfelt thanks.

My deepest gratitude is to my supervisor, Philippe de Reffye, for his warm kindness in France and patient guidance from the preliminary stage to the end. I have been amazingly fortunate to have had a real friendship with the founder of AMAP and the GreenLab model, whom I had heard a lot about. He shared with me his Laohuli (old fox's) philosophy in work and life. His big heartedness and optimism, his faith, persistence and passion in modelling, his support and encouragement inspired and motivated me to go ahead and finish this thesis.

My co-supervisor, Daniel Auclair, was always there to keep track of my thesis progress and provide advice. I am deeply grateful to him for consistently guiding and encouraging me in my dissertation writing. I am also thankful to him for the great effort in perfecting the writing and academic expression of our manuscripts, which composed significant parts of this thesis.

I am extremely grateful to Hervé Rey for his consistent help and patience, for spending a lot of time with me on field experiments, for introducing me to valuable agronomic/botanical knowledge and practical approaches. His strict logical thinking and constructive comments on my studies were thought-provoking and they helped me regulate and focus my ideas.

I am indebted to Sébastien Griffon for his continuous support in software development and visualization applications. He is in charge of developing Xplo, which provided the crucial aspects of plant architectural organization and operation, thereby enormously facilitating my programming work and enabling me to finish my thesis on time over three years.

I am grateful to J-F Barczi, who works in the same office as Hervé and Seb. His perceptive analyses and smart questions during discussions were not only interesting but often enlightening from a thoroughness perspective.

I am also indebted to François de Coligny for his professional aid for program implementation. His organization, concise expression, and rigorous thinking set a high standard for my engineering work, and stimulated me to do better.

I would like to thank Marie-Laure de Guillen and Nora Bakker for their careful assistance in administrative procedures over the three years. I would like to thank Michaël Gueroult and François Pailler for the technical support in experiments. I would like to thank Philippe Borianne for his support in software development. I would like to thank Yves Caraglio and René Lecoustre for their botanical aid for Black Pine. I would like to thank Yannick Brohard for her literature support to the whole lab. I also wish to extend my thanks to all the colleagues at AMAP, because they have inherited and built a free, cooperative, open-minded, atmosphere together for this research laboratory that is of benefit to

everyone working there. I am greatly indebted to Peter Biggins for the tremendous effort he put in the improvement of the English language of this thesis.

I am also indebted to the following important people involved in this thesis study.

- Marie Launay for inviting me to INRA Avignon to learn the process-based model (PBM) STICS and exchange data, so that I could carry out preliminary in-silico computation of the combined modelling study.

- Jean-Claude Mailhol of Cemagref for providing the PILOTE PBM and thereby collaborating in this thesis. Thanks to the experimental site and crop field growth data study supplied by his team, this thesis benefited from the practice on maize and explored the interconnection between plant individuals and community performance.

- Philippe Dreyfus from INRA-URFM for providing the empirical forest model, PNN, and valuable studies and data from his team and thereby collaborating in this thesis, so that the application to import architecture into the dimension dynamics of a black pine stand could be carried out.

I would like to acknowledge two reporters, Prof. Yan Guo and Prof. Paul-Henry Cournède, for their constructive comments to improve this thesis.

My friends both in Montpellier and China are very important parts of these three years of my life in France. I greatly appreciate them for countless joyful and pleasant moments with me and their strong bulwark of friendship. Some of them are also my thesis “comrades-in-arms”. We shared the experience and encouraged each other to face the hard work and pressure together, which inspired my final effort.

I would like to express my heartfelt gratitude to Laurent, Papa, Mama and my extended family. Your love, understanding, support and faith in me have been the constant source of my courage throughout this endeavour.

Finally, I am indebted to the Chinese Government and the China Scholarship Council for funding my PhD from 2008 to 2011.

And, I thank all those who, directly or indirectly contributed to this thesis.

Table of contents

Abstract

Plant architecture involves the development of both topological and geometric structures over time, which determines resource acquisition, which, in so doing, interacts with physiological processes. However, it has long been overlooked in traditional community dynamic models. Functional-structural plant models (FSPM), which are based on plant architecture, have shown their particular suitability for addressing issues such as interactions between plants and the environment (e.g. light interception), and between structural development and growth (e.g. carbon allocation), as they take into account morphogenesis with explicit organ-level descriptions. However, FSPMs are time consuming and require a lot of memory space, which prevents greater use of them in agricultural or silvicultural practices. This thesis attempts to combine a mathematical FSPM, GreenLab, and a crop model or an empirical forest model (EFM), in order to introduce individual-based architectural support for community growth studies. In the case of maize, disagreements between stand level growth stimulations (by the PILOTE crop model) and individual level growth stimulations (by GreenLab) implies different individual emergence times, which are used to quantify distribution. Assuming that the theoretical projective area (S_p) is determined by the growth situation and the final size of the individual architecture, the variance of S_p is reversely computed with the variance in organ compartment measurements, in order to characterize individual variability. In the case of Black Pine, the architecture dynamics built in GreenLab according to Rauh's model (architecture model for the pine tree) were adapted to the simulation of an EFM, PNN. As a consequence, thinning scenarios are well incorporated in the final stand visualization. From these preliminary applications, the following conclusions can be drawn: (i) FSPMs are able to provide individual performances (i.e. organ development and expansion) inside an area of a crop field for crop models. (ii) The crop model may regulate the combined form of individuals from an integral level. Both aspects are significant for a clearer understanding of stand growth. (iii) Architecture designs integrated into FSPMs can be adapted to EFM simulations for data-driven visualization. (iv) EFMs can guarantee ecological/silvicultural functions for 3D stand visualization. In order to take biomass processes into consideration, additional observations are needed. As models are independent in combinations, the same methods can be extended and linked to other stand models.

Keywords: Crop model, functional-structural plant model, plant architecture, visualization, GreenLab, *Pinus nigra nigra*, *Zea maïs*

Résumé

1 Introduction

1.1 Complexité du système plante

Une plante est un système hiérarchisé constituée d'éléments qui communiquent entre eux non seulement au sein de la même structure, mais encore entre plantes voisines (compétition pour la lumière, etc.. Selon l'échelle ou l'on se place, au plus haut niveau les organes végétatifs sont les constituants du fonctionnement écophysiologique alors qu'au plus bas niveau les cellules des organes sont le siège du fonctionnement physiologique. Selon les problématiques il convient de situer le niveau d'observation.

La croissance (expansion des organes) et le développement (création des organes) d'une plante sont la conjonction de divers processus, comme l'ontogenèse qui caractérise le programme morphogénétique du développement et la photosynthèse qui concerne la production de la biomasse et sa répartition dans l'architecture.

L'environnement (température, lumière, eau) peut modifier à la fois le développement et la croissance et même leurs interactions.

1.2 Etats des modèles de croissance de plantes

1.2.1 Les modèles de culture

On distingue les modèles de cultures et les modèles forestiers. Parmi eux on détaille les modèles empiriques basés sur des statistiques sur des périodes plus ou moins longues et les modèles fonctionnels basés sur l'interception de la lumière. Ces derniers utilisent l'indice foliaire, la biomasse produite/m2 et l'indice de récolte. Selon les conditions de stress on postule une efficience de l'eau ou de la lumière. Ici c'est la production par unité de surface qui compte et la morphologie de la plante est complètement ignorée.

1.2.2 Les modèles structures fonction

La simulation des plantes virtuelles et leur visualisation sont apparues il y a plus de 30 ans avec la naissance des ordinateurs, pour prendre leur part dans le monde de l'image de synthèse. C'est le réalisme qui était avant tout visé et non la modélisation des processus biologiques. Mais petit a petit ces derniers ont été pris en compte.

D'abord le développement de l'architecture a été modélisé et récemment le fonctionnement de la structure a suivi. Cependant ces modèles se heurtent dans leur simulation à de grandes difficultés qui engendrent des coups de calculs et de mémoire importants et qui sont dus à la construction de la structure topologique, à la répartition de la biomasse, au calcul de l'interception de la lumière etc. .

D'autre part ils concernent des plantes individuelles et ne sont pas taillés pour aborder le fonctionnement des populations.

Les modèles de plantes simulés les plus en vue ont été les L_systems et Amap.

1.3 Objectifs et hypothèses

Le modèle structure fonction pris en exemple dans ce document est le modèle GreenLab, issu d'AMAP et qui partage toutes ses hypothèses botaniques et écophysiologiques. Il a été développé dans un esprit plus mathématique de façon à résoudre les problèmes de coup de calcul (factorisation de l'organogenèse, interception de la lumière, production et répartition de la biomasse etc.) et aussi les méthodes inverses qui doivent nécessairement accompagner les modèles pour qu'ils soient utilisables. Le but de cette thèse est de permettre une meilleure utilisation du concept d'architecture de plante en agriculture pour améliorer la production végétale.

2 GreenLab et le développement végétal.

2.1 La méthode GreenLab

2.1.1 Aspects botaniques

Les notions de phytomères, d'unités de croissance et pousses annuelles sont celles utilisées dans AMAP. Le temps thermique basé sur le phyllochrone est celui couramment utilisé en écophysiologie. L'âge physiologique caractérise le degré de différentiation des méristèmes et pilote les notions de type d'axes, d'acrotonie et de mutation (voir AMAP).

Les modèles Architecturaux (Halle & al 78) raffinés par Barthelemy et Caraglio, sont la base même des simulations du modèle GreenLab. Les aspects stochastiques, indispensables pour prendre en compte la variabilité individuelle ont été spécialement développés par de Reffye (79, 88,…). Ceux-ci pilotent le fonctionnement des bourgeons (croissance, pause, mortalité, mutation, branchement, pré et néo formation). Kang (09) a étendu GreenLab aux herbacées dans lesquelles croissance et développement des organes ne sont pas synchronisés.

2.1.2Représentation du développement dans GreenLab

Le fonctionnement rythmique caractéristique des arbres nécessitent une approche multi échelle. Pour la plus part des cas un automate double échelle est suffisant. Il permet la simulation des phytomères qui s'assemblent en unités de croissances qui elles mêmes forment finalement une branche. Ces processus construisent par simulation l' « Axe de développement » notion très utile car on sait aussi en calculer la distribution statistique qui en découle. Celle-ci remplace avantageusement les milliers de simulations nécessaires pour l'obtenir empiriquement.

Le modèle GreenLab se décline en plusieurs versions.

- GL1 développé au Liama qui concerne les plantes à architectures déterministes (Tournesol, Betterave, …)
- GL2 développé au Liama et au Cirad qui concerne les plantes stochastiques (caféiers)
- GL3 développé a l'ECP qui étudie les interactions croissance développement à un niveau déterministe
- GL4 développé au Liama qui étudie les interactions croissance développement à un niveau stochastique.
- GL5 développé au Cirad qui concerne plus spécialement les arbres et la gestion des pauses entre la fabrication des unités de croissance successives.

2.1.3 Représentation de la croissance dans GreenLab

La croissance se fait pas à pas par récurrence. Tous les organes ont une fonction puits qui est modélisée par une fonction Beta très polymorphe et qui peut prendre des formes en cloche très déformées. Le mode de la fonction puits est normalisé à un. A un âge donné la fonction puits prend une valeur qui multiplié par un scalaire appellé intensité du puits donne le puits de l'organe, La somme des puits de la plante donne la « demande « . Celle-ci se calcule rapidement au moyen d'une fonction grâce à la factorisation du développement. L'expansion de l'organe est proportionnelle à son puits multiplié par l'offre et divisé par la demande.

La production de la biomasse s'obtient en définissant une surface de projection par plante. Le rapport entre la surface foliaire et la surface de projection correspond à l'indice foliaire par plante. Cette méthode calque le procédé des modèles de culture. Dans le cas de haute densité il est évident que l'indice foliaire/m2 et celui par plante est le même. Mais pour les faibles densités ce n'est plus le cas. La surface de projection n'est en fait qu'une inconnue parmi les autres (les puits, la résistance…) dans l'équation de production. Elle est résolue par méthode inverse, ce qui est très avantageux par rapport à un calcul de transfert radiatif.

La forme des organes est donnée au moyen d'allomètries mesurées et associées aux volumes. Ainsi la surface d'une feuille est égale à son volume divisé par le poids.

2.1.4 Le problème inverse

Il s'agit ici de calculer les paramètres du modèle à partir des mesures effectuées sur la plante. Celles-ci (poids, dimensions d'organes) sont collectées et assemblées en une cible. Chaque élément correspond exactement à une sortie spécifique du modèle.

Minimiser l'écart entre les valeurs observées et calculées c'est le rôle des méthodes de calibrations. Le modèle GreenLab a donné de bons ajustements sur toutes les plantes cultivées qui ont été étudiées dans ce cadre. La méthode inverse utilisée est le modèle non linéaire généralisé. Une autre heuristique a été testée dans cette thèse il s'agit du PSO : particule swarm optimization.

2.2 Développement de GL5

2.2.1 Historique des logiciels Greenlab

Les laboratoires qui utilisent le modèle GreenLab ont développé les outils logiciel pour faire tourner le modèle.

- Cornerfit CAU de niveau GL1
- GreenScilab Liama de niveau GL2
- Digiplante ECP de niveau GL1 GL3
- Qing Yuan Liama de niveau GL4 GL5
- Gloups Java de niveau GL5. C'est le logiciel qui a été développé dans le cadre de cette thèse et qui représente une partie importante du travail.

2.2.2 La plate forme Xplo

La version java de Gloups est connectée sur la plateforme Xplo qui permet la visualisation 3D, l'animation et la représentation de plantation.

2.2.3 Les besoins de GL5

Il est nécessaire d'un point de vue pratique de développer des interfaces, des modules de construction, des procédures itératives de croissance et des méthodes inverses permettant l'utilisation du modèle. La visualisation ne se fait qu'en bout de chaine.

2.2.4 Interfaces avec Xplo

Un développement important a été réalisé pour interfacer le logiciel Gloups Java avec Xplo.

2.2.5 Implémentation de classes d'objet

Ce chapitre très technique ne peut etre détaillé ici. Il concerne l'organisation des données en classes lors du passage de Gloups java à Xplo.

2.2.6 Démonstration de Gloups Java sur la plateforme Xplo

A titre d'exemple est donnée la calibration et la simulation d'un Mais cultive au Cemagref qui a été mesuré pour cette thèse. Les interfaces avec Xplo sont détaillés . La plante est analysée et simulée. D'autres plantes Tournesol, concombres, tomates, betteraves sont données en démonstration ainsi qu'un prototype d'arbre typiquement GL5.

3.Etude de la variabilité individuelle. Exemple du Mais.

3.1 Introduction

La variabilité entre plantes dans une même culture est un fait constant. Les origines sont multiples : densité locale hétérogène, retards variables à la germination, distribution des ressources hétérogènes. Les modèles de cultures et les modèles structure-fonction ont permis des analyses de l'hétérogénéité au niveau du champ, entre plantes et intra plantes, mais sans entrer dans les

mécanismes. La thèse a pour but de combiner le modèle de Culture Pilote et le modèle structure-fonction GreenLab pour analyser précisément la croissance du Mais en prenant en compte la variabilité individuelle.

3.2 Matériel et méthode

3.2.1 Observation en champ

L'expérience a été conduite en champ au Cemagref de Montpellier sur du Mais avec une densité de 7.5 pied/m2. L'indice foliaire était mesuré avec l'instrument LI-COR ainsi que la biomasse produite à cinq dates différentes. Parallèlement des prélèvements de plantes au même stade de développement étaient effectués dans le champ (6 individus par date) pour mesurer finement la biomasse fraiche et sèche des organes ainsi que la surface foliaire. Les mesures correspondent donc aux moyennes de six individus.

3.2.2 Description des modèles et comparaison

GreenLab et Pilote partagent la même philosophie pour le calcul de l'interception de la lumière et la production de biomasse, mais n'ont pas le même niveau d'échelle. Pilote lit l'évolution présumée de l'indice foliaire en fonction du temps thermique et déduit la biomasse produite au m2 en fonction des données climatiques air- sol. Le modèle est forcé par le temps thermique qui contrôle bien l'indice foliaire. Une équation empirique la décrit (Eq 3).

Dans le modèle GreenLab, le phyllochrone est forcé par le temps thermique, mais tout le reste est calculé par récurrence d'un pas à l'autre de la croissance.

La surface foliaire (Eq 4) de la plante est calculée a partir de la répartition de la biomasse et des relations d'allomètrie et par optimisation on déduit l'indice foliaire individuel de façon à équilibrer l'équation de production. Cet indice foliaire est le rapport entre la surface foliaire et la surface de projection calculée. La clé du modèle GreenLab est la définition mathématique de la demande de la plante à chaque instant. Les paramètres sources puits sont cachés et doivent être calculés par méthode inverse.

Le tableau 3-1 compare les équations des deux modèles en soulignant les analogies.

3.3 Resultats et discussion

3.3.1Comparaison entre GreenLab et Pilote

La figure 3-1 montre l'excellente concordance entre les données du champ et les prévisions de Pilote en ce qui concerne l'évolution de l'indice foliaire et la biomasse produite pour l'année 2009.

Pour GreenLab il s'agit de trouver les paramètres sources puits invariants qui contrôlent toute l'architecture de la plante aux divers stades de son développement. Neuf paramètres cachés : sources (résistance et surface de projection) et puits (paramètres des fonctions), sont calculés par méthode

inverse. La cible est constituée pour chaque stade de croissance par le poids des organes (feuille, gaine, entre nœuds, épis femelle et male) selon leur rang, ce qui fait plusieurs centaines de données à ajuster avec seulement 9 paramètres. La figure 3-2 montre la bonne calibration du modèle et la figure 3-3 montre l'architecture simulée en utilisant la plateforme Xplo.

Cependant aux points de rencontres figure 3-4 des deux modèles on constate un décalage temporel entre les indices foliaires et la biomasse produites par les deux systèmes. L'hypothèse basée sur l'observation est que ces décalages sont dus aux délais de germination en champ. En effet les plantes choisies en nombre de 6 à chaque prélèvement étaient homogènes pour leur développement pour des raisons de traitements mathématiques, ce qui élimine la variabilité du champ.

On recherche donc la loi composée des distributions des délais de germination qui en mélangeant en proportion les sorties du modèle GreenLab, s'ajuste au mieux aux sorties du modèle pilote. Cette loi est supposée être une loi binomiale négative. La solution fournit un bon résultat (fig 3-6,3-7) et on peut admettre que l'origine des décalages des modèles est établie. Il manque toutefois des observations précises sur ces variations de délais de germination dont l'existence est bien établie par ailleurs.

3.3.2 Etude de la variabilité individuelle entre plantes.

Bien que les échantillons de six plantes prélevés avaient le même stade développement, ils n'étaient pas homogènes pour le poids. La biomasse produite par plante pour un développement donné, se caractérise par une moyenne et une variance non négligeable. Cette variabilité affecte d'une plante à l'autre les poids des différents organes selon leur rang et par conséquence des compartiments. Au premier chef, l'origine de cette variabilité peut être recherchée dans la compétition spatiale provenant de l'hétérogénéité de la densité locale à chaque plante. Les individus sont en effet contingentés à partir du moment où le feuillage recouvre le sol sur une surface limitée (la surface de projection) qui capture la lumière en proportion. Une variation de cette surface induit une variation de production de biomasse. L'effet se propage pas à pas au cours de la croissance. Il faut donc attribuer à la surface de projection un écart type dont la valeur redonne par calcul l'écart type de la production de biomasse.

Il est plus simple d'un point de vue numérique de considérer la variance des compartiments en tant que somme des organes, plutôt que la variance individuelle des organes.

L'outil dit des « statistiques différentielles » est exactement adapté à cette problématique. La formule 5 montre que sont impliquées la fonction de production ainsi que ses dérivées. A chaque étape de croissance la variance se propage. Dans ce cas simple ou seule la variance d'un facteur est prise en compte les corrélations entre facteurs sont égales à un. La variance optimisée de la surface de projection ajuste correctement à la fois les variances des différents compartiments. Sur la figure 3-8 on peut constater que le modèle GreenLab ajuste à la fois la moyenne et l'écart type des différents stades de croissance de la plante pour chaque compartiment.

Sur la figure 3-9 un champ de Mais est reconstitue dans sa variabilité en ce qui concerne les retards à la germination et l'hétérogénéité de la densité.

4 Combinaison de modèles pour la visualisation de foret de pins

4.1 Introduction

Les modèles empiriques sont couramment utilisés pour la gestion des plantations forestières. Ils ont une bonne valeur prédictive si l'environnement est stable. Les modèles fonctionnels sont mieux adaptés aux conditions variables de l'environnement. Toutefois il n'y a pas de simulation d'architectures comme le font les modèles structures fonctions. L'intérêt des forestiers pour ceux-ci est à mettre en parallèle avec celui des agronomes limités aux modèles de culture.

Dans le cadre de cette thèse, on vise à coupler le modèle empirique forestier PNN de Dreyfus, avec le modèle GreenLab dans le but de créer une valeur ajoutée, notamment en terme de visualisation des parcelles forestières.

4.2 Matériel et méthode

4.2.1 Architecture du pin noir

L'architecture pseudo verticillée du pin noir est décrite (fig 4.1) selon la méthodologie d'AMAP. Celui ci appartient au modèle de Rauh dont tous les axes végétatifs sont orthotropes. Les âges physiologiques correspondent ici aux ordres de ramification. AMAP a par ailleurs réalisé des études architecturales qui ont fourni des données complémentaires pour cette étude.

4.2.2 Mesures disponibles

Le modèle PNN dispose d'une très grande base de données recouvrant des plantations d'âges différents et de densités différentes.

4.2.3 Le modèle empirique PNN

Celui-ci intègre les mesures classiques hauteur, diamètre à la base, dimension du houppier, angle, longueurs et nombre des branches par pseudo verticille, etc. pour des arbres allant de 10 ans a 100 ans. Un exemple de donnée est fourni dans le tableau 4-1.

4.2.4 Le modèle structure fonction Greenlab

Limité à sa composante développement en détaillant l'architecture, et en la complétant par de la géométrie, le modèle Greenlab peut simuler des architectures d'arbres réalistes.

4.2.5 Simulation de scenario

Deux itinéraires culturaux sont simulés par le modèle. L'un en croissance libre en utilisant les tables de mortalité naturelles des branches, l'autre avec des élagages de branches à 45, 60 et 75 ans.

4.3 Combinaison de modèles

PNN et GreenLab ont été synchronisés de façon à pouvoir communiquer. GreenLab travaille dans ce cas au niveau de l'année alors que PNN a un pas de 5 ans. De plus pour le premier seules les troncs et les branches d'ordre deux sont détaillées alors que pour le second c'est le phytomère qui est l'unité de construction.

4.3.1 Mortalite des branches

Les longueurs de houppiers de PNN ont été traduites en mortalité des méristèmes terminaux, qui donnent le même résultat.

4.3.2 Nombre de branches par verticilles

Les statistiques du nombre de branches d'ordre deux par verticille sur le tronc sont connues dan PNN. AMAP fournit des éléments pour les ordres supérieurs.

4.3.3 Longueur et diamètre des unités de croissance

Celles-ci ne sont pas directement accessibles dans PNN mais peuvent être déduites des mesures liées aux accroissements.

4.3.4 Angles de branchements et flexions des branches

Ceux-ci sont répertoriés dans PNN. De plus la longueur de la corde qui relie l'extrémité de la branche au tronc donne une idée de sa flexion.

4.3.5 Modélisations des aiguilles

Pour le rendu visuel de l'arbre un symbole aiguille a été fabriqué.

4.4 Résultat en simulation

La figure 4-4 montre l'architecture du pin noir simule à trente ans, après adaptations des données de PNN au modèle GreenLab. La figure 4-5 montre la croissance du pin noir selon les deux scenarios précités. Ces pins sont disposés en plantation dans la plate forme Xplo afin de donner des images réalistes de la culture (figure 4-6). Celles-ci montrent l'intérêt du couplage PNN-GreenLab par rapport à la visualisation classique rudimentaire dans la plate forme Capsis.

4.5 Discussion

La combinaison PNN Greenlab permet d'ajouter à l'information provenant de la sylviculture une information botanique. Celle-ci permet à priori d'avoir plus d'information sur la biomasse fabriquée et sur sa répartition dans l'architecture. Il est sans doute possible de remonter d'avantage aux processus physiologiques, grâce à cette combinaison, en prenant plus en considération la biomasse.

4.6 Conclusion

GreenLab peut être un outil intéressant pour les modèles empiriques ou fonctionnels forestiers, pour les transformer en modèles structure-fonction et donc pour augmenter leur efficacité prévisionnelle.

5 Conclusion et suggestion pour une continuation

5.1 Les modèles structures fonction en agriculture

5.1.1 Architecture et variabilité individuelle

L'explication des causes de la variabilité individuelle a été souvent abordée, mais celle-ci restait assez floue faute d'avoir un modèle quantitatif permettant de décrire la répartition de la biomasse au sein d'une plante et dans une population. Sur le Mais, la combinaison des modèles Pilote et Greenlab a permis une description détaillée du phénomène. Les délais de germination et l'espace individuel disponible, peuvent a eux seuls expliquer la plus grande partie de la variabilité entre plantes d'une même population.

5.1.2 Sur la combinaison des modèles de culture et des modèles structure fonction.

Les modèles de culture ont des limitations dans l'évaluation des indices foliaires et des indices de récolte. La cause en est la non prise en compte des données de l'architecture de la plante. Celle-ci contient en effet toute l'information nécessaire pour remonter aux processus de croissance et aussi d'avortements des organes qui influent directement sur l'indice de récolte.

Les modèles structure-fonction ont aussi des limitations sévères. La prise de données est en soi un problème et les méthodes inverses pour remonter aux paramètres du modèle sont loin d'être facile à mettre en œuvre. Pour finir la simulation parallèle de la croissance d'une plante, le calcul de l'acquisition et de la répartition de la biomasse sont des freins sévères à l'utilisation de ces modèles, sans compter le passage de la plante au peuplement qui n'a rien d'évident.

Cette thèse montre que le modèle GreenLab propose un bon point de vue même si il n'est pas le seul. Sa proximité avec les modèles de culture fait qu'il est rapidement assimilable par eux et permet justement le passage de la plante au peuplement. D'autre part, par rapport aux modèles structures fonctions, il a une forme plus mathématique ce qui permet la factorisation des processus et l'utilisation de méthodes inverses efficaces permettant la calibration du modèle sur les plantes cultivées. Les paramètres du modèle devraient être un nouvel atout pour les sélectionneurs dans la recherche de QTL et aussi permettre d'optimiser plus rationnellement les itinéraires culturaux, (amendements, éclaircies, tailles, etc.)

5.2 Les modèles structure-fonction en sylviculture

5.2.1 Architecture des arbres

Pour les arbres l'architecture semble incontournable, par rapport aux plantes cultivées, bien qu'elle soit encore plus complexe et due aux fonctionnements rythmiques des méristèmes. De plus les phénomènes stochastiques, de différentiation, de branchement, de mortalité des méristèmes, rendent a priori la tache encore plus difficile, notamment dans la constitution de échantillonnage. Cependant les travaux entrepris avec le modèle GreenLab permettent de minimiser le problème. Dans sa forme GL5 le modèle permet d'aborder la calibration d'espèces forestières, comme des conifères, des peupliers, des ormes, qui semblaient hors de portee encore récemment. Ceci est du principalement au passage de la simulation de la plante au calcul de la plante grâce aux équations de production du modèle, déduites des réglés de l'automate de développement. La surface de projection individuelle de l'arbre, paramètre qui sert à la fois à calculer l'interception de la lumière et à positionner l'arbre dans la population est certainement un atout du modèle, mais il faut l'affiner sur les arbres par rapport à l'expérience qu'on a sur les grandes cultures.

5.2.2 Combinaisons des modèles forestiers et des modèles structure-fonction

Les modèles empiriques forestiers ont leur limite dans leur rigidité à répéter des scénarios basés sur des statistiques. Ils ne peuvent s'adapter à de nouvelles conditions environnementales. Néanmoins ils constituent l'unique base de connaissance. Tels quels en y ajoutant des données botaniques architecturales, ils peuvent simuler des architectures réalistes en empruntant aux modèles structures fonctions leur partie développement associée à de la géométrie.

De leur côté les modèles structures fonctions sont quasiment inexistants à l'échelle de l'arbre. Le modèle Finlandais Lignum reste unique pour ses applications forestières sur les conifères et les feuillus. Il reste cependant limité à cause des temps de calculs qui le confinent à la simulation qui peut facilement dépasser une dizaine d'heures. De plus l'architecture reste sommaire et déterministe. Le fonctionnement stochastique des méristèmes n'est pas intégré. Une combinaison Lignum GreenLab est parfaitement possible, car les paramètres écophysiologiques d'un arbre, ne sont pas ceux qui alourdissent les calculs, dûs surtout à la complexité de la structure. Or la factorisation réduit considérablement les temps de calcul. Les simulations réalisées gagneraient en finesse et en réalisme.

L'introduction combinée de la production de biomasse et de l'architecture des plantes dans les modèles de cultures et les modèles forestiers semblent donc dignes d'intérêt comme cette thèse a essayé de le démontrer.

Références bibliographiques

161 références sont citées

Annexe 1 Liste des paramètres du modèle Greenlab

Annexe 2 Exemple de cible végétale sur le Maïs pour la calibration du modèle GreenLab

Annexe 3 Méthode des statistiques différentielles.

1. Introduction

1. Introduction

1.1 Complexity of plant systems

Plants are primary producers that provide the ultimate source of energy for creatures on earth. Through photosynthesis, they use energy from sunlight, convert carbon dioxide and water to organic compounds, and release oxygen. Such a process is crucial for balancing oxygen in the atmosphere and maintaining a stable ecological environment. The ultimate aim of plant studies is for the benefit of people, such as improving food productivity, achieving sustainable development in agriculture or silviculture. However, plants are complex systems, and they have three major features that are a challenge for research.

1) Hierarchical organization. At the top end of the scale, plants can present as a field or a forest, whilst as individuals they can be regarded as a constitution of specialized and interrelated organs, lower level tissues and cells, even molecules. Such hierarchical levels characterizing processes at the higher level are the integration of lower level processes (Bouman et al. 1996). For example, canopy photosynthesis is mainly the sum of the photosynthesis of single leaves, whereas photosynthesis for a leaf is the result of biochemical actions taking place in chloroplasts (cell level). It should be noted that such integration can be very complicated when hierarchical levels have their respective influences on the same processes. For instance, the photosynthesis effect depends on light interception, which itself can be influenced by plant population densities (stand level), the architecture and space attributes of leaves (individual level), and the position and geometric attributes of a single leaf (organ level). Generally, the lower levels are closer to the mechanism of a problem, but they can be very complicated to deal with. Consequently, a definite objective of a plant study is always necessary, whereby the appropriate level(s) can be determined.

2) Cooperation of multiple internal processes. Basic physiological processes include ontogenesis and architectural development, resource uptake, photosynthesis, respiration and carbon allocation (Gifford and Evans 1981; Fourcaud et al. 2008). During plant growth they work simultaneously and interact with each other as both cause and effect. For instance, ontogenesis is the origin of plant growth and architectural development, yet its occurrence requires sufficient energy (by respiration) and biomass (from seed). Photosynthesis produces biomass and stores energy for architectural development and organ growth (carbon allocation). Conversely, leaf distribution (dependent on architectural development) and areas (dependent

on carbon allocation), and root structure (dependent on architectural development and carbon allocation) can each determine the capture of light, water and nutrients to influence photosynthesis.

3) Interactions with the environment. As plants are immobile, their growth is greatly constrained by the environment; likewise it depends on adaptive responses too. On the one hand, resources (i.e. water, carbon dioxide and nutrients) from the environment are essential for biomass production and organism construction. On the other hand, plants per se receive signals (i.e. light, temperature, water, nutrient, gravity etc.) from the environment, and then control or regulate their physiological processes according to their "perception". A good example is the temperature effect on leaf emergence, which can be found in plastochron or phyllochron observations. The regulation of flowering time by photoperiod is another example. The plasticity of plant behaviour in relation to the environment is the main cause of plant variability, and such a situation increases the difficulty in plant growth studies.

1.2 Current situation of plant growth models

Modelling as a main approach to plant growth is a powerful tool. The advantages include: 1) Modelling can quantify problems, thus classic mathematical and physical methods can be used to serve research. 2) With an explicit description of problems, modelling is controllable and hypotheses can be tested with the same explicit results. 3) Modelling is effective in integrating diverse knowledge, information, theories, and even sub-models, making it suitable for dealing with complex systems. Nevertheless, given the complexity of plant behaviour, models always involve a lot of simplification and approximation, by building empirical relationships or reducing the factors under consideration, so models always have their limitations as well as their advantages.

1.2.1 Advances in traditional models

Traditional models include crop growth models (Bouman et al. 1996; Marcelis et al. 1998) and forest growth models (Pretzsch 2009). They were built for agricultural and silvicultural research and management. Such models are mostly carried out at stand level, and some forest growth models also predict variables for single trees. Over approximately a half century's development, they have become accepted tools for use and application in their fields. They provide yield predictions based on environmental conditions and resource supplies, and carry out scenario simulations, giving rise to advice for farmers on cultivation, and for managers or stakeholders for strategic decision-making.

Empirical models. At the outset of modelling studies, the methods used were mainly empirical, based on statistical analyses. Empirical crop and forest growth models are based on the knowledge of systems, whereby various factors such as climate (e.g. temperature, light radiation, precipitation), field conditions (e.g. soil status) and management treatments (e.g. irrigation, fertilization, thinning of forest stands) can be taken into account, but without consideration of the underlying mechanisms. They are suitable for economic management, by supplying efficient predictions of growth and yield. However, as they are rigorously calibrated with particular cultivars or species and with well-defined conditions, their applicability is mostly limited to that aspect (Cheeroo-Nayamuth 2000; Landsberg and Sands 2011).

Process-based models. The need to deepen understanding of eco-physiological processes underlying crops and to provide widely applicable model tools has greatly increased in the face of climate change and food security issues. In this context, physiological process-based approaches are increasingly being encouraged in crop and forest growth models (i.e. process-based model, PBM, Landsberg and Sands 2011). These models set out to take into account interactions between physiological processes and abiotic factors, and plant growth is mainly considered as a change of matter in organ compartments based on uptake processes (e.g. photosynthesis), and loss processes (e.g. senescence in the case of trees) that, in turn, depend on environmental conditions (i.e. light, temperature, water and nutrient availability) (Pretzsch et al. 2008; Fourcaud et al. 2008). The studies are mostly based on populations at stand level (e.g. STICS, Brisson et al. 2003; APSIM, Keating et al. 2003; DASSAT, Jones et al. 2003; Pretzsch et al. 2008), but also include a few individual cases (e.g. TOMSIM, Heuvelink et al. 1996; 1999). Usually, morphogenesis and explicit descriptions of plant structure are not considered in such models. PBMs emphasize photosynthate computation, but generally disregard allocation processes (Marcelis et al. 1998), which are actually relevant to organ or organ compartment construction, and crucial to some key components of the models, such as LAI and grain yield (computed by the harvest index). As the allocation process adapts to environmental changes as well as to photosynthetic functions, this can be a major limitation to PBM use for wider environmental conditions. In recent years, studies with genetic information have become a new tendency in crop growth models (e.g. Garvin et al. 2007; Hammer et al. 2010; Lizaso et al. 2011), in an attempt to improve the identification of genotypes and understand differences between genotypes and phenotypes. One perspective

for this is as a breeding aid. Another is to introduce genotype-environment interactions in plant growth models (Dingkuhn et al. 2005).

1.2.2 Functional-structural plant models

Plant development and structure dynamics are important components in plant behaviour, but for a long time the right conditions were not available for them to be taken into account in plant growth studies. The advent and development of 3D plants has changed this situation. Functional-structural plant models (FSPM) are just such a particular type of plant model built on the basis of interrelations between plant structure dynamics and growth functions. Models taking into account the interaction between plant development, organ functions (e.g. root uptake, leaf photosynthesis, and stem transport) and plant growth processes have been developed extensively over the last decade (Perttunen et al., 1996; de Reffye et al., 1997a; Prusinkiewicz, 2004; Fourcaud et al., 2008).

Plant morphology and visualization. Interest in plant morphology in modelling has emerged with the advances made in computer graphics technology. It has gradually become another intriguing means for plant modelling studies, as the most straightforward means of perception. 3D plant visualizations have been greatly promoted by various algorithms. Some of them mostly involve smart-looking image synthesis (e.g. particle systems, Reeves 1983; fractals, Oppenheimer 1986), while others pay more attention to realistic structural features (e.g. by parameterization of branching attributes, Honda, 1971; L-systems, Prusinkiewicz and Lindenmayer, 1990; AMAP, de Reffye et al. 1988). Nowadays, highly realistic 3D plants can be generated by computers, which have been widely using in city landscape designs, visualization of farm land or forests, scene production for films or games, teaching, and scientific demonstrations; some nice examples are shown in Fig.1-1.

Structure representation. Vivid plant visualization often greatly impresses people, but for a botanist or a plant physiologist the more rational attraction of plant morphology is likely to be its mechanistic sense for plant studies involving abundant information mirroring plant development and very important physiological processes. For this purpose, efficient and accurate representations of plant structures and their dynamics are a prerequisite.

The most representative methods for that purpose include L-systems and AMAP, the former being the most widely used and the latter for botanists' purposes.

Inspired by the fractal features existing in plant morphology, Prusinkiewicz and Lindenmayer (1990) adapted the parallel rewritten formalism, L-system (Lindenmayer 1968),

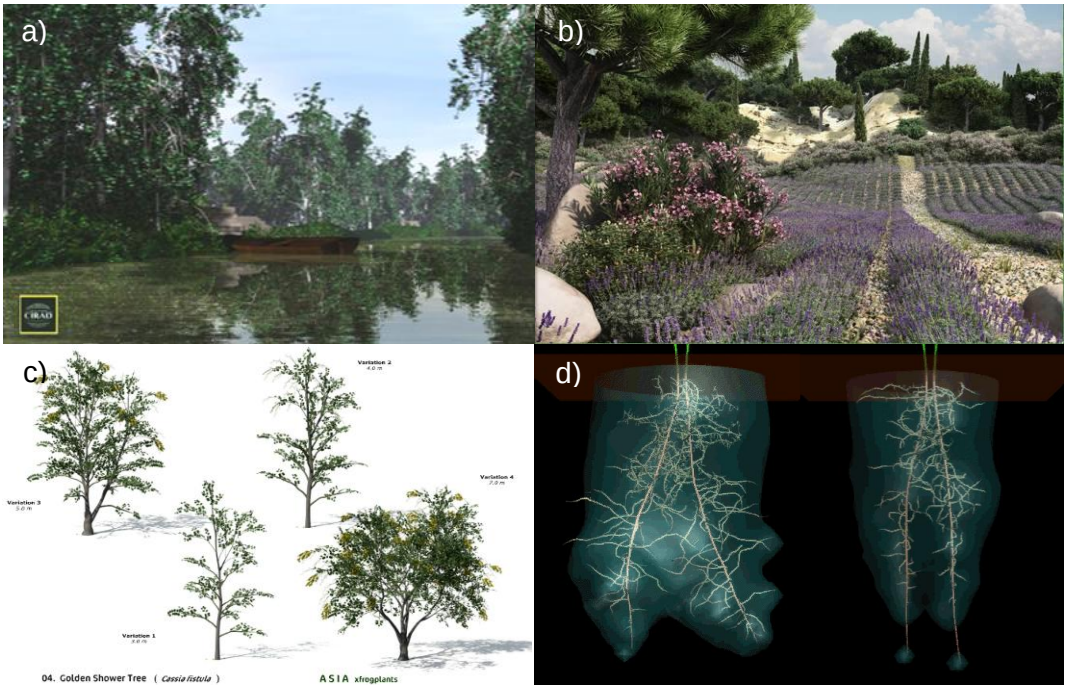

Fig.1- 1 Some demonstrations of computer-generated plants, or scenes of early periods of plant form simulation. a) Canal, generated by Marc Jaeger in 1992 using AMAP software http://marcjaeg.free.fr/Amap_Classics/index.html**; b) Generated by landscape architect Frederic Bec 2009, all plants are modelled in OnyxTree,** http://www.onyxtree.com**; c) Golden shower tree (*Cassiafistula*) in XfrogPlants library,** http://issuu.com/xfrog/docs/asia_xfro **d) A comparison of the effects of different rates of uptake on root system development, simulated by L-system (Měch and Prusinkiewicz 1996)**

to describe the dynamic organization of plant compositions. The development of a plant is abstracted and defined using grammatical rules; stochastic, delay and specific inflorescence patterns can be configured with parameters (Prusinkiewicz et al. 1988). The merits of this method are: 1) the essential theory is easy to understand and provides a universal framework to be followed for plant building; 2) very complex structures can be achieved by some simple grammatical manipulations. While most plants display great plasticity in structural development, for large plants with a complex structure, it can be very difficult to faithfully abstract topological development into a grammar.

Based on plant architectural concepts (reviewed by Barthélémy and Caraglio 2007), de Reffye and co-workers (1988), from the AMAP laboratory (http://amap.cirad.fr), proposed a mechanistic method for faithful simulation of plant development. On the one hand, morphogenetic construction is strictly established based on botanical knowledge of plant architecture. A very significant contribution made by Hallé et al. (1978) was 23 architectural models, amounting to an abstraction from all the existing plant growth patterns. These models provided generalized approaches for simulating the features of plant structures and their development. On the other hand, given the relation between meristem activities and the

resulting architecture, they also put forward an explanatory way of quantifying plant structures by the probability of meristem growth, branching and mortality, which gives an explanation of the random characteristics of plant structure. This stochastic algorithm provides a way of characterizing the growth and cessation processes by analysing the final distribution of organ numbers in branches. Good coherence can be found in both tropical and temperate trees (de Reffye et al. 1991b), as well as for flowering sequences (Guédon et al. 2001). The value of this method is that: 1) It provides a mathematical way of structuring development simulation, which takes into account the general situation and not only certain specific cases; 2) It is possible to build access to real plants.

Two kinds of emphasis in FSPMs. FSPMs, which are a recent addition to plant growth models, emphasize the connection between plant morphology and growth functions, where morphology is mainly considered in two ways: one is the 3D spatial occupancy of the plant structure, the other is the dynamic process of the plant constructing its structure, which is also known as morphogenesis.

Plant spatial occupancy greatly determines resource acquisition both above and below ground. With the 3D reconstruction of plant structures, we are able to study light interception by the canopy (e.g. Sinoquet et al. 2001; Soler et al. 2003; Pearcy et al. 2005; Wang et al. 2006; Dauzat et al. 2008; Rey et al. 2008), competition for water and resources within the root area (e.g. Měch and Prusinkiewicz 1996; Dunbabin et al. 2003; Lambers et al. 2006;Wu et al. 2007; Danjon and Heubens 2008), and even the kinetics of mass and energy inside the plant structure or between the structure and the environment (e.g. Dauzat et al. 2001).

For instance, LIGNUM (Perttunen et al. 1998) is an FSPM which takes into account plant functions by emphasizing the aspect of spatial occupancy of the plant structure in interaction with the environment. Carbon accumulation and new tree segment creation in LIGNUM are both determined by global or local radiation interception.

Comparatively, the time scale dynamics of plant morphology (i.e. morphogenesis) can be a crucial determinant of plant growth too. In botany, studying plant development according to the evolution of its structure has become a new discipline known as “plant architecture” (Barthélémy and Caraglio 2007). Plant architecture not only concerns plant structure but more importantly also examines the strategy of structural evolution and the corresponding time information. In detail, the time information includes the time of organogenesis, expansion and death, which directly determines the type, the quantity and the active duration of the organs.

Such information is very important for precisely describing organ processes (e.g. photosynthesis, biomass partitioning) and thereby plant growth.

In order to distinguish them from FSPMs focusing on spatial structure, the FSPMs based on comprehensive knowledge of plant architecture and taking advantage of that information to study growth processes are called functional-architectural plant models (FAPM). For instance, GreenLab is such a model, which is based on the architectural models (de Reffye et al. 1988) developed by the AMAP laboratory and takes into account the interaction between the dynamic number and type of organs abstracted from the architectural model and physiological processes (i.e. biomass assimilation and partitioning).

Advance in FSPMs. The progress made in reconstructing the structures of real plants is of great interest for FSPM studies. The 3D digitizing technique allows exact geometric reconstruction of real plants (e.g. Sinoquet et al. 1991), but the work involved is very laborious. New theories (e.g. Multiscale Tree Graph, Godin, 1998) and graphic technical methods (e.g. Cheng et al. 2007) have attempted to simplify the work involved in analysing and measuring plant structures for 3D reconstruction.

The objective of FSPMs is to integrate interactions between plant morphology and physiological functions, but initially most attempts focused on the effect of structural components on functions (e.g. de Reffye et al., 1997a; Perttunen et al., 1998). In recent years the importance of morphogenesis and its response to the environment or to plant growth status have attracted more and more attention (Prusinkiewicz and Rolland-Lagan, 2006; Evers et al. 2007; Chelle et al. 2007; Buck-Sorlin et al. 2008; Letort et al. 2008; Ma et al. 2011).

Organ level biomass allocation, as well as biomass assimilation, is often taken into account when simulating plant growth (Drouet and Pagès 2003; Yan et al. 2004). Several platforms designed to incorporate extensive physiological processes with plant structure have been developed based on the L-systems (L-studio, Prusinkiwicz 2004; Allen et al. 2005; GroImp, Hemmerling et al. 2008) or other approaches (e.g. AMAPsim, Barczi et al. 2008, OpenAlea, Christophe et al. 2008).

It is worth mentioning that the GreenLab FSPM (de Reffye et al. 2003) was developed specifically for solving the source-sink process regulated by plant architecture development. After long-term practice, the generalized least squares method (Zhan et al. 2003) was found to be feasible for estimating parameters according to organ measurements, which is the first example of FSPMs usable for access to real plants.

The great power of FSPMs is that interactions between physiological processes (associated with organ functions) and environmental conditions can be described and analysed in connection with 3D plant architecture (Fourcaud et al. 2008). After development over a period of ten years, the potential of FSPMs to deal with some intractable issues, such as plant morphogenesis, interactions with the environment, plant plasticity, genotype and phenotype studies, has begun to emerge. However, models that fully take into account the relation between physiological processes and dynamic structural development for whole plant growth have yet to become popular for applications to crop fields or forests.

1.3 Objective and work plan

As FSPMs are promising for improving mechanistic plant growth studies, the objective of this thesis was to combine them with crop models or forest growth models in order to jointly study problems in agriculture or silviculture.

However, some challenges generally exist in practice. Firstly, the passage from individuals to population is unknown. For instance, the maximum productivity of a crop field or a forest stand does not imply that each individual inside the field or forest has reached optimum growth, the performance of a population is not a simple sum of individuals, but a result of the combined actions of population density, available resources and individual behaviours. However, the pattern of these components, and interactions between them, are not clear.

Secondly, some processes in FSPMs, such as ray-tracing light interception, transport resistance based carbon allocation, are time consuming and require a great deal of memory space. Although the advances in hardware and algorithms have shown the potential to cope with the heavy computing in FSPMs in the future (e.g. ECOPHYS, Host et al. 2008; Zheng et al. 2011), implementation is currently still restricted by the population scale, plant age and complexity of plant architecture.

Thirdly, most FSPMs are built on simulation processes and do not have equations, which is very difficult or impracticable for parameter estimation. For instance, without equations, reverse computation can only be solved by some heuristic methods (e.g. PSO), which call for numerous repetitions of possibly heavy simulation.

The solution in this work was to use GreenLab (de Reffye et al. 2003; Yan et al. 2004) as the FSPM. GreenLab is not only an FSPM but also an FAPM, which contributes to providing realistic plant architecture dynamics (de Reffye et al. 1988; Kang et al. 2003) and

establishes source-sink processes on that basis, even with feedback from growth functions to plant development (Letort et al. 2008; Ma et al. 2011). GreenLab has effectively solved the two challenges facing FSPMs:

1. Dynamic equations (de Reffye et al. 2003) are generally established in GreenLab, which supports fast calculation. For development, the algorithm of structure factorization (Yan et al. 2002; Cournède et al. 2006) can compute dynamic organ production based on substructure instances without architecture construction. Biomass accumulation is adapted from an empirical function based on Beer's law (Yan et al. 2004, Cournède et al. 2008). Biomass allocation is carried out by the sink strength of organs (Yan et al. 2004), which does not depend on the transport path in plant architecture.

2. Parameter estimation is available. GreenLab has been used many times on real crop plants (e.g. maize, Guo et al. 2006; sweet pepper, Ma et al. 2010; tomato, Dong et al. 2008; cucumber, Mathieu et al. 2007, etc.), or young trees (e.g. Scots pine, Wang et al. 2010), which guarantees further applications.

For the combination, GreenLab was assumed to provide individual-based development and growth information, including: 1) Morphogenesis configuration based on botanical knowledge. 2) Source-sink processes associated with organ level functions based on the dynamic architecture. 3) Parameter estimation for the growth system. 4) 3D architecture generation and visualization. Crop growth models commonly provide field-level computation of economic yield by accounting for photosynthetic processes in accordance with the amount of available environmental data and agricultural knowledge (Cheeroo-Nayamuth 1999; van Ittersum et al. 2003). By contrast, an EFM generally provides accurate and rapid predictions of stand-level forest growth performance (i.e. diameter, height and crown growth and mortality) based on long-established statistical relationships for economic forest management. Causes involving resource supplies, environmental conditions at a site and extending to thinning management are taken into account, through a regression analysis of relations with the responses expressed in the above-mentioned growth performances (Pretzch 2009, in Chapter 11; Landsberg and Sands 2011).

Consequently, the modelling combinations were expected to benefit from both parties: the FSPM offers dynamic plant architectures and relations with organ-level functions as a support; the crop growth model supplies productivity computations with field-level accuracy based on agricultural knowledge; the EFM then provides accurate forest growth estimations based on silvicultural functions. Lastly, the capability provided by each model can be

expanded, one example being that the corresponding dynamic stand level 3D canopy can be visualized.

1.4 Structure and content

The relevant GreenLab methodology and my engineering work on the Xplo platform are presented in Chapter 2.

Two applications of model combinations were carried out using the developed software. One was between GreenLab and a crop model, PILOTE, on maize. The other was between GreenLab and an EFM, PNN, on black pine. They are studied and discussed in Chapter 3 and Chapter 4.

Lastly, further applications of modelling cooperation and the future promising direction of architecture exploitation in plant growth modelling research are described (Chapter 5).

2. GreenLab model and development

2. GreenLab model and development

2.1 GreenLab method

2.1.1 Botanical aspects of plant architecture (according to Barthelemy and Caraglio 2007)

Phytomer. The phytomer (or metamer) is the basic structural unit in plant organization. It usually consists of an internode and its insertion part including a leaf (or leaves) and axillary bud(s) (Fig.2-1). Successive phytomers build up a leaf axis, whereas an axillary bud in a phytomer can produce another axis.

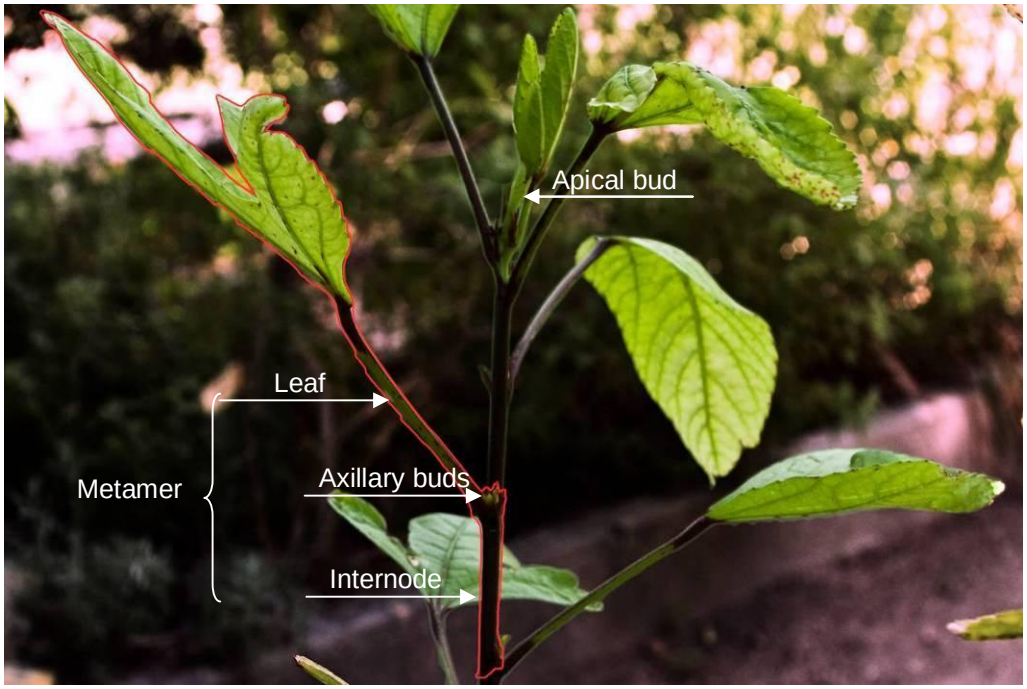

Fig.2- 1 An example of a phytomer in a leaf axis (marked by a red line)

Growth unit. The growth unit (GU) is a succession of phytomers that generates over an uninterrupted period. In fact, a small proportion of plants under constant tropical conditions (e.g. coffee) and some other herbaceous plants (e.g. maize, cotton, wheat, tomato) have *continuous growth*, which does not have significant rest periods for distinguishing GUs. However, most plants have *rhythmic growth*, which involves alternating resting and active periods of meristem activity. Such alternations leave morphological separations between GUs indicated by special markers (i.e. short internodes, cataphylls).

In a growing season, one GU (i.e. monocyclism) or a succession of several GUs (i.e. polycyclism) may expand, constructing an "annual shoot". GUs generated in one annual shoot may be identical or distinctive.

Time measurement. Plant growth universally exhibits periodicity with climate (i.e. phenology). On the assumption that phytomer appearance is driven by temperature at a constant rate, GreenLab takes thermal time as the default time measurement. Thermal time is accumulated by daily mean air temperatures after subtraction of a base temperature for a specific plant.

The time units frequently used are the *phyllochron*, which corresponds to the thermal time taken to generate a phytomer, the *growth cycle* (GC), which is a quite regular period in a growing season taken to generate a growth unit, and the *computing unit* (CU), which is the smallest time unit used in the model. The computing unit can correspond to a phyllochron or a growth cycle or to another time unit, depending on the model design.

A period since the formation of an organ, a phytomer, a GU, an annual shoot or a plant is called the chronological age (CA). However, another concept of age (i.e. physiological age) is used by botanists for understanding the gradient features in the construction of plants.

Physiological age. Meristem gives birth to new phytomers to construct an axis, where differential features, such as vegetative or reproductive shoots, long or short shoots, can be regularly found along the axis as it develops. The physiological age (PA, Barthélémy et al. 1997) is used to identify meristems with the same particular combination of features of derivations, consequently characterizing axes of different architectural development. The PA of the main stem is set to 1 by default. Usually, PAs of axillary buds are older than the apical buds of an axis, except in the *reiteration* case, where plants duplicate their own elementary architecture during their development, and where the axillary bud is equal to the apical bud in terms of PA. For this reason, the branching order often shows good correspondence with the PA gradient between axes. The PA value depends on both the position of the meristem in the plant architecture and the plant development stage. Fig.2-2 is an example that demonstrates the morphogenesis gradients represented by the PA along the axes (right) in a black pine tree (left).

In fact, gradient features (i.e. size of GU, branching complexity, size, form and anatomy of vegetative organs, features of lateral branches, and the capacity to flower) observed from topological hierarchies arise from a transition of meristem production during

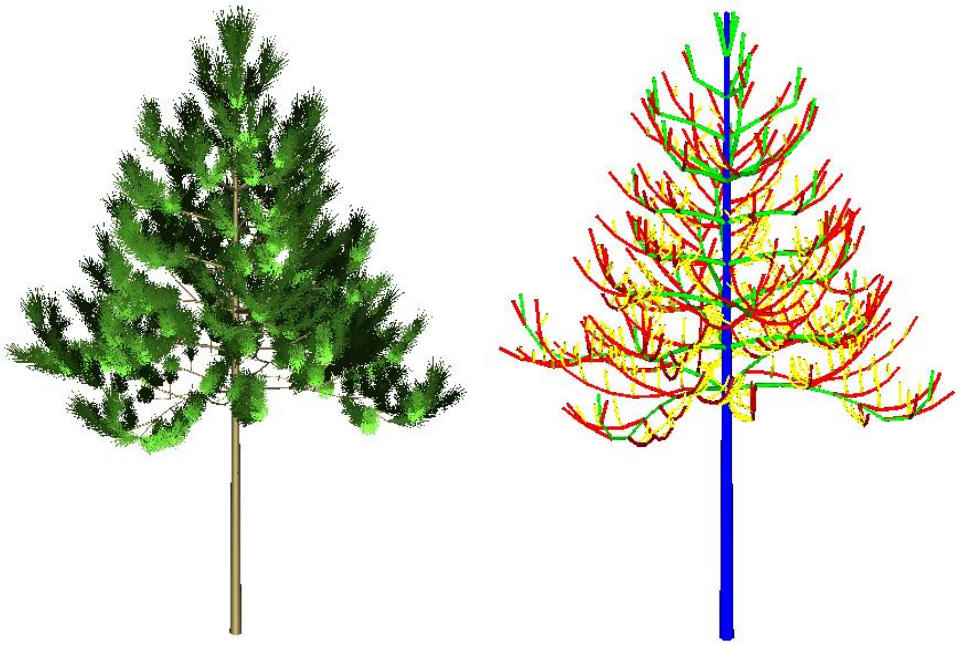

Fig.2- 2 3D Simulation of a black pine with four PAs at age=15 years old (left) and the schematic diagram of a PA gradient along the axis (right). Blue, PA=1, green, PA=2, red, PA=3, yellow, PA=4

the development stages. The *"morphogenetic gradient"* concept (defined by Barthelemy et al.1997; also defined as heteroblasty by Diggle 2002) is used rather to describe intrinsic morphological differentiation of plant development.

Architectural model. The architectural model is a systematic method summarized by botanists (Halle and Oldeman 1970) for identifying plants by collective endogenous growth patterns and the resulting architecture. Architectural models are defined based on investigations involving four major aspects: 1) The growth pattern, 2) The branching pattern, 3) The morphological differentiation of axes 4) Lateral or terminal flowering. Each aspect can then be described by one or more grouped features. For example, considering whether the apex meristem can constantly expand (i.e. abscission, abortion or transformation into a specialized structure), the growth pattern can be *determinate* or *indeterminate*; considering whether or not shoot expansion has a marked cessation, the growth pattern can still be rhythmic or continuous. The number of theoretical possible combinations of morphological features is high, but only 23 architectural models have apparently been found in nature, for which reference can be made to Halle and Oldeman (1970) and Halle et al. (1978) for detailed information.

The study of architectural models provides a theoretical foundation for constructing a universal plant model, since if the model can describe these 23 architectural models of plants then it can simulate the development of any plant. GreenLab (de Reffye and Hu 2003; Yan et al. 2004) and its predecessors AMAP (Jaeger and de Reffye 1992), AMAPsim (Barczi et al.

1997; Barczi et al. 2008), AMAPpara (de Reffye et al. 1997a), AMAPhydro (de Reffye et al. 1999) are based on the same theory of architectural concepts and models to account for morphogenesis and plant development.

Plasticity in plant architecture. Plasticity, which is ubiquitous in nature, is an adaptive response in plant growth and development to external environmental constraints, which is a concept contrary to "gene expression". For plant architecture, plasticity is governed by meristem behaviour (i.e. differentiation, abortion, dormancy), which gives rise to variation in the number of organs, and in the distribution and morphology of botanical entities. Based on this situation, de Reffye et al. (1988) proposed a mathematical approach, which described stochastic expressions of plant architecture as a result of the probability of meristem behaviours.

In fact, plasticity with regard to resource uptake and use under given environmental conditions generally combines with intrinsic regulations such as a "morphogenetic gradient" to jointly determine an ontogenetic phenotype and the resulting architecture (Diggle 2002).

Time relevant behaviour. Organogenesis and extension constitute the development and growth of plants. Depending on a certain fitness strategy, organ extension and initiation can take place simultaneously or separately. For a specific plant, the patterns occurring in the growth processes commonly have a cause linked to its physiological and/or phenological features, whereby the occurrence and period of growth can better adapt to climatic conditions (Geber et al. 1997, Sabatier et al. 2003). With different patterns, the ways in which organs participate in resource uptake and use processes are different.

"*Preformation*" and "*neoformation*" (Barthélémy et al. 1997) are the precise terminologies for the two above-mentioned patterns. In many plants with rhythmic growth, the organs in a shoot are partially differentiated and rest in a bud for days, months or years prior to expansion; such organs or phytomers are termed preformation. Very often, after preformation expansion, more phytomers or organs grow that undergo simultaneous extension and initiation, termed neoformation. A shoot may be formed by preformation or neoformation or a mixture of the two, depending on the plant species, the morphogenetic gradient, the growth status and environmental conditions (Geber et al. 1997, Puntieri et al. 2002). The number of organs in a shoot is determined by the number and the proportion of preformed and neoformed parts. Preformation is relatively more stable than neoformation in organ production at specific positions within the plant architecture, whereas neoformation displays more fluctuations related to environmental changes (Guedon et al. 2006).

However, in specific cases of branching with inflorescences or fruit-set, preformation only partially describes the features. A more essential characteristic is the time taken for organ initiation or extension, flowering or fruit yielding depending on their branching locations (Jassen and Lindenmayer 1987). Such processes have been found to be determined by genes which can be sensitive to the environment or can be regulated by hormonal or physiological signals (Bernier 1988; Cline 1991; Bernier et al. 1993; Reeves and Coupland 2000; Teale et al. 2006). Possible types of orders include: acropetal, basipetal, centripetal and centrifugal, which represent the occurrence in succession towards the apex or towards the base, or towards the centre from the outside, or outwards from the centre respectively. However, the initiation and extension orders of vegetative organs, inflorescences or fruit-setting in branching do not necessarily follow each other, and neither do the initiation and extension of structures inside an inflorescence or a cluster of set fruit. For example, in Compositea plants, the branch-growth sequence is typically acropetal (Fig.2-3a, b), the flowering sequence over the whole branching system is basipetal (Fig.2-3 c), while the construction sequence within a capitulum is acropetal (Jassen and Lindenmayer 1987).

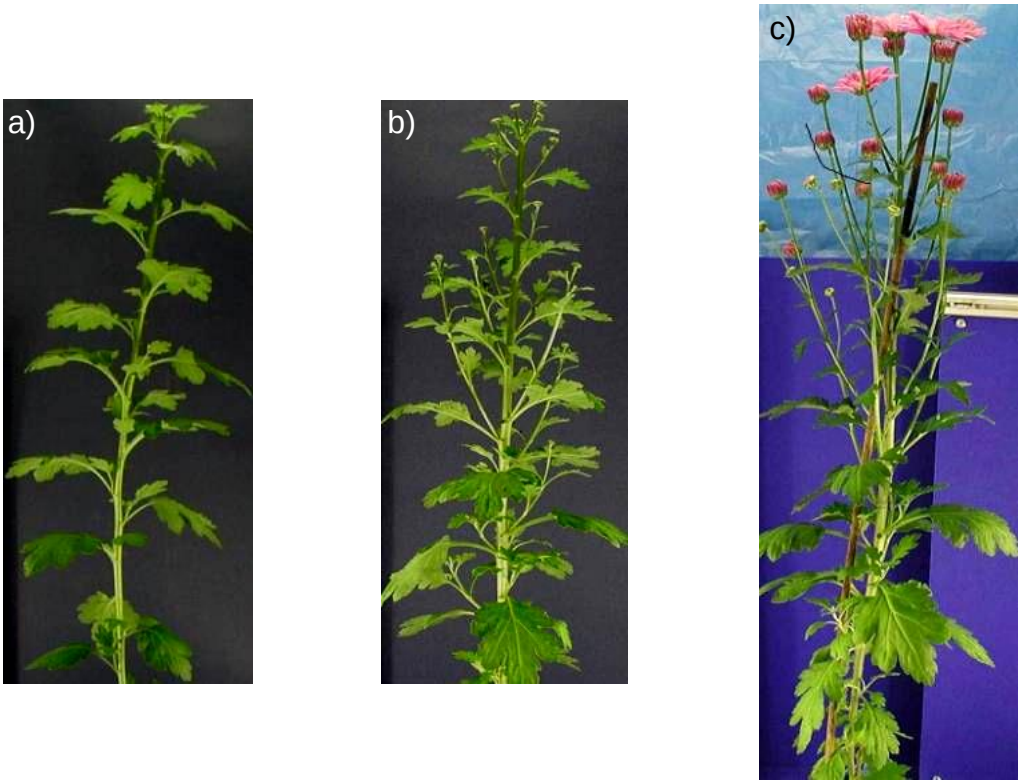

Fig.2- 3 Photos of a chrysanthemum. Main stem and lateral branch development is acropetal during vegetative growth (a & b), whereas the flowering sequence is basipetal (c) (from the presentation by Kang et al. 2009)

In terms of architectural representation, Prusinkiewicz et al. (2007) simulated apical dominance in basipetal growth by an activation relay starting from the main apex. Based on a similar assumption, Kang et al. (2009) proposed parameterized mathematical expressions taking into account both the pathway of signal transmission and a quantified time delay, so that the organ development sequence in plant architecture could be further connected with the resource acquisition and allocation process.

2.1.2 Architectural representation in GreenLab

Dual-scale automaton. Zhao et al. (2001) proposed an approach using two scales to describe structural organization in plant development, defined as the dual-scale automaton. In the automaton, the GU is represented as a "macrostate", and the phytomer is represented as a "microstate". Such a method has been adopted by GreenLab given its efficiency in plant architecture simulation: 1) It can address all the 23 architectural models (Zhao et al. 2001); 2) It is convenient for introducing the probability of meristem activity (i.e. apex bud and axillary bud) (Zhao et al. 2001); 3) It can be used to achieve the specific time sequence process for inflorescences (Zhao et al. 2003).

PAs are used to represent development differentiation. Each microstate is associated with two PAs, one is the PA of the apical meristem of the internode, and the other is the PA of the axillary bud (Fig.2-4 a). Repetition and transition rules for microstates define the construction of the macrostate, and then repetition and transition rules for the macrostate define the axis of development (Fig.2-4 b). The axis of development is represented by a sequence of PAs, which is very close to the "*reference axis*" concept (de Reffye et al. 1991a; Barczi et al. 1997, 2008). With complete axis definition, the behaviours of all the meristems in both apical buds and axillary buds are defined; architectural development can thus be translated step by step (Fig.2-3 c).

For mathematical representation, the dual-scale automaton can also be written in a group of matrices:

$$MI = \begin{bmatrix} m_{1,1} & m_{1,2} & m_{1,3} \\ 0 & m_{2,2} & m_{2,3} \\ 0 & 0 & m_{3,3} \end{bmatrix}, \quad MA = \begin{bmatrix} M_1 & M_2 & M_3 \end{bmatrix}, \quad MU = \begin{bmatrix} r_1 & r_2 & r_3 \end{bmatrix}$$

Matrix *MI* states transition rules for the microstate into the macrostate. The microstate (phytomer) is represented by item $m_{i,j}$ ($i \leq j$), *i* indicates the PA of the apex bud, and *j* indicates the PA of the axillary bud. The value of $m_{i,j}$ indicates replication of this microstate. Matrix

MA states transition rules for macrostates. Each item M_i represents a macrostate, i indicates the PA of the apex bud of the macrostate, the value of M_i indicates the number of GC before the macrostate transition. Matrix MU states the PA (r_i) after transition for each macrostate (M_i). If r_i=0, it means the action of the apex bud has terminated.

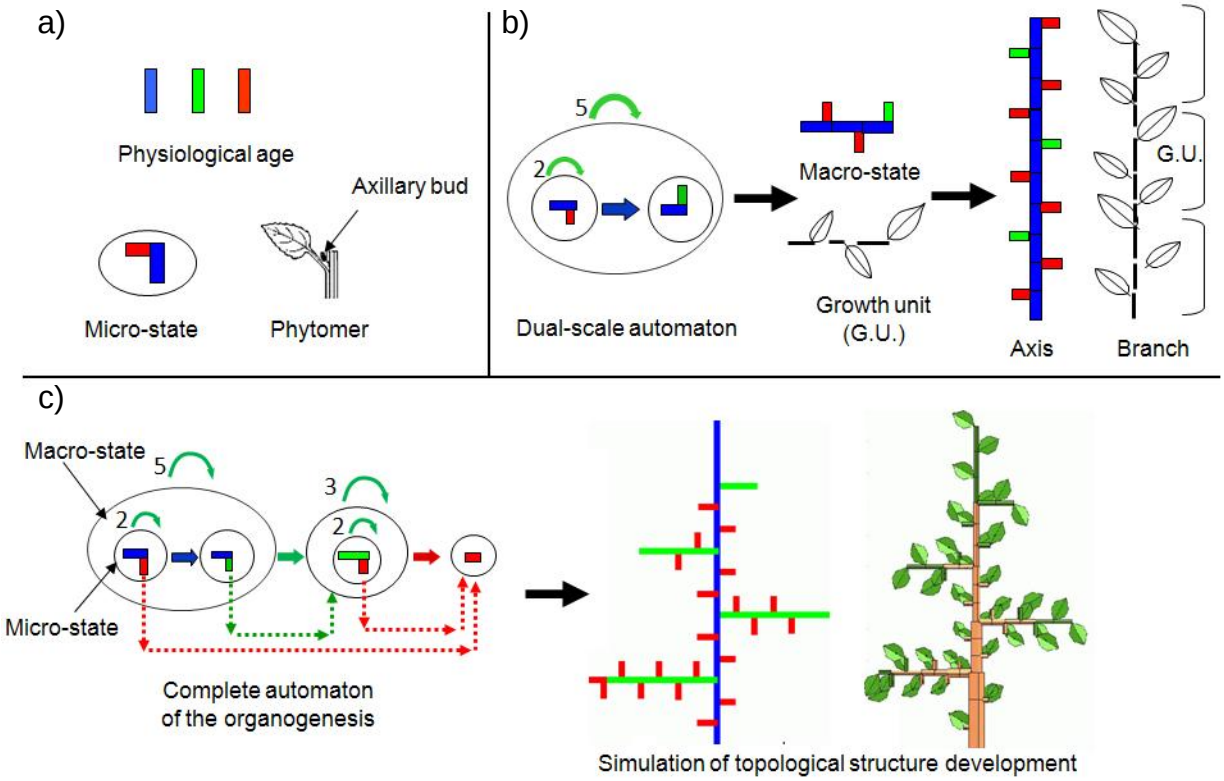

Fig.2- 4 A sketch map of dual-scale automaton construction. Colours denote the physiological ages (PA) of the meristem, blue=1, green=2, red=3. a) To represent a phytomer with a microstate, blue denotes that the PA of the apical meristem of the internode is 1, whereas red denotes that the PA of the axillary bud is 3. b) A macrostate corresponding to a growth unit consists of microstates. The curving arrows indicate replication of the microstate or macrostate; the figure indicates the number of replications. A branch (repetition of growth units) can then be represented as an axis. c) Shows the complete automaton representing plant organogenesis.

Development of the GreenLab model. To date, GreenLab has been implemented on five levels. Each level represents a plant architecture solution, from arbitrary to increasingly mechanical, and to more interactive with growth functions. GL1 to GL5 are used to represent these five levels.

In GL1 (de Reffye et al. 2003; Yan et al. 2004; Guo et al. 2006; Ma et al. 2008) architecture is deterministic, which means the morphogenesis of plants is determined as an average performance, as is the resulting structure and number of phytomers or organs (n_o) (Cournède et al. 2006). It is effective for most crop plants, whose life cycles usually last several months and whose growing environment is quite stable. However, this approach is

limited for the general situations of plants in the wild, whose architectures always vary between individuals and in response to environmental conditions.

Thus, in GL2 (Kang et al. 2008a) stochastic models controlled by the probabilities of meristem activities (i.e. growth, death, pause) were introduced; the methodology was first published by de Reffye et al. (1988). In this case, morphogenesis is a probability event, and n_o is a distribution determined by the probability of meristem activities. Consequently, functional simulation and computation carried out accordingly can represent the integral level of a species or cultivar by assessing the mean and variance performance. Fig.2-5 shows an example from the work of Kang et al. (2008a).

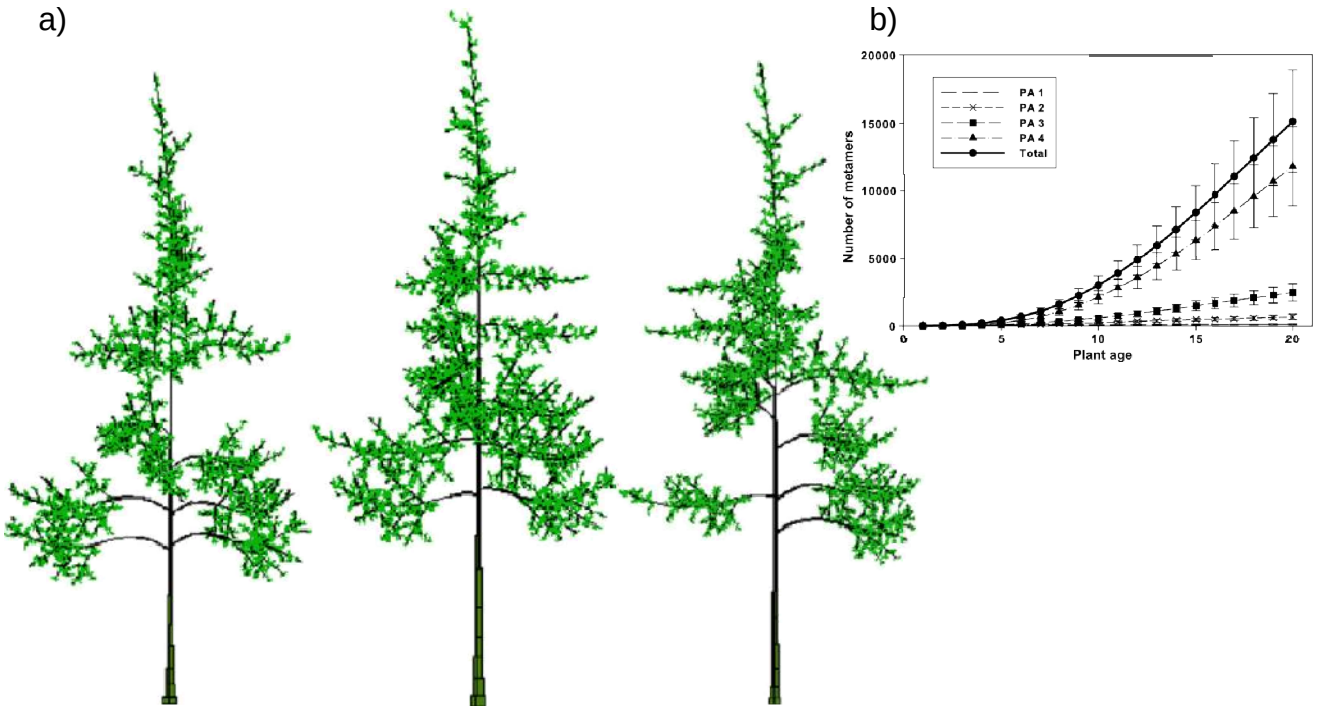

Fig.2- 5 Stochastic simulations of the *Gingko Biloba* tree from the same set of parameters. a) three examples of individual *Gingko Biloba* trees at age=20 years old; b) the mean and standard deviations of the number of metamers in axes of different PAs over time (from Kang et al. 2008a)

GL3 (Cournède et al. 2006) was proposed because in studies of plants with cyclic fruit-set patterns, the dynamic source-sink ratios are found to be regularly related to the appearance of fruits (Marcelis et al. 1994; 2004; Mathieu et al. 2007; 2008). During the plant's life span, where fruits emerge the source-sink ratio is higher than some thresholds (Fig.2-6, the example of cucumber from Mathieu et al. 2007; re-arranged in Kang et al. 2009). Consequently, a feedback mechanism between architectural development and the source-sink is supposed. The new numbers of organs, metamers or branches (n_o) appearing are controlled by functions of the source-sink ratio (Mathieu et al. 2009), which simulate the threshold of

regulated competition for assimilates between organs. Letort et al. (2008) and Ma et al. (2011) have applied this theory to beech and sweet pepper respectively.

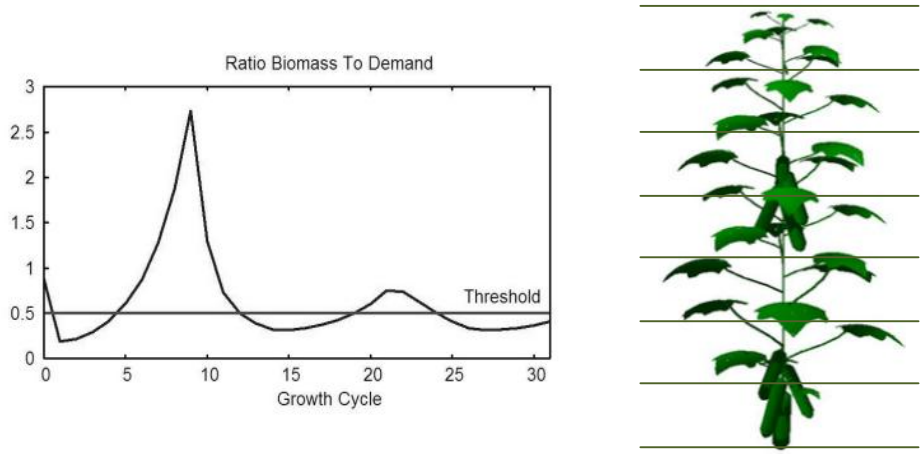

Fig.2- 6 Feedback simulation of cucumber growth. The positions and number of set fruits correspond to a growth rate twice as high as the threshold. (Mathieu et al. 2007; Kang et al. 2009)

GL4 was then proposed for a more generalized case where the threshold control of the source-sink ratio can have variations corresponding to the gradient transition of organogenesis over time. The first use and identification can be found in Pallas et al. (2009) and Pallas et al. (2011) on grape.

Although the modelling assumption of GL4 and the reverse computation of GL3 were preliminarily achieved, the CU of GCs largely prevented dynamic processing of the feedback on plant development for complicated plants (e.g. temperate trees, multi-cyclic plants). This is why GL5 was launched over two years ago by Philippe de Reffye. It is still in progress. The most obvious difference from the previous version is a smaller CU, a phyllochron, used instead of the GC.

The GC time step is rather coarse and not sufficient to represent perennial plants, especially temperate tree growth. For such plants, annual growth often has two or more continuous organogenesis periods with intervals that distinguish the annual shoot into different successions of phytomers (i.e. GU). On a GC scale, we can predict the accurate number of phytomers constructed in a GU, whilst the real growth time of each phytomer, which depends on both the time of appearance and plant rest period, are not explicit, not to mention the more complex events, such as preformation, neoformation, inflorescence with the branching process. A finer time scale is therefore needed.

With the phyllochron, we have to clearly state the time of organ appearance and the real growth time each year, so that the growth duration of an organ is explicit. Furthermore, it is possible to explore the time-related interactions between architecture dynamics and the resource uptake and use process.

Figure 2-7 gives an example of the different visions for the phyllochron and GC respectively. For a monocyclic plant, an annual shoot with an apical meristem having a growth probability p=0.5 can have various possible development sequences, as seen for the phyllochron in Fig.2-7. Each development sequence represents a unique process of shoot growth, which is determined by the specific sink development (emergence of new organs) and the resulting source-sink ratio. With the phyllochron, we can obtain an explicit description of the occurrence of new phytomers or new organs, hence the resting periods in plant development; however with the GC, the time scale information is lost inside a GC (illustration for the GC in Fig.2-7).

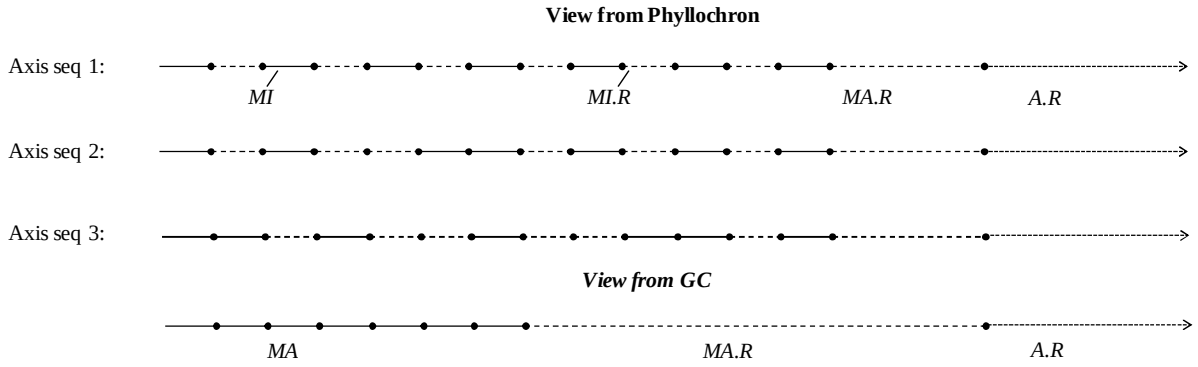

Fig.2- 7 Comparison of the sequences of axis development (Axis seq) represented by the Phyllochron and the GU for an annual shoot with an apex meristem active probability of 0.5 to generate a phytomer. *MI*, microstate, corresponds to the organogenesis of a phytomer; *R*, organogenesis resting period; *MA*, macrostate; *A*, year. *MI.R*, *MA.R* and *A.R* are the organogenesis resting periods between microstates, or between macrostates, or growth resting period over a year. In the simulation by the GU, the organogenesis resting periods are invisible for the sequence, whereas simulations by the phyllochron have an explicit description of the organogenesis and resting period sequence.

From a modelling viewpoint, the time line of an annual shoot development (T.A.) can be broken down as:

$$T.A = m \cdot \left[n(MI) + n(MI.R) + n(MA.R) \right] + n(A.R)$$

Where, *MI* is the generation of a phytomer (microstate); *MI.R* is an organogenesis resting period between microstates; *MA.R* is the organogenesis resting period between

macrostates; *A.R* is the growth resting period over a year; $n(X)$ is the cumulative number of events *X*; *m* is the number of GCs in a year. m>1 is the case of polycyclism.

2.1.3 Growth simulation

Organ functions. Growth simulation in GreenLab is centred on assimilative production by photosynthesis and carbon allocation to organs. All the organs containing a blade (b), petiole (p), internode (e), secondary growth of cambium on stems (c), female fruit (f), male fruit (m) and root (r) are assumed to be sinks. Sink organs can compete with other organs for biomass for their extension during the expansion period. Green leaves are regarded as a source, which intercepts light radiation to carry out photosynthesis and provides biomass as a common pool. In addition, the initial source providing for initial plant development comes from a seed. Assimilative production and biomass allocation interact with each other depending on the developing architecture (especially green leaves), which is inversely an accumulative consequence of the source-sink process.

Recursive computation. Recursive processes in plant growth are represented by a series of equations in GreenLab. Taking CU= GC as an example, the principle is illustrated in Fig.2-8. In each GC, new organs are firstly generated, processed by a defined dual-scale automaton. Together with the existing organs, they share or compete for the biomass accumulated in the previous GC for their extension. At the outset, the first biomass is initiated from seed. Biomass production is then computed according to the exposed green leaf area. Topological structures are managed and recorded according to a dual-scale automaton. Geometric attributions are converted from biomass by allometric relationships. Lastly, the development of 3D architecture can be visualized.

Biomass allocation. All organs undergoing expansion (i.e. $0 < ca_o$: age of the organ $\leq T_x$: expansion duration) can procure biomass allocation according to their sink strength (p_o), which is the relative capability of organs to compete for assimilates. The sink strength of an organ is the product of the sink factor (P_o) and variation function (f_o) as in Eq.2-1. P_o (o=b, p, e, f, m, r) is the relative value among types of organs, and by default P_b=1.

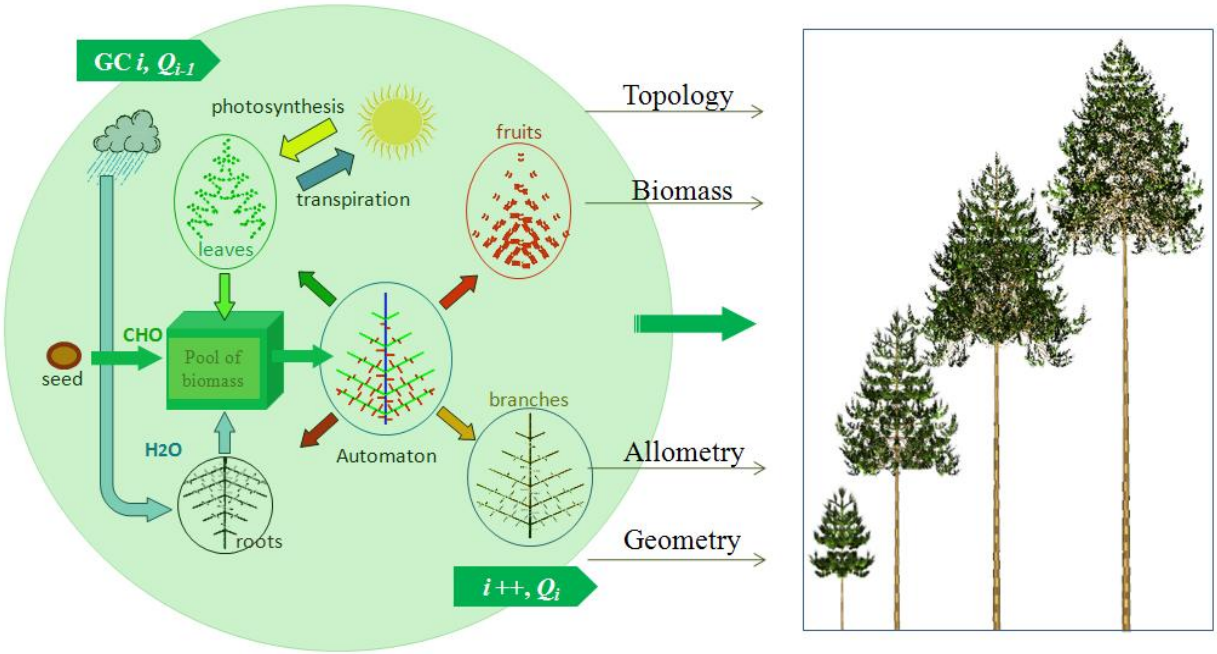

Fig.2- 8 Principal organization of the GreenLab function. The automaton computes the architectural development sequence and generates new organs. Biomass sources originate from a seed or are produced by green leaves. All expanding organs commonly distribute biomass. After recursive calculation of plant functioning, topology, biomass, allometry and geometry data can be completely provided, which can be used for 3D visualization

$$\begin{cases} p_o(ca_o) = \begin{cases} P_o \cdot \left(f_o / f_{o,MAX} \right) & \left(0 < ca_o \le T_{x,o}\right) \\ 0 & \left(ca_o \le 0 \text{ or } ca_o > T_{x,o}\right) \end{cases} \\ f_o(ca_o) = \left[(ca_o + 0.5)/T_{x,o} \right]^{\alpha-1} \cdot \left[1 - (ca_o - 0.5)/T_{x,o} \right]^{\beta-1} \cdot 1/T_{x,o} \\ f_{o,MAX} = MAX\left(f_o \right) \end{cases} \quad \text{(Eq.2-1)}$$

The shape of f_o is characterized by a beta law distribution function; the value is normalized by its maximum. "α" and "β" are the parameters that need to be calibrated. As a beta law distribution function is flexible to adjust, in order to obtain different curve shapes, it often makes one of the variables α and β stable and just fits the other one.

Biomass allocated to an organ (q_o) (Eq.2-2) depends on the ratio of the organ sink strength ($p_{o,j}$) to total demand (cumulative function in the denominator) and the accumulated biomass in the previous GC (Q_{i-1}).

$$q_o(j) = Q_{i-1} \cdot \frac{p_{o,j}}{\sum_o \sum_{ca} p_{o,j} \cdot N_{o,j}} \qquad \text{(Eq.2-2)}$$

$N_{o,j}$ is the number of organs o at age=j, i is the current GC. This equation is based on the assumption that organs of the same type in a phytomer with the same PA and generated at the same time are regarded as identical. Yan et al. (2002) proposed a method of factorization of plant structure to compute the number of organs. It factorizes plant structure into substructures ($S_p^k(i)$) of the GU or substructures of the shoot (of GUs), which are characterized by the PA of the apex bud (p), the CA of the substructure (k) and the age of the plant (i). By representing the revolution of a substructure ($S_p^k(i+1)$) by its previous structure ($S_p^k(i)$) with the transition matrix (see 2.1.2), the number of phytomers can be computed from simple matrix operations. In this manner, the number of organs can be computed even without constructing the plant architecture, which can accelerate processing efficiency in the complex case of plant architecture.

Biomass acquisition. Assimilative production in GreenLab is simulated by an empirical function, which is based on Beer-Lambert's law to account for light interception by all green leaves, as in Eq.2-3:

$$Q_i = \frac{E_i \cdot S_p}{r}\left(1 - \exp\left(-k \cdot \frac{S_b(i)}{S_p}\right)\right) \qquad \text{(Eq.2-3)}$$

Q_i is current biomass production. Where i=0, Q_i the seed biomass. E is the environmental factor providing a growth potential. Leaf area index (LAI) is represented by the ratio of total green blade area (S_b) to a theoretical projective area (S_p). k is the extinction coefficient. Parameter r indicates resistance factors in plant growth.

Current green blade area (Eq.2-4) is converted from the total biomass of green blades by mass per leaf area (e), which is the blade fresh weight per unit area.

$$S_b(n) = \frac{1}{e} \cdot \sum_{i=n-t_b+1}^{n} N_b(i) \sum_{j=i}^{n} q_b(j) \qquad \text{(Eq.2-4)}$$

Where the total biomass of green blades is accumulated by the current biomass of blades from the initialization date n-t_b+1 up to the current GC (n), and the current biomass of each blade is accumulated by the biomass increment (q_b, see Eq.2-2) from the initialization date (i) up to the current GC (n). Parameter t_b is the function duration of the blade.

Size and organ geometry. The computation of organ size is based on the assumption that the dimension of the same type of organs has a regular relationship with the constructing biomass. Constant or piecewise allometric parameters, calibrated from observations or adopted from the literature, were applied for this conversion. The use of allometric parameters depends on the similar geometric form of the organ. For example, a specific leaf area ($SLA = e^{-1}$) is used to estimate the area of blades, as the blades are considered plane even though they may have different outlines. Parameters "*a*" and "*b*" are used to describe the radial (area, *s*) and axial (length, *l*) relationship based on the biomass (*q*) for organs that have a shape approaching a cylinder (e.g. internode pith, petiole), as in Eq.2-5.

$$\begin{cases} l = \sqrt{b} \cdot q^{\frac{1+a}{2}} \\ s = \frac{1}{\sqrt{b}} \cdot q^{\frac{1-a}{2}} \end{cases} \quad \text{(Eq.2-5)}$$

Geometric attributes include orientation (i.e. insertion angle, phyllotaxy angle), size and geometric shape (e.g. representing geometric symbols, mesh). Parameters related to geometric attributes were obtained from observations or the literature. The specific morphological characters of plants may make sense of ecophysiological functions; for example, the orientation of leaves has an effect on light interception. However, as a simplified mathematic model, only the effect of the green blade area is taken into consideration in the GreenLab growth function.

In order to improve computation efficiency, sizes and geometric computations that are not necessary for plant growth processes can be designed as independent modules from recursive calculations, and just executed when 3D visualization is required.

Secondary stem growth computation. Secondary stem growth comes from cambium activity, which brings about internode increments by growth rings. Secondary stem growth is taken into account in the source-sink process and in internode diameter growth for vascular plants. As growth rings have a very high degree of confidence with the calendar year (Hughes 2002), and are sensitive to climatic conditions, the endogenous growth gradient and exogenous constraints (Cook 1985) that limit growth throughout the whole tree, and happen simultaneously in all existing internodes, carbon allocation to secondary stem growth is dealt with as a whole to compete with the expansion of other organs in the source-sink process, as described in Eq.2-6:

$$\begin{cases} p_c(i) = P_c \cdot \left[Q(i-1) / D(i) \right] \\ D(i) = \sum p_o(i) \qquad \text{o=b, p, i, f, m, r, c} \end{cases} \qquad \text{(Eq.2-6)}$$

where the total demand for cambium growth ($p_c(i)$) is the product of the cambium sink factor (P_c) and the current growth rate, which is represented as the previously accumulated biomass ($Q(i\text{-}1)$) divided by total demand ($D(i)$). In return, $D(i)$ is the sum of the demand of all organs (p_o, i.e. blade b, petiole p, internode i, female fruit f, male fruit m, root r and cambium c). By replacing the equation of $p_c(i)$ in the summary function of $D(i)$, total demand $D(i)$ can be determined as the solution of the quadratic equation, and thus the cambium demand ($p_c(i)$) and biomass partitioning to cambium ($Q_c(i)$) can be assessed sequentially.

Within a tree, ring width distribution in the higher portion of stems has a high degree of correspondence with foliage capacity in the upper part, but does not necessarily express a response to the macroclimate. Whereas in the lower portion of stems, ring width growth is likely to receive a limited biomass supply caused by environmental conditions in unfavourable years (Fritts 1966). In order to perform the two kinds of phenomena, a mixed model is used (cf. Letort et al. 2008; Eq.2-7).

$$\begin{aligned} D_{Pressler,i}(n,ca,pa,s) &= \sum_{ca=1}^{n} \sum_{pa=1}^{PA_{\max}} \sum_{s=1}^{n} N_b(n,ca,pa,s) \cdot S_b(n,ca,pa,s) \cdot P_{c,pa} \cdot l(n,ca,pa,s) \\ D_{uniform,i}(n,ca,pa) &= \sum_{ca=1}^{n} \sum_{pa=1}^{PA_{MAX}} N_B(n,ca,pa) \cdot sign(S_b) \cdot P_{c,pa} \cdot l(n,ca,pa) \\ q_c(n,ca,pa,s) &= \left(\frac{1-\lambda}{D_{uniform,i}(n,ca,pa)} + \frac{\lambda \cdot S_b(n,ca,pa,s)}{D_{Pressler,i}(n,ca,pa,s)} \right) \cdot P_{c,pa} \cdot l(n,ca,pa,s) \cdot Q_{c,n} \end{aligned} \qquad \text{(Eq.2-7)}$$

On the one hand, carbon allocation to an internode (at tree age = n, age of internode = ca, PA = pa, distance from trunk base = s) depends on the area of the upper leaves (S_b) and is proportional to the cambium sink factor (P_c) at PA=pa and length of the internode (l). This is the Pressler rule (de Reffye et al. 1997b; Deleuze and Houllier 2002) related to the 'pipe model' (Shinozaki et al. 1964). The total demand under this theory is $D_{Pressler}$. On the other hand, carbon allocation to an internode is carried out uniformly, only according to the sink factor (P_c) and the length of internode (l) (Letort et al. 2008). Such a method takes into account growth limitation due to environmental conditions. The two models are thus mixed by a proportion coefficient λ in [0,1], so that the two effects can be balanced.

2.1.4 Inverse problem (parameter estimation)

Parameter estimation is a necessary process to run a model in a simulation, prediction or control study. The parameters in the GreenLab model are divided into two types, the visible

and the hidden. Visible parameters often have a realistic sense and can be measured or estimated directly from observation, such as environmental factors (e.g. air temperature, solar radiation, and precipitation), allometric parameters (e.g. *e*, leaf specific weight) and geometric attributes and shape. Visible parameters also involve general morphogenesis definitions (i.e. parameters to configure the dual-scale automaton), which are derived from classic plant architecture studies and complementary observations. On the other hand, some parameters in the model are merely theoretically defined and immeasurable, they are hidden parameters. Such parameters are mainly the variables relative to the hypotheses of the source-sink process, which include growth resistance (*r*), the theoretical projective area of plant architecture (S_p), sink factors (P_o , o=b, p, i, f, m, r, c) and the beta distribution parameters (α_o, o=b, p, i, f, m, r) for the sink variation function (Appendix I).

Target file. Solving hidden parameters is the inverse problem, in which the modelling targets are given whereas the parameters need to be estimated. In GreenLab, the targets are placed in a file recording the field measurements in detail. The records include: 1. The GCs (date) of measurement (converted by thermal time); 2. General information about each measurement, such as the number of each organ, organ compartment weight or organ compartment weight according to PA; 3. Organ (i.e. blade, petiole, internode, female fruit and male fruit) weights listed according to the axis of the PA, to the GC of the measurement and to the rank of the phytomer. It should be noted that organ weights are not noted according to the exact position in the architecture, but noted according to the time-relative position along an ideal axis characterized by the PA. For instance, all the phytomers appearing in the last GC on the axis of PA=2 are treated as being at the same position. In this way, the organs with the same type and having the same chronological age (CA) on the same PA of axes are regarded as identical, thus the average weight of identical organs is the actual value noted for the organ weight. An example of a maize target file can be found in Appendix II.

Lastly, a target vector Y is made up of *k* measurements throughout the growth season, and each measurement is the ranged data P, which includes 2 optional and 1 necessary type of observations: 1) Optional - plant level organ compartments (G), 2) Optional - axis level organ compartments (A), and 3) Necessary - organ weight (W):

$$\mathbf{Y} = \left[\mathbf{P}^T{}_1 \cdots \mathbf{P}^T{}_k \right]^T{}_{n\times 1}$$
$$\mathbf{P}_i = \left[\left\{ \mathbf{G}^T{}_o \right\} \left\{ \mathbf{A}^T{}_{o,pa} \right\} \mathbf{W}^T{}_{o,pa,pos} \right]^T{}_{l\times 1} \qquad \text{(Eq.2-8)}$$

where index o is the organ type category, which may be a blade, petiole, internode, female fruit, etc., index pa is the PA category, which depends on the complexity of the plant architecture, and index pos is the category of position from the bottom of the axis. Thus, the plant level organ compartments $\mathbf{G}_o=(g_o)^T_{Oi\times 1}$, the axis level organ compartments $\mathbf{A}_{o,PA}=(a_{o,pa})^T_{(Oi\times PAi)\times 1}$, $\mathbf{W}_{o,pa,pos}=(w_{o,pa,pos})^T_{(Oi\times PAi\times POSi)\times 1}$, and Oi, PAi and POSi are respectively the number of three categories, and $n=\sum_{i=1}^{k} l_i$, $l=Oi+Oi\times PAi+Oi\times PAi\times POSi$.

Iterative generalized least squares estimation. The common fitting method applied for GreenLab is the iterative weighted generalized least square method (IGLSQM, Green 1984, Zhan et al. 2003).

GreenLab is a recursive discrete-time non-linear model; the relationship of the model (**G**) and predictor result vector (**Y**) can be represented as:

$$\mathbf{Y}=\mathbf{G}(\boldsymbol{\theta})+\boldsymbol{\varepsilon} \qquad \text{(Eq.2-9)}$$

where **Y** is an $n\times 1$ vector corresponding to the organ measurement, n equals the number of measured data. **G** is a vector function representative of GreenLab. $\boldsymbol{\theta}$ is a $1\times m$ vector of the unknown parameters, m equals the number of parameters to be solved. $\boldsymbol{\varepsilon}$ is a vector of residual errors.

Thus we can use the least squares criterion:

$$\min\left[\sum_{i=1}^{n}\omega_i(\boldsymbol{\theta})\cdot\left|y_i-g_i(\boldsymbol{\theta})\right|^2\right], \text{ or } \min\left[\left(\mathbf{Y}-\mathbf{G}(\boldsymbol{\theta})\right)'\boldsymbol{\Omega}\left(\mathbf{Y}-\mathbf{G}(\boldsymbol{\theta})\right)\right] \qquad \text{(Eq.2-10)}$$

where ω or $\boldsymbol{\Omega}$ is the value or vector of weight indicating different influences of the observation points, which is inversely proportional to the variance of each data point, i.e. $\boldsymbol{\Omega}=\boldsymbol{\Sigma}^{-1}=1/\sigma^2\mathbf{I}_{(n,n)}$. However, the problem is that the optimum weight cannot be known before the problem is solved, hence it needs to be corrected repeatedly during computation. Moreover, to apply the usual least squares estimator, the G model needs to be transformed into linear form.

The transformation is achieved with the aid of an iterative procedure. For the iterative procedure, a primary estimate of $\boldsymbol{\theta}$, $\boldsymbol{\theta}_1$ and $\boldsymbol{\Sigma}$, $\boldsymbol{\Sigma}_0$ is given. At iteration i with $\boldsymbol{\theta}_i$ and $\boldsymbol{\Sigma}_{i-1}$, we can deduce from Equation 2-9:

$$\begin{aligned}\mathbf{Y}&=\mathbf{G}\left(\boldsymbol{\theta}_i+\left(\boldsymbol{\theta}-\boldsymbol{\theta}_i\right)\right)+\boldsymbol{\varepsilon}\\ \mathbf{Y}&=\mathbf{G}\left(\boldsymbol{\theta}_i\right)+\mathbf{X}_i\left(\boldsymbol{\theta}-\boldsymbol{\theta}_i\right)+\boldsymbol{\varepsilon}\end{aligned} \qquad \text{(Eq.2-11)}$$

where $\boldsymbol{\theta}$ is the solution of parameters, $\mathbf{X}$ is an $n \times m$ matrix made up of partial derivatives of $\mathbf{G}(\boldsymbol{\theta})$. And at coordinate (i,j)

$$\mathbf{X}_{i,j} = \frac{\partial \mathbf{G}_i(\boldsymbol{\theta})}{\partial \boldsymbol{\theta}_j} \qquad \text{(Eq.2-12)}$$

As the model has no analytical expression of $\boldsymbol{\theta}$, the partial derivatives are numerically computed as an approximation:

$$\frac{\partial \mathbf{G}_i(\boldsymbol{\theta})}{\partial \boldsymbol{\theta}_j} \approx \frac{\mathbf{G}_i(\boldsymbol{\theta} + h_k) - \mathbf{G}_i(\theta)}{h_k} \qquad \text{(Eq.2-13)}$$

where, h_k is a finite difference increment.

Thus we can rewrite the $\mathbf{G}$ function as:

$$\mathbf{Z}_i = \mathbf{Y} - \mathbf{G}(\boldsymbol{\theta}_i) = \mathbf{X}_i(\boldsymbol{\theta} - \boldsymbol{\theta}_i) + \boldsymbol{\varepsilon} \qquad \text{(Eq.2-14)}$$

Then a new linear form function can be derived:

$$\mathbf{Z}_i = \mathbf{X}_i \boldsymbol{\beta}_i + \boldsymbol{\varepsilon}$$

where $\boldsymbol{\beta}_i = (\boldsymbol{\theta} - \boldsymbol{\theta}_i)$ is the vector of the distance from the current estimate parameter to the true solution.

Consequently, the estimation of $\boldsymbol{\theta}_{i+1}$ is derived from:

$$\begin{aligned} \boldsymbol{\beta}_i &= \left(\mathbf{X}_i' \boldsymbol{\Sigma}_{i-1} \mathbf{X}_i\right)^{-1} \mathbf{X}_i' \boldsymbol{\Sigma}_{i-1} \mathbf{Z}_i \\ \boldsymbol{\theta}_{i+1} &= \boldsymbol{\beta}_i + \boldsymbol{\theta}_i \end{aligned} \qquad \text{(Eq.2-15)}$$

And $\boldsymbol{\Sigma}_i$ can be computed too. The procedure works until the estimation of $\boldsymbol{\Sigma}$ becomes stable.

2.2 Development of GL5

2.2.1 GreenLab software

Different software have been used in the development of GreenLab theoretical studies over the last ten years.

Cornerfit. Cornerfit (Zhan et al. 2002; Yan et al. 2004) is designed to compute biomass acquisition and partitioning for simple plants that have a single stem with determinate growth, such as maize, sunflower, tomato. The name “Cornerfit” is taken from the name of this type of architectural model. The major contribution of the software has been to solve the inverse problem of computing the source and sink parameters of real plants from the data collected from their architecture using IGLSQM (see section 2.1.4).

GreenScilab. GreenScilab (http://liama.ia.ac.cn/greenscilab, Kang et al. 2006) is for more generalized use built on the basis of Cornerfit. Twenty-three classic architectural models are available in this software open to all plants. Moreover, stochastic developments in architecture caused by meristem behaviour (GL2) are taken into account. Substructure factorization (Yan et al. 2002; Kang et al. 2004; Cournède et al. 2006) is used to handle architectural development and to speed up tree simulation. The GU concept has been integrated without temporal consideration.

For deterministically structured plants, GreenScilab provides both simulation and computation (i.e. inverse method), whereas for stochastically structured plants, it provides an accurate description of architectural development.

DigiPlant. Digiplant software was developed by the Laboratory of Applied Mathematics at the Ecole Centrale in Paris (Cournède et al. 2006). It is dedicated to interactions between plant growth and architectural development (GL3). Simulation and the inverse method of deterministic plants are available in Digiplant. New releases with GL2 and GL5 are in progress.

Qing Yuan. Qing Yuan (Hu et al. 2003) software is an extension of GreenScilab and also developed at LIAMA (Laboratoire franco-chinios d'Informatique, d'Automatique et de Mathematique Appliquees). The complex behaviours of meristems including seasonal pauses, polycyclism (i.e. GL5), are implemented. It can simulate the effect of the local environment on tree architecture and the results of pruning. The inverse method is to be developed for agronomic applications.

GLOUPS. GLOUPS was initiated by Philippe de Reffye, the creator of GreenLab, since 2009. In GLOUPS, both the spatial attributes and the temporal information of each phytomer are explicitly described (GL5), which promises a more powerful means for plant development and growth studies. From the outset, implementation has been geared towards generalized plants (i.e. herbaceous plants, shrubs and trees), and aims to run all previous versions of GreenLab (GL1-GL4). It should be available for end-users in 2012. The software mainly focuses on solving the source and sink parameters for plants with complex growth and development.

During studies for this thesis, I also tried to develop my GL5 software in JAVA, in order to have a flexible environment to extend the possible interface for applications. The implementation has greatly benefited from Xplo, which is a well managed platform at the

AMAP laboratory open for plant architectural studies. My development of GL5 is based on it. In accordance with the requirements of this thesis, growth simulation and reverse computation of plants with a deterministic architecture have been implemented in this software, which has been used to study maize and black pine. However, development ambitions are to continue until GL2, GL3, or even GL4 have been integrated into the implementation with the phyllochron time scale (GL5).

2.2.2 Xplo platform

Xplo (http://amap-dev.cirad.fr/projects/xplo/wiki) is a free open-source software under LGPL license, intended to provide a user-friendly interface for editing, visualizing, exploring and simulating plant architecture. Sebastien Griffon has been developing it since 2008, supported by UMR AMAP. It has been built to be extendable (Fig.2-9), inheriting the Capsis methodology. In this way, various tools can be plugged in flexibly, independent plant models can be integrated as modules too, so that modellers can take advantage of functions in this platform for hypothesis testing.

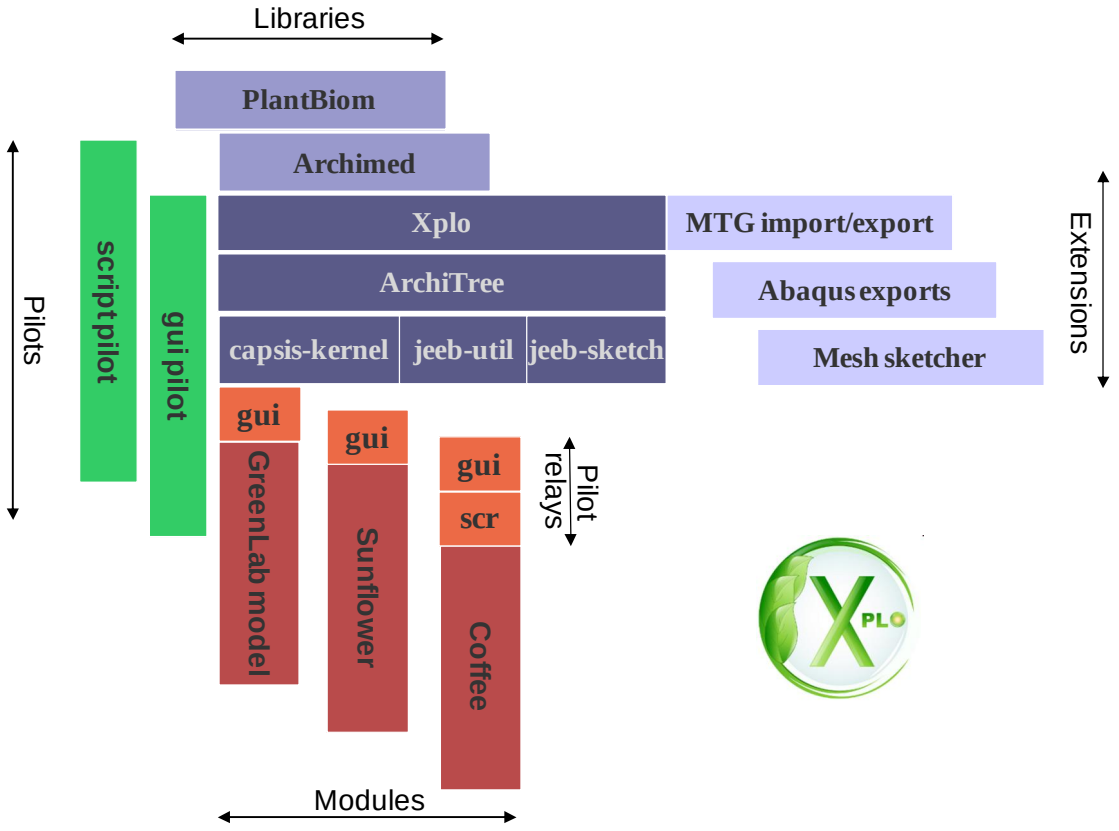

Fig.2- 9 Extensive framework of Xplo (S. Griffon, refers to Xplo CAQ, April 2011, http://amap-dev.cirad.fr/attachments/729/Xplo_CAQ_050411.pdf)

Xplo supports various interactions (Fig.2-10), including topological structure edition (i.e. organ insertion/deletion), geometric manipulation (i.e. 3D selection, edition and rotation) and dynamic design (through time line and scenarios). Scenario computation can be launched not only by the modification of model parameters, but also by operations on 3D architecture (e.g. pruning). In addition to multi-language user interface, a script mode is also available (i.e. Groovy/Python) for interactive operation.

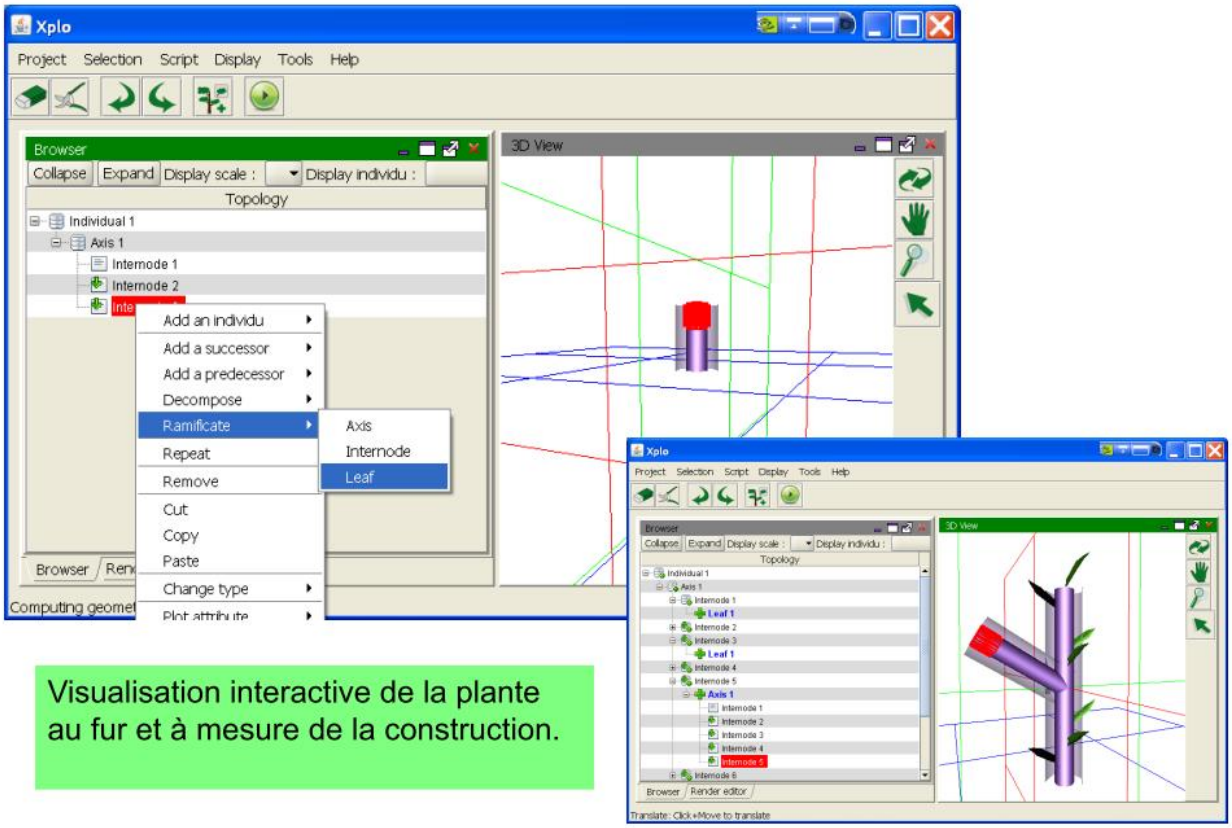

Fig.2- 10 Screenshots of Xplo (S. Griffon, refers to Xplo CAQ, April 2011, http://amap-dev.cirad.fr/attachments/729/Xplo_CAQ_050411.pdf). The top-left demonstrates adding a leaf from the apex internode. The bottom-right demonstrates the top internode of a branch being selected.

Multi-scale tree graph and Xplo data structure. Multi-scale tree graph (MTG) is a methodology specially designed to represent topological structures, proposed by Godin and Caraglio (1998). Depending on different objectives or points of view, users select different scales to analysis or describe a plant. For this reason, a multi-scale design is required for flexible adaptation. In this method, each component has a scale attribute. Components on a relatively low scale can be compositions of components on a higher scale (i.e. composition). Components on the same scale and their connections (i.e. succession or branching) represent one scale of the plant (Fig.2- 11, from Godin and Caraglio 1998).

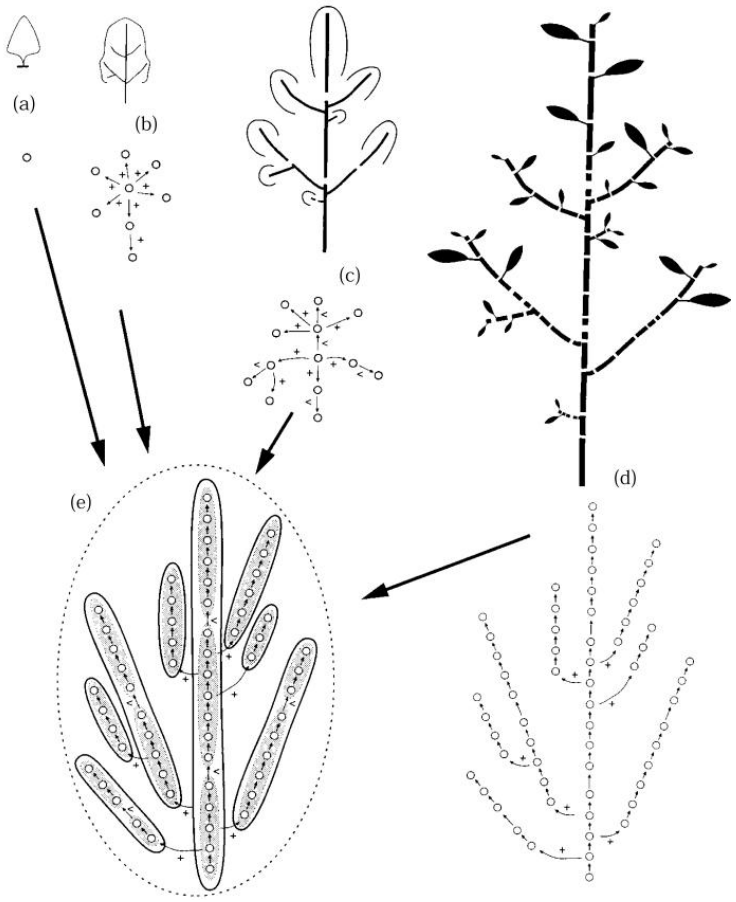

Fig.2-11 Different scales of a tree and their topological representation. a) Tree scale, b) Axis scale, c) GU scale, d) Phytomer scale. e) MTG representation of the Tree. The dotted circle corresponds to the tree scale, smaller solid circles and their connections indicate the axis scale, shaded circles and their connections indicate the GU scale, and small rings and their connections indicate the phytomer scale. "+": insertion; "<": succession (Godin and Caraglio 1998).

In Xplo, ArchiTree is designed to deal with plant architectural data, which is fully compatible with the data structure of MTGs. ArchiNodes as a composition of an ArchiTree are identified by type and scale. They memorize topological structure by recoding the spatial relationships including branching, composition and succession. Node attributions, such as weight, length, width, geometry or user-defined properties can be attached to ArchiNodes. In addition, these attributions can be extracted in tables or visualized in plots. With topological structures and geometric attributions, integrated plant geometry builders take charge of computing 3D plant mockups for rendering.

The Xplo platform has been used in several plant architecture studies, such as sunflower (Rey et al. 2008) and fir tree (Taugourdeau et al. 2010).

2.2.3 Requirements of GL5

Apart from a greater precision in terms of time scale, the new version of GreenLab shares most of the principles with the past versions. The main requirements include:

1) A user interface for plant growth configuration (i.e. to build, import or edit parameter files, details in Appendix I) and for result visualization, which already has a foundation in Xplo.
2) An architecture computation module, which builds plant architecture development according to the dual scale automaton setting. It should be executed independently if possible, so that unnecessary complexity arising from mixed processing with recursive growth functions can be avoided.
3) A recursive procedure for plant growth computation, which commonly includes initiation of new organs (i.e. organogenesis), carbon partitioning from the previous biomass pool, and new biomass production. In order to ensure high efficiency, fast access to the necessary information of expanding or functioning organs is necessary. For example, for biomass production, the number of identical organs is crucial information and an effective method should be applied, such as structural factorization (Yan et al. 2002; Cournède et al. 2006).
4) Independent computation of allometry and geometry, if the result is solely useful for visualization, which can largely reduce the calculation burden.
5) Reverse computation to calibrate parameters with field measurements.

In line with the requirements of this thesis, only computations for deterministic architecture were carried out.

2.2.4 Framework under Xplo

GL5 is independently developed in a project, by way of a module (See Fig.2-9) embedded in Xplo, called “GL5”. In functional-structural plant models, a common difficulty is the inevitable organ level interaction between architecture and function. In fact, Xplo has good supports for this.

ArchiTree and ArchiNode handle scaled plant architectures, and provide interfaces for locating, tracing and editing the composing nodes, whereby the plant architecture is easy to store or consult. To take advantage of this feature, with a view to implementing GL5, I designed a framework as demonstrated in Fig.2-12. GLArchiTree and GLArchiNode classes

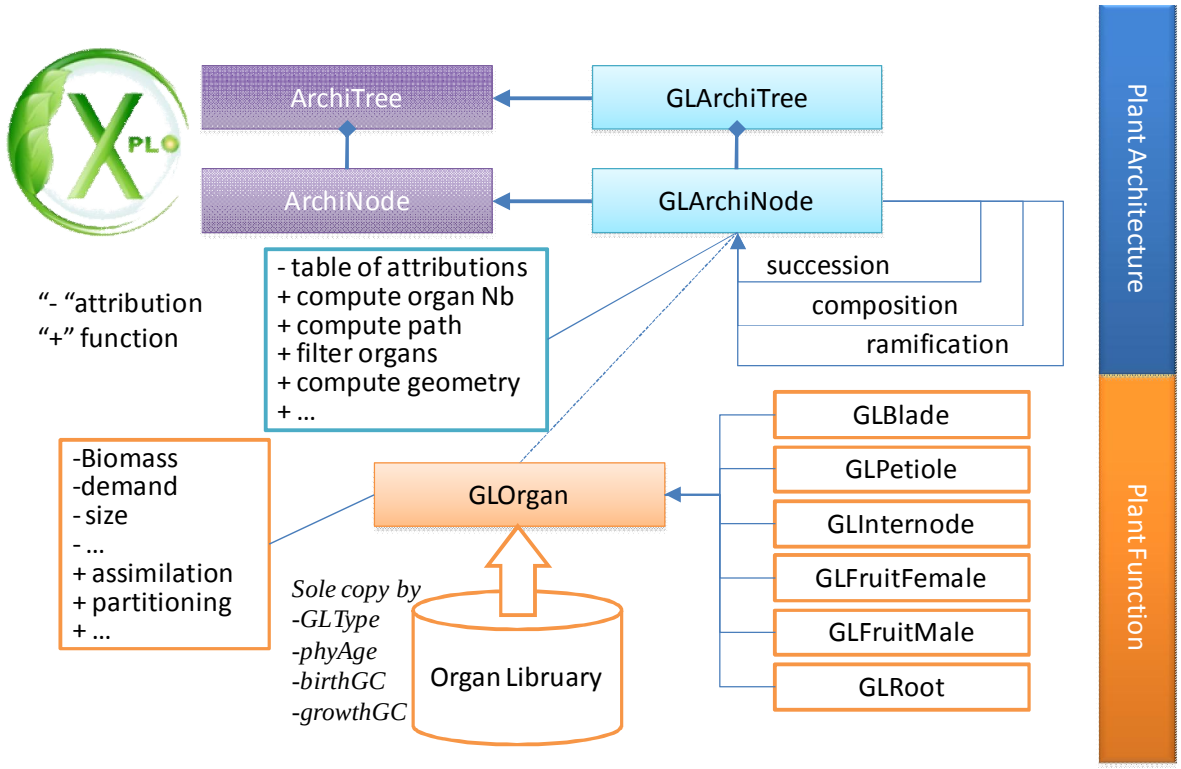

Fig.2-12 Framework to develop GreenLab on Xplo, taking advantage of the data structure of ArchiTree and ArchiNode in Xplo, GLArchiTree and GLArchiNode inherit their ability to manage plant architecture. GLOrgan, which is the organ instance, takes charge of function computation. And GLOrgan and GLArchiNode refer to each other by pointers.

are created by inheriting from ArchiTree and ArchiNode respectively, so that they inherit their data structure. An object from GLArchiTree is constructed by objects from GLArchiNode, which connect with each other through the relationship of succession, composition or ramification. They are specific to GL5 and also manage additional attributes and functions. Another aspect is for functions. Since organs of the same type, on axes of the same PA, with the same age and the same duration of expansion are regarded as identical and perform the same function, unique organs are in fact a subset of whole organs. Or, in other words, if organ functions are executed according to plant architecture, it would be a waste of computing resources in repeated computations for identical organs. I therefore decided to extract and position organ functions independently. A group of new classes was created to encapsulate organ functions, and they are referred to by pointers from GLArchiNode. GLOrgan is an abstract class used to declare common attributions and functions of all organs, and classes GLBlade, GLPetiole, GLInternode, GLFemaleFruit, GLMaleFruit and GLRoot inherited from it manage functions specific to each type of organ. For instance, each type of organ has a specific method for computing size depending on their geometric shape definition. The GLInternode function contains pith and cambium. All the organs have just one copy

stored in a library (organLibrary), and for high consulting efficiency, they are saved with the key attributes of the organ type (GLType), physiological age (phyAge), appearance date (birthGC) and start of growth date (growthGC). This method is actually a substitution of substructural factorization (Yan et al. 2002; Cournède et al. 2006), which has high efficiency not arising from structure computation, but benefits from information management. Taking an estimation of the number of organ as an example, since links will be established between GLArchiNode and a unique organ during the instantiation of a tree, it is convenient to use an attribute in GLOrgan to note the repetition of the unique organ, which takes no time. However this advantage is not universal, but depends on using this software. To sum up, organ level functions can be carried out quickly according to the unique copy of identical organs, with no more need to traverse the plant structure.

2.2.5 Implementation with classes

Data and functions are organized with objects, which are defined by classes. The design and implementation of classes is such that they can be reused with existing programs, extended to new requirements, their code maintained according to object-oriented programming (Jacobson et al. 1992). The class diagram (Booch et al. 1998) in Fig.2-13 demonstrates the relationships of kernel classes in “GL5”.

GLPlantAgent is a pivotal class, which takes charge of calling other classes to carry out plant growth computation. Inverse calculation for unknown parameters is managed by the GLFittings class and its subclasses, which work with the aid of GLPlantAgent too.

Input. The GLSettingsAuto class (Fig.2-13) manages general model configuration. We can set environmental data (EType), define the automaton and other diverse parameters (e.g. sink factors, beta function, expansion duration, allometric variables, geometric attributes) for organs (i.e. leaf, internode, fruit and root), which also includes the fitting configuration. In order to be flexible, specific settings or additional data are also taken into account; the GLAppSpecific class is designed for that.

For a new specific setting, it is enough merely to create a new class extended from GLAppSpecific to deal with the specific settings. As in Fig.2-14, four classes are inherited from GLAppSpcific to deal with specific inputs, including GLPiloteMaize and GLBlackPine, which are respectively for two model applications to be introduced later. In GLPiloteMaize, attributes APAR and RUE are used to load photosynthetically active radiation and radiation use efficiency as specific environmental data, GerminationDate takes charge of computing the

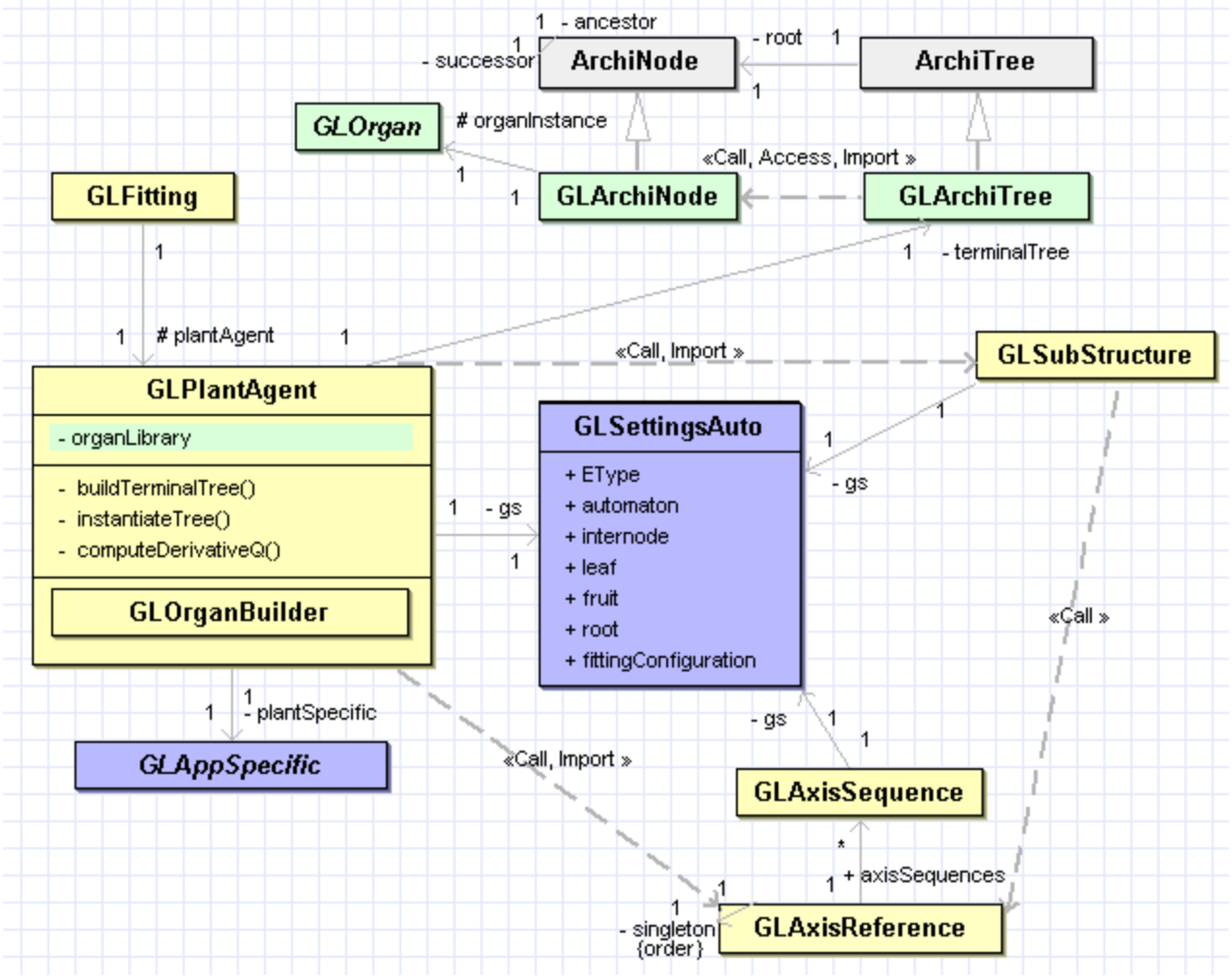

Fig.2-13 Diagram of kernel classes in "GL5", yellow classes, mainly for function, green classes, mainly for data management, blue classes for input, grey classes for heritable classes outside the GL5 module. GLPlantAgent is a pivotal class, which handles the growth computation process. GLPlantAgent also helps GLFitting with inverse calculation.

distribution of the germination date for the maize population by combining with the output from a crop model, PILOTE. In GLBlackPine, simulated geometric data for Black Pine need to be inputted from the forest model PNN, and to have further processes. Consequently, the corresponding storage arrays and methods are prepared. The GLSettingsAuto interface is used to assign specific settings files and handler selection.

Architecture computation and storage. In 2.2.3, the basic design for architectural data management has been introduced, inheriting the existing data structure from Xplo. In GL5, a significant procedure for model simulation is to calculate the architecture according to the automaton and other parameters. It takes place in two steps (Fig.2-15). The first step is the reference axis pre-computation administered by GLAxisReference. Axes with the same PA

share the same development sequence, which is an assumption of the model. Consequently, it should compute an axis sequence for each PA. The length of the development sequence is determined by the maximum age of the plants (maxCUNb). If it is a perennial plant (perennial=True), features of the annual shoot will be taken into account. If it is a temperate plant (temperatureMode=True), the computing unit in one year (cuInYear) will be considered to calculate the axis development resting time in one year.

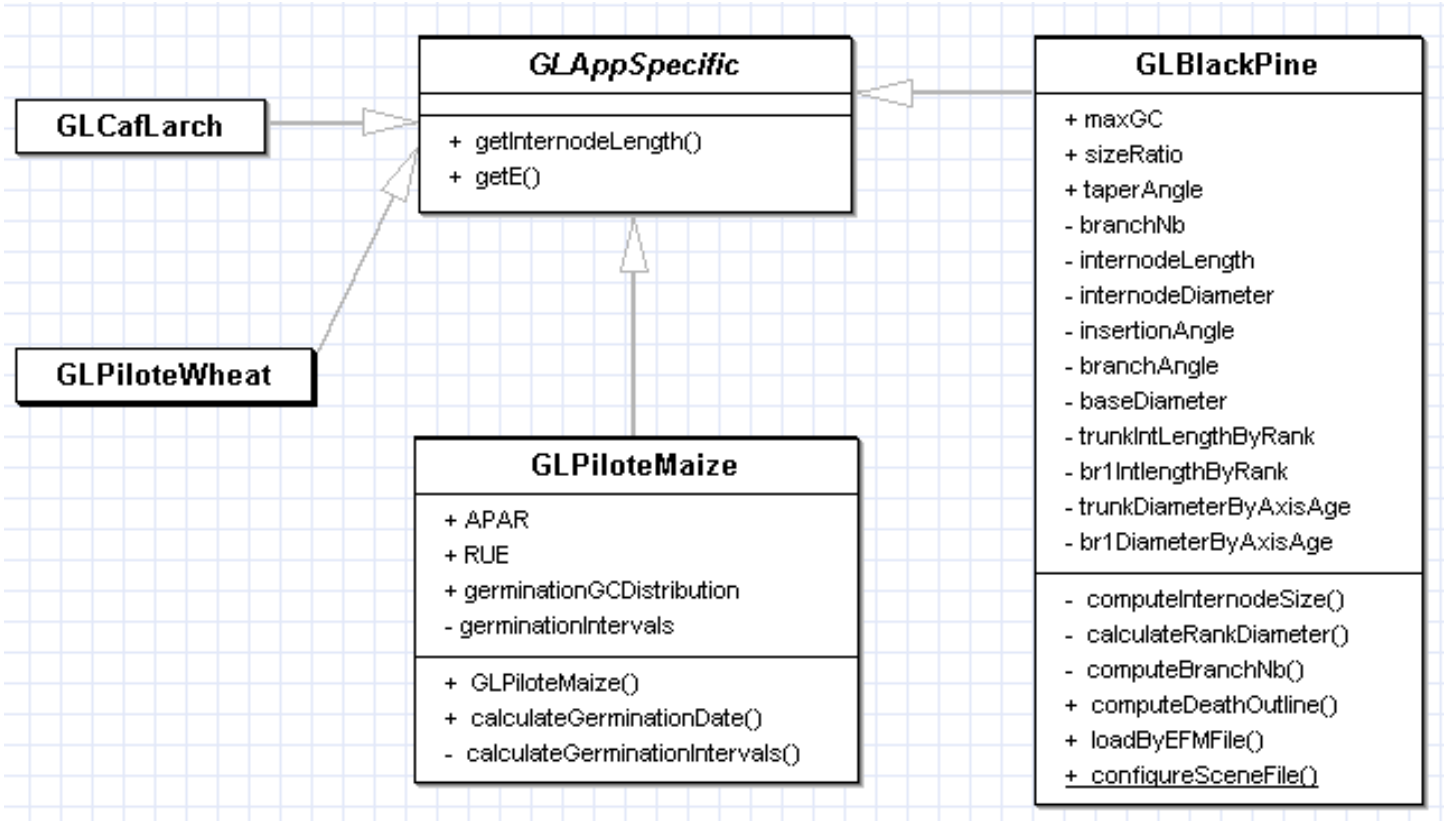

Fig.2-14 Specific input is extendable in "GL5", managed by the GLAppSpecific class and its subclasses.

If the inflorescences of the plant have a specific mode, the specific pattern of the inflorescence will be processed by setting inflorescenceMode=True and further configuration. Essentially, the sequence of phytomers along an axis is determined by the automaton settings. According to the above parameters, GLAxisSequence computes the development sequence of the axis by the computeDevelopmentSequence method. Lastly, the result is saved in four arrays. Array developmentSequence stores the sequence of phytomer status (i.e. physiological age of axillary buds). Array developmentBranchNumber stores the number of axillary buds that corresponds to the number of branches. Array developmentMixedBudNumber stores the number of mixed buds (i.e. the short shoots inserted on the same rank of the long vegetative shoot). Array developmentOrganNumber stores the sequences of the number of organs by type. These data stored in the objects of GLAxisSequence are finally saved in

GLAxisReference for reference to GLSubStructure for further architectural computation.

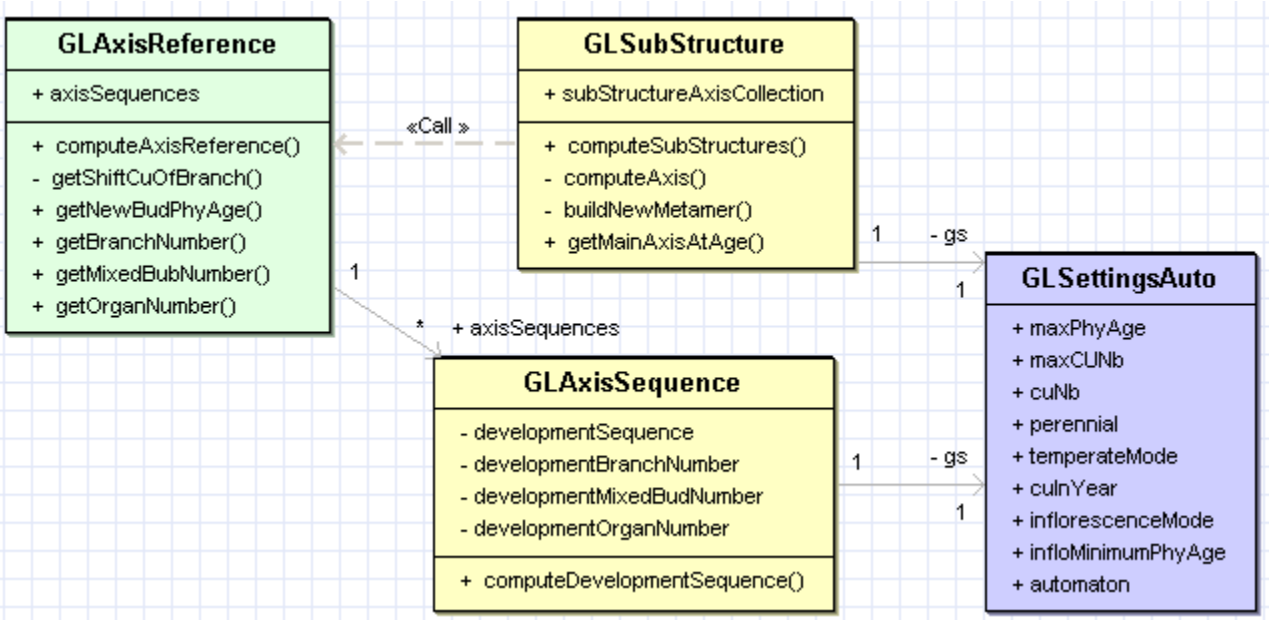

Fig.2-15 Classes relevant to architecture computation, for which the definition comes from GLSettingAuto. GLAxisReference manages development sequence computation for each axis of the different PAs, the real procedure is carried out by GLAxisSequence. With the pre-computed reference axis, GLSubStructure then computes substructures (i.e. axes of different PAs and different ages), whereby the evolution of the main axis can be derived.

The second step is that the GLSubStructure class computes main axis development. In fact, what it calculates is substructures through the computeSubStructures function, in which substructures (i.e. axes of different PAs at different ages) are computed from high PA to PA=1 (main axis), and computed according to the age, increasing up to the maximum age. An advantage of this order is that the branching axis attached to the substructure computed later can always be found from the previously computed substructures, which have been stored in a collection (subStructureAxisCollection). After this computation, development of the main axis is derived from it. Substructures are saved as collections of GLArchiNodes, which not only store the architecture structure, but also attach information about the organ type, PA and age, and growth duration. It should be noted that the axis development resting time is also recorded in substructures, where an “emptyMetamers” is built.

For plant simulation, GLPlantAgent calls GLAxisReference to compute development sequences first, then it calls GLSubStructure to carry out computation of the substructures. The final full architecture of the main axis, which is the aerial part of the plant, is then produced. To build a tree, this main axis is added to the empty GLArchiTree and attached to a scaled frame of a plant. Importantly, at that moment, information relative to age and growth

duration attached to nodes is converted into the birth date and start of growth date in reference to the plant age. At this stage, a tree is finally built and it is saved in GLPlantAgent. This tree is named terminalTree, because it is the final architecture of the plant, and according to the time information attached to the nodes, it also gives a clue as to how such a final architecture developed.

Growth computation. In order to compute the plant growth source-sink process, the architecture needs to be attached with real organs. An "instantiateTree" method in GLPlantAgent is used to do this. In fact, each node needs the basic information of the organ to be attached with it, namely the type, PA, birth date and the start of growth date, so that it knows the target organ. In order to have a unique copy of identical organs, during the program dealing with nodes one by one with mapping, it first checks in the organLibrary to see if the target organ exists already; if it does, it will use a pointer referring to it directly, otherwise it creates a new one and saves it into organLibrary thereafter.

Attachment with organs is necessary because GLOrgan and its subclasses encapsulate the attributes and functions relevant to growth, which, when called by GLPlantAgent, can execute the functions for plant growth. Let us take a look in the three key procedures in the growth process defined in GreenLab how the organ classes serve for computation (refer to Fig.2-16).

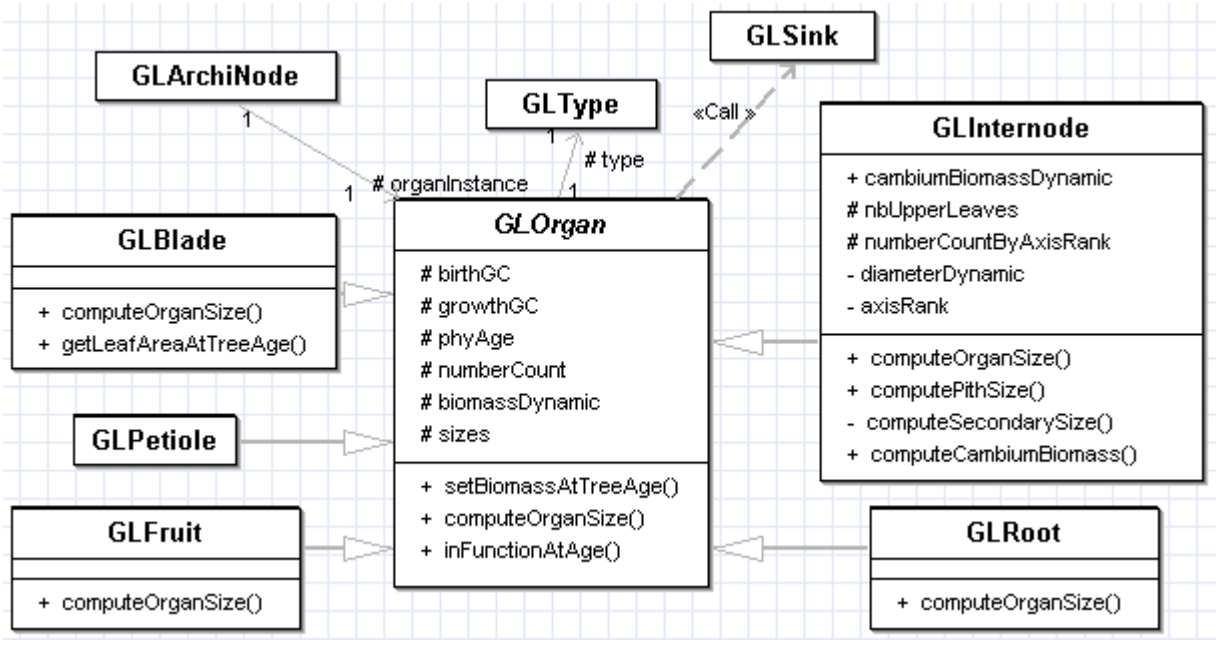

Fig.2-16 Attributes and functions of organ classes, which is the basis of plant growth computation

First, there is biomass partitioning. The initial state of a plant is a seed, which conserves the initial biomass, followed by the first architecture development and the first expansion of organs. Biomass allocation to organs depends on the relative strength of organ demand, which is quantified by a sink factor and a variation curve characterized by a beta distribution function (see *Biomass partitioning* in 2.1.3). As sink computation is independent from other procedures, a GLSink class is created to take charge of it. In fact, sink strength computation requires the organ type, PA, expansion duration, and age of the organ (see *Biomass partitioning* in 2.1.3). Of these, the expansion duration is known from the GLSettingsAuto configuration, whereas the other parameters are the organ information, which is integrated with the organ object. Consequently, organs themselves are able to visit GLSink to acquire sink strengths. A getSinkAtTreeAge method is created in GLOrgan for this access, and it is inherited by all its subclasses too. With this, computation of the relative sink strength of organs for GLPlantAgent is relatively facilitated. By visiting organs in organLibrary and with knowledge of their number, the computation of relative sink strengths is simply additions and divisions. The allocated biomass is assigned to the organ at the same time, which is noted by a biomassDynamics member array of organ classes.

The second procedure is assimilative calculation, which crucially depends on total green leaf areas solely related to the organ blade. However, GLBlade has corresponding supports for it. This calculation implies two requirements for blades: one is that the blade should be functional (green), the other is the blade area. The blade area can be converted to the allometric relationship with accumulated biomass, which was saved in a member array with organs. The allometric variable is the specific leaf weight (e) defined in GLSettingsAuto. The functional state of the blade should be judged according to the birth date and its function duration, which are also configured in GLSettingsAuto. Such a function is built in GLOrgan, inherited by GLBlade directly. As a collection of blades can be accessed directly from organLibrary by mapping with the organ type, the total green leaf areas can be derived easily. Consequently, assimilation can be computed according to the production function (see *Biomass acquisition* in 2.1.3).

The third procedure is allometry and geometry computation, which is mainly used for 3D visualization. For this procedure, the real executor is still organs. As different organs have specific allometric definitions and quite different geometric characteristics, the method used is size computation (computeOrganSize), which is defined in GLOrgan and re-implemented respectively in the subclasses (i.e. GLBlade, GLPetiole, GLInternode, GLFruit and GLRoot).

The result of size computation is converted into two variables: the length and the width, and saved in member array “sizes”. For leaves, length and width describe the longitudinal and horizontal scales of the surface; for internodes, they describe the length and diameter; for fruits, as their default form is spherical, length is equal to width, and they describe the scale of the volume. Their specific allometric and geometric parameters have been taken into account in GLSettingsAuto correspondingly. Uniform geometric symbols are practical for visualization and are usually appointed for each organ type, and their scales are then the computed sizes.

It should be mentioned that blade area is used as a function variable for internode length and is also a function variable for secondary computation (described in *Secondary stem growth computation* in 2.1.3). As one determinant of cambium growth is the number of upper leaves, cambium biomass depends on its location along the axis. Consequently, if there is secondary growth (i.e. in GLSettingsAuto withCambium=true), in the organ internode, which is attached to the architecture, the position of the internode on the axis (axisRank), the number count of the same axisRank (numberCountByAxisRank) and the dynamic number of upper leaves over time are also noted in arrays. In biomass partitioning, the pith of the internode follows ordinary computation, whereas cambium is computed according to axisRank and the corresponding number of upper leaves (nbUpperLeaves). Internode size computation thus consists of pith (computePithSize) and cambium (computeSecondarySize). The length of the internode is determined by the pith, but the diameter is determined by both pith and cambium. Thus, diameter dynamics are saved alone in the diameterDynamic array.

Inverse computation. Access to inverse computation is via the GLFitting class; specific fittings (Fitting method) are implemented in its subclasses (Fig.2-17) including the classic iterative generalized least squares fitter (GLGLSFitting) and a heuristic particle swarm optimizer (GLPSO). In this way, new fitters are extendable when they are needed.

GLFitting defines the basic variables and methods for fitting, such as the matrix of parameters (matrixPara), matrix of target data (targetY), matrix of simulated data (simulatedY), to load data from a target file (getData), to compute fitting criteria (computeVariance), and to compute model simulations (computeSimulatedData). In subclasses they manage themselves, with the additional variables and methods serving for their computation. Three exterior classes are associated as an aid for peripheral functions.

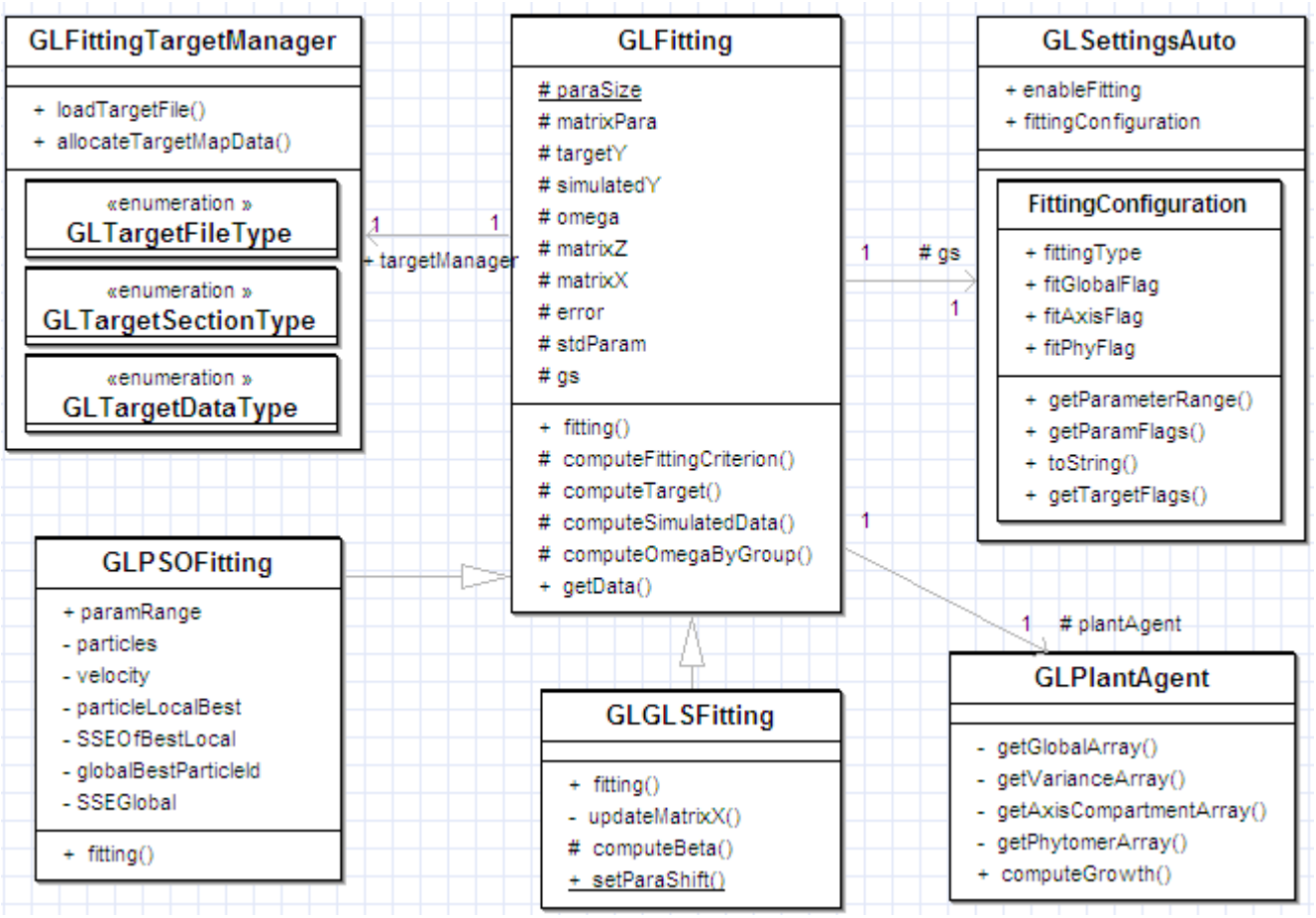

Fig.2-17 Classes for fitting: specific methods are applied in the GLFitting subclasses. GLFittingTargetManager is designed to read target files and load valid data to arrays for fitting classes. Through GLSettingsAuto, the parameter for fitting is configured, including the selection of parameters to be fitted, the target file and other settings for fitters. GLPlantAgent is used to execute growth computation and return the result of modelling to the fitting classes used for inverse computation. These three classes are associated in GLFitting, and such linkages are inherited by its subclasses.

GLSettingsAuto undertakes parameter configuration with an inner class, FittingConfigure. The configuration contains the selection of parameters to be solved, assignation of a target file, selection of target data composition (i.e. phytomers, compartment, variance of compartment) and settings for specific fitters. GLPlantAgent is associated with GLFitting to simulate the model (computeGrowth) and provide the simulated data (by the getGlobalArray, getAixsCompartementArray, getPhytomerArray and getVarianceArray methods), which are referred by fitters. GLFittingTargetManager is specially defined to manage the data composition of the target, which is defined in GLSettingsAuto. It loads data from the target file (by loadTargetFile), and provides fitters for the organized data by mapping (allocateTargetMapData). The composition information is also referred to to build the corresponding simulated data.

2.2.6 Demonstration of GLOUPS-JAVA

Embedded in XPLO, GLOUPS is launched in Xplo by building the new project of GL5 (Fig.2-18).

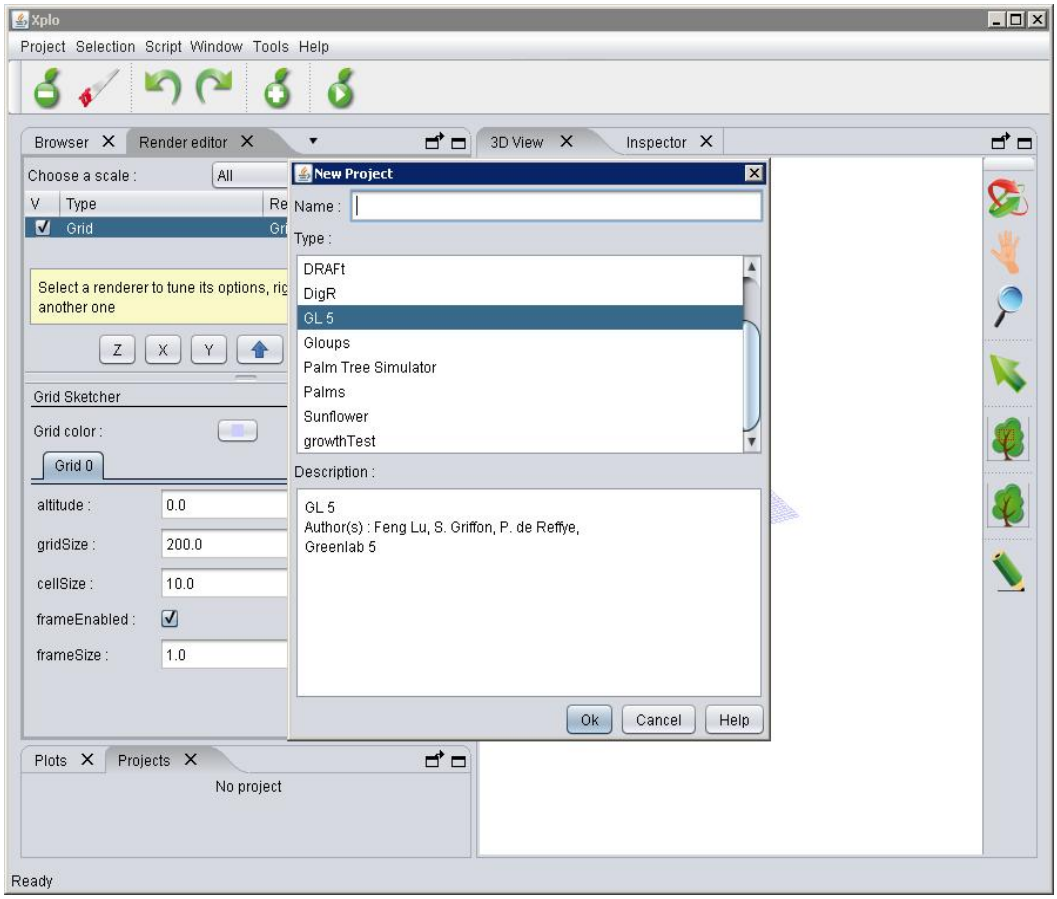

Fig.2-18 Launching GLOUPS from Xplo

User-friendly interface. This embedded relation has effectively inherited the user-friendly interface design from Xplo. Diverse windows take charge of different interactions for modelling execution (Fig.2-19). A “Projects” panel (window a) manages plant development steps by a computing unit. By activating the target step, the architecture and detailed data of the instantiated plant can be accessed. “3D View” (window b) demonstrates the integrated result of the instantiated plant by architecture visualization. The tool bar on the right-hand side provides basic geometric operations (i.e. rotation, transferring and zoom) and selection. On the other side of the user interface, a “Browser” (window c), which is based on the same data set of 3D view, presents details of plant components in an exchangeable and extendable table. Components are organized by tree hierarchies. All the attributes, including component status (i.e. functional, in expansion or not), biomass, age and various geometric variables are convenient to check. In addition, the historical value of attributes can be plotted for a better understanding (“Plots” window e). "Browser" also supports components selection, which is

linked with "3D View". “Render editor” (window d) can be used for further rendering options, such as texture.

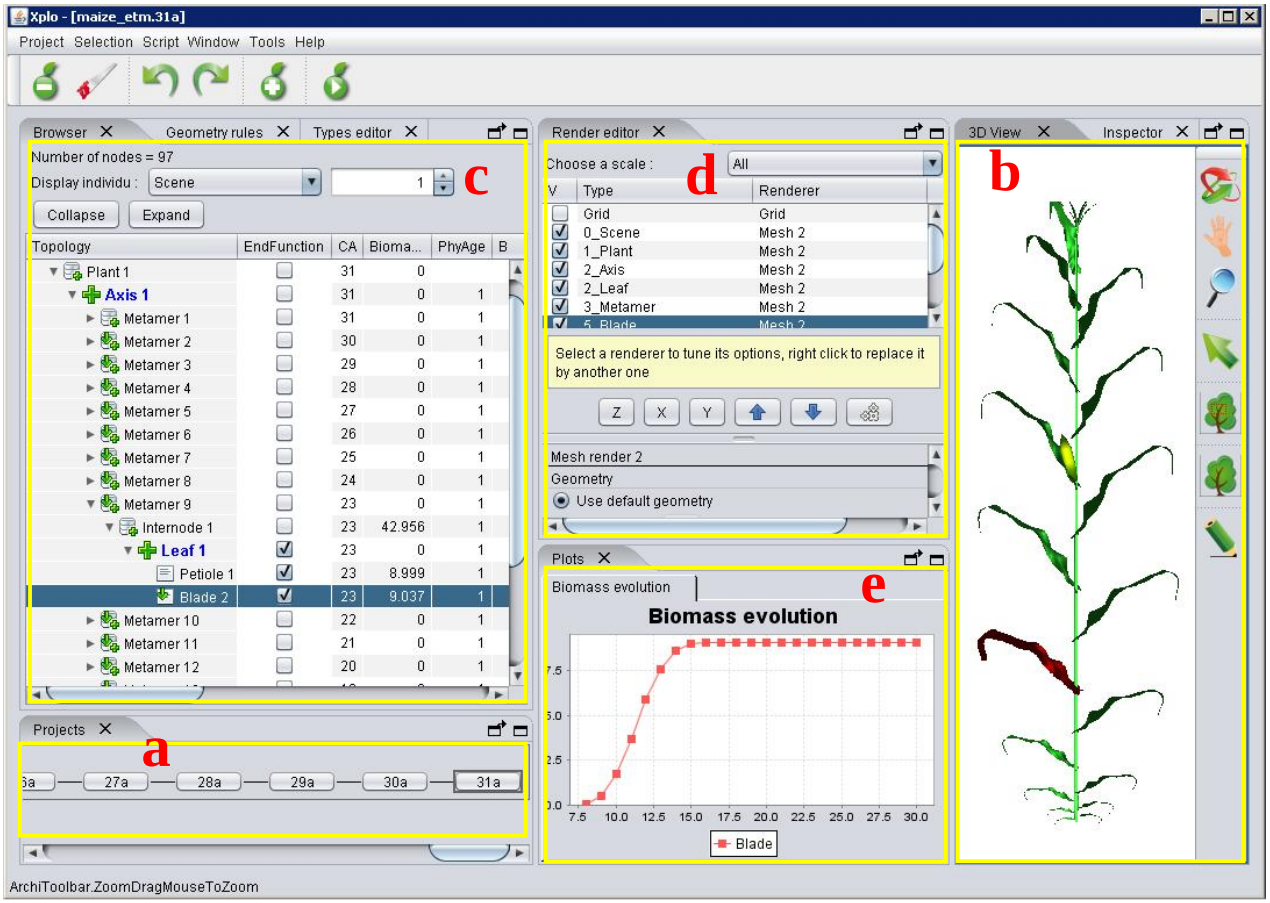

Fig.2-19 GLOUPS user-friendly interface inherited from Xplo. The "Projects" panel (a) manages plant growth steps. "3D view" (b) demonstrates output assembly by visualization. "Browser" (c) provides details in an exchangeable and extendable table, which are organized by topological hierarchies. Historical data for certain attributes can be plotted in the "Plots" window (e). "Render editor" (d) supports further rendering options.

GLOUPS configuration by GLSettingsAuto. On entering GLOUPS, the GLSettingsAuto interface will allow the user to configure plant computation (Fig.2-20 a). The parameters are divided into several groups, such as general (plant level), sink (by organs), automaton, geometry, allometry and fitting.

The settings in the automaton (Fig.2-20 b) are all the details of plant development. “1-Time” notes the important time definition, such as the number of GCs in one year, the resting time between GCs, delay of axis development time, ratio of different growth rates among PAs. “3-Mutation” defines when the axes will have mutation, and to which PA it will transit. “4-Transition” and “5-Vertcille” define phytomer transition and the corresponding branching number, mixed branching. “6-Mask” provides special organ sequence definitions.

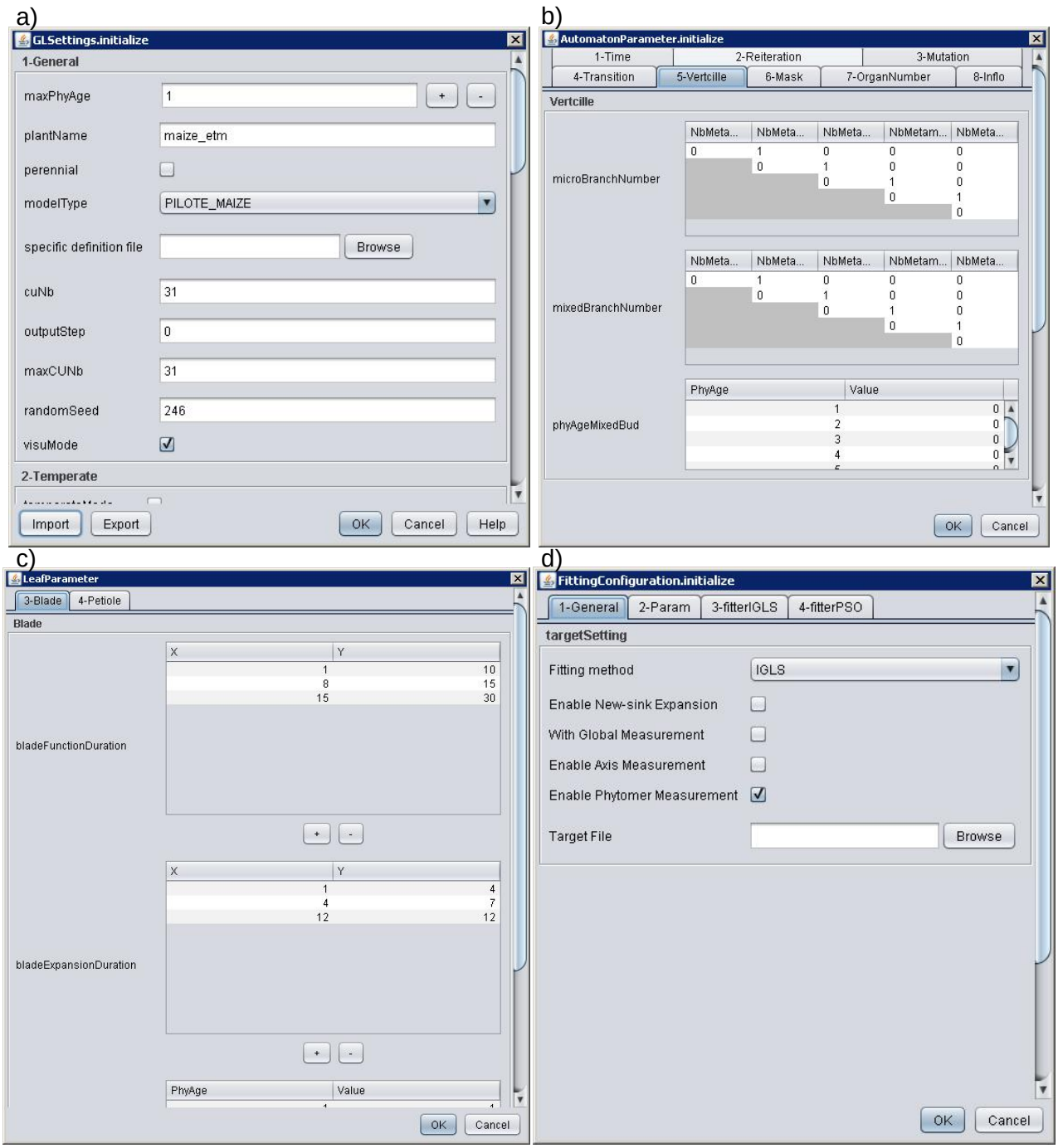

Fig.2-20 Interface of GLSettingsAuto for plant computation configuration. a) main interface b) setting for automaton c) relevant sink setting for organ (blade) d) configuration for reverse computation

"7-OrganNumber" defines the default number of organs in a phytomer. "8-Inflo" defines variables related with signal transduction for inflorescence mode.

Organ level definition (Fig.2-20 c) is mainly about sink variables, such as sink factors over PAs, beta law variables for variation, delay of expansion and the expansion duration according to position. Function duration, which is crucial for leaves, is also defined here.

When reverse computation is needed, it is necessary to configure parameters for fittings (Fig.2-20 d). “1-General” chooses the fitter type, designates the target file and defines target data. The parameters to be fitted are selected in “2-Param”. “3-fitting IGLS” and “4-fitter PSO” respectively configure variables and options for the iterative generalized least squares method and the particle swarm optimizer.

In addition, there are settings for geometry and allometry, but these will not be covered in detail here.

Plant galleries. Before developing GreenLab modelling geared towards universal plants, a smaller version was first developed on kernel functions, but specifically only for plants from Corner’s model (Barthélémy and Caraglio, 2007). At the moment, previous studies by GreenLab on several of Corner’s plants are used to test for this core version, both for simulation and reverse computation. They are sunflower (Fig.2-21 a) and cotton (e) from Zhan et al. (2003) and Li et al. (2009), maize (b) from Guo et al. (2006) and Ma et al. (2008), cucumber (c) from Mathieu et al. (2007), beetroot (d) studied at the “Institut Technique de la Betterave” (Lemaire et al. 2008; de Reffye et al. 2008) and tomato (f) from Dong et al. (2008).

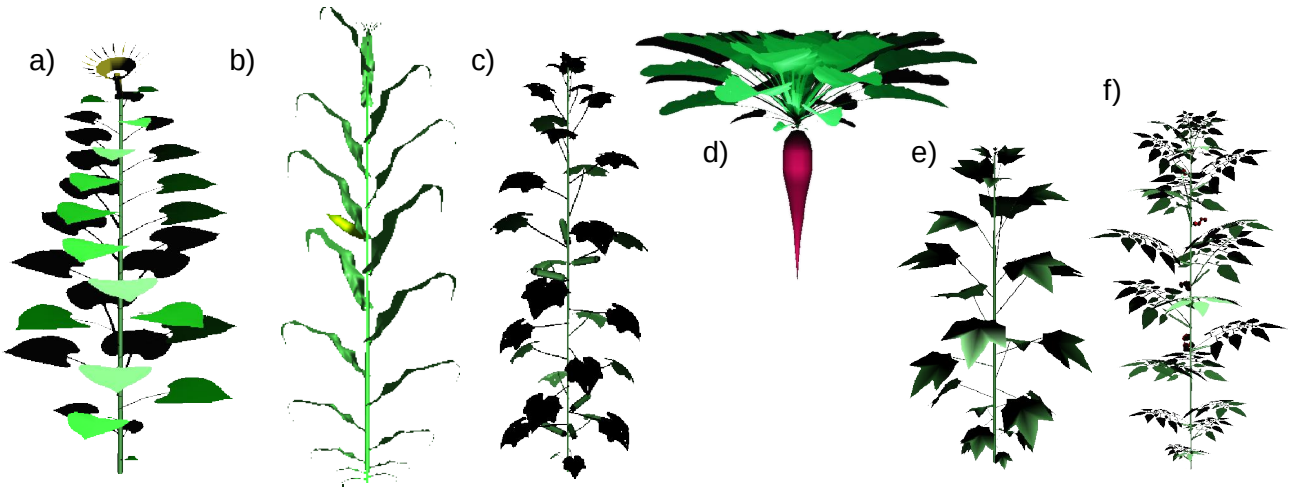

Fig.2-21 Corner’s model plants used in previous studies with GreenLab have been tested in GLOUPS core development; this is the architecture visualization. a) sunflower, b) maize, c) cucumber, d) beetroot, e) cotton, and f) tomato.

After core completion, further efforts were made in the configuration and representation of various plant architectures under the hypothesis of GL5. So far, this part of the work is still limited to the deterministic level, and neither stochastic effects nor feedback from the growth rate on plant architecture have been implemented. However, the newly added representation of explicit morphogenesis resting time has opened up new prospects for

studying and understanding the hidden behaviours behind the complex structure of plants. A virtual example of a temperate tree is given (Fig.2-22). This tree has four orders of branching, corresponding to four PAs, and is monocyclic with acrotonic branching characteristics (i.e. having larger lateral branches at the distal position). The growth duration in one year converted to CU is 11, each year's development for the main axis (PA=1) happens in the first 6 CUs, for 2nd order axes (PA=2) it happens in the first 4 CUs, for the 3rd order axes (PA=3) it happens in the first 2 CUs and in the first CU for the 4th order axes (PA=4). Leaves and short branches of PA=4 (yellow in the figure) have a life-span of 3 years. Up to CU=60, the tree architecture develops as in Fig.2-20 a. However, this visible structure comes from both the active and resting times of architecture development, which are fully visualized in Fig.2-20 b.

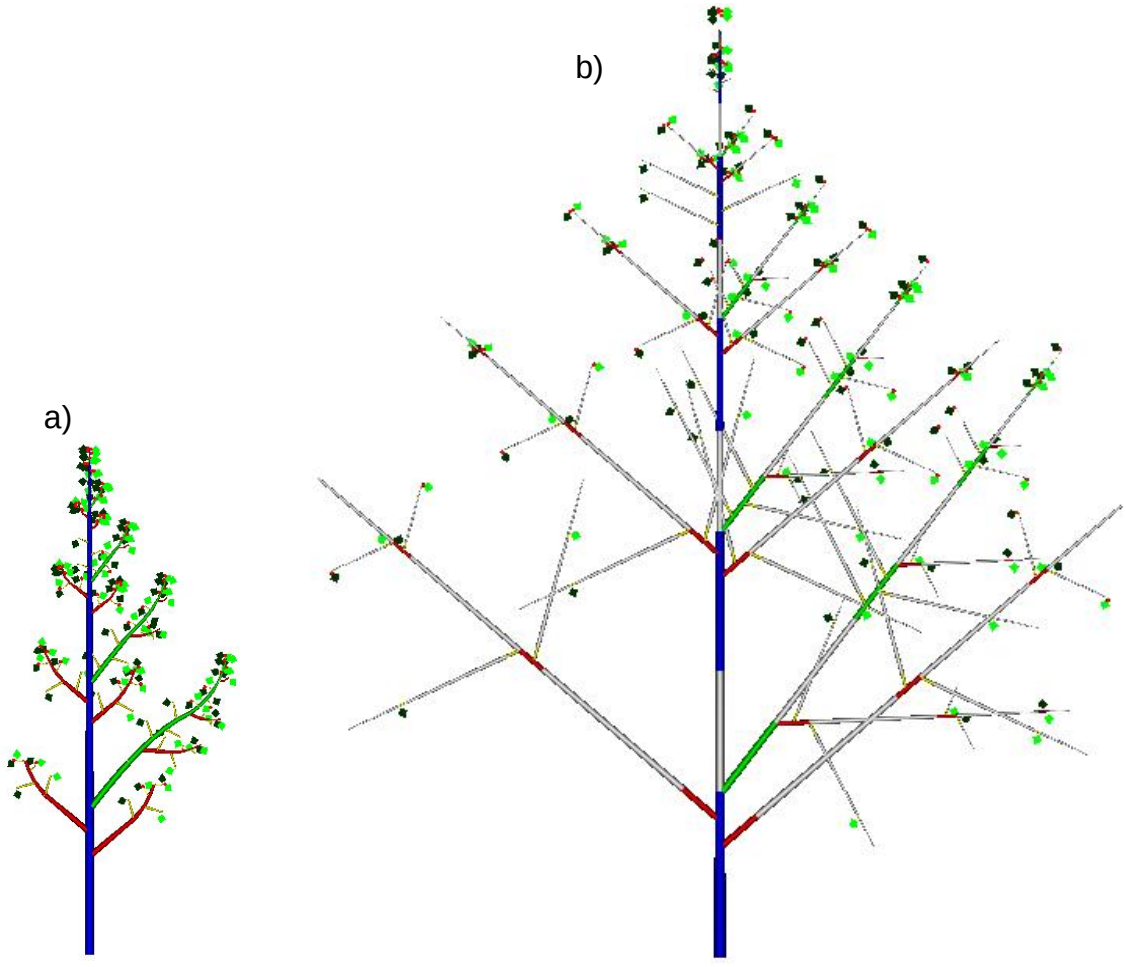

Fig.2-22 A virtual temperate tree visualized according to PAs, blue, PA=1; green, PA=2; red, PA=3; yellow, PA=4, white represents morphogenesis resting time. At CU=60, the tree could be seen as on the left, but the existence of the morphogenesis resting time is a partial cause of this final architecture, and is visualized inside the real architecture on the right.

3. Individual variability study: using maize as an example

3. Individual variability study: using maize as an example

Based on

1) A presentation at the 6th International Workshop on Functional - Structural Plant Models (FSPM10)

Title: Combining a process based model with a functional structural plant model for production partitioning and visualization

Lu Feng[1], Jean-Claude Mailhol[2], Hervé Rey[1], Sébastien Griffon[1], Daniel Auclair[3], Philippe De Reffye[1,4]

[1]CIRAD, UMR AMAP, F-34398, Montpellier, France
[2]Cemagref, UMR G-eau, F-34096, Montpellier, France
[3]INRA, UMR AMAP, F-34398, Montpellier, France
[4]INRIA Saclay Île de Fance, EPI DigiPlante, F-91893, Orsay, France

2) A manuscript submitted for publication in the European Journal of Agronomy

Title: Combining an empirical crop model with a functional structural plant model to account for individual variability

Lu Feng [a], Jean-Claude Mailhol [b], Hervé Rey [a], Sébastien Griffon [a], Daniel Auclair [c] Philippe De Reffye [a]

[a] CIRAD, UMR AMAP, F-34398, Montpellier, France
[b] Irstea, UMR G-eau, F-34096, Montpellier, France
[c] INRA, UMR AMAP, TA A-51/PS2, F-34398, Montpellier cedex 5, France

Combining a process based model with a functional structural plant model for production partitioning and visualization

Lu Feng[1,*], Jean-Claude Mailhol[2], Hervé Rey[1], Sébastien Griffon[1], Daniel Auclair[3] and Philippe De Reffye[1,4]

[1]CIRAD, UMR AMAP, F-34398, Montpellier, France
[2]Cemagref, UMR G-eau, F-34096, Montpellier, France
[3]INRA, UMR AMAP, F-34398, Montpellier, France
[4]INRIA Saclay, EPI DigiPlante, F-34398, Montpellier, France
*Corresponding author, fyafeng@gmail.com

Keywords: Process Based Model, Functional Structural Plant Model, Plant Architecture, Crop Production, Visualization

Introduction

Process Based Models (PBM) are used to compute crop yield, they treat a field as a homogenous medium, total production is computed accurately, but there is little information on individual variability of plants, and number and size of organs. Functional Structural Plant Models (FSPM) simulate individual plant development and growth, they build plant architecture on the basis of biomass production and partitioning according to botanical rules, but generally lack the ability to upscale to the field level to address crop production. In the present study we combined crop biomass production of maize estimated by the PBM PILOTE with biomass partitioning and individual plant architecture generated by the FSPM GreenLab, in order to benefit from the field-level accuracy of the former and from the heterogeneity of individual architecture of the latter.

Model description and comparison

PILOTE (Mailhol et al., 1997) is a model designed for crop yield simulation. GreenLab (Guo et al., 2006) is an FSPM designed for individual plant architectural development and biomass partitioning. Although GreenLab and PILOTE address different scales, they take into account similar processes for biomass computation, based on Beer's Law for light interception (Table 1).

Table 1. Comparison of biomass computation by PILOTE and GreenLab

PILOTE (PBM)	GreenLab (FSPM)
$Q = RUE \cdot \sum_{\text{sowing}}^{\text{harvest}} PAR_{(i)} \cdot \left(1 - e^{-k \cdot LAI_{(i,stress)}}\right)$ (Eq.1)	$q_{(n)} = \frac{RUE_{(n)} \cdot PAR_{(n)} \cdot Sp}{r}\left(1 - \exp\left(-k \cdot \frac{Sa_{(n)}}{Sp}\right)\right)$ (Eq.2)
Q: final total dry matter (t ha^{-1})	q: total biomass of individual plant at GC n (g)
RUE: radiation use efficiency	RUE: radiation use efficiency
PAR: daily photosynthetically active radiation (J m^{-2})	PAR: photosynthetically active radiation at GC n (J m^{-2})
k: extinction factor	k: extinction factor
LAI: daily LAI according to water stress (m^2 m^{-2})	Sa: total area of living leaves (cm^2)
sowing: sowing day of year	Sp: theoretic projection surface (cm^2)
harvest: harvest day of year	r: resistance to water transpiration
i: day i	n: current growth cycle ("GC")

The differences between the two models come from different spatio-temporal scales: PILOTE addresses plant population per unit area, GreenLab addresses individual plants. PILOTE computation is on a daily basis, GreenLab computation is by growth cycle (GC), based on thermal time. LAI in GreenLab is optimized by Sa/Sp ratio for an individual plant: leaf area is estimated from the source-sink balance, and the projection surface Sp is computed by multi-fitting and Eq.2 inversion (Ma et al., 2008). If the field is homogeneous, the LAI and total biomass computed by both models should be identical; on the contrary, if the results are different, it could be explained by field heterogeneity.

3.1 Combining an empirical crop model with a functional structural plant model to account for individual variability: Introduction

Crop yield generally presents individual plant variability, and the higher yields often occur in fields with higher uniformity (Liu et al., 2004a; Muldoon and Daynard, 1981; Tollenaar and Wu, 1999). In addition to variations of the local environmental conditions (soil, sunlight, temperature…), plant uniformity is related to initial conditions in the field. Plants situated at lower local density (Nafziger, 1996; Pommel and Bonhomme, 1998) or emerging earlier grow better (Ford and Hicks, 1992; Liu et al., 2004b; Nafziger et al., 1991), whereas plants grow weaker and may even undergo abortion at higher local density or late emergence, due in particular to the fact that they suffer from more intensive competition (Lauer and Rankin, 2004) and at earlier stages (Tollenaar et al., 2006).

Plant uniformity also responds to resource stress intensity. For instance, plants at high density, low nitrogen or low water supply show significant differences from control experiments (Edmeades and Daynard, 1979; Ipsilandis and Vafias, 2005; Maddonni and Otegui, 2004; Rossini et al., 2011; Sangoi, 2000). As a result, breeding programmes propose to select hybrids with higher tolerance to stress, and/or which show less variability, to achieve higher production (Tollenaar and Wu, 1999).

However, such plant-to-plant variability is poorly accounted for in crop models. This paper is an attempt to combine an empirical crop model that computes crop yield at the stand level with a functional structural plant model (FSPM), which addresses the individual plant level, in order to represent the individual production variability.

The two kinds of models consider different scales, but they are complementary to each other for agronomic purposes. Crop models (Bouman et al., 1996; Marcelis et al., 1998), which simulate plant growth at the field level according to a variable environment, are able to predict yield under different kinds of stress. However, individual plants are generally regarded as identical, and individual variability including plant-to-plant interactions is poorly taken into account (Marcelis et al., 1998). Furthermore, crop models focus mainly on biomass acquisition and have a crude representation of biomass partitioning, often limited to the total above-ground biomass of the plants associated with a harvest index which describes the ratio of "useful" biomass (fruit or grain) used for estimating the yield. Seldom is the below-ground biomass taken into account, or the detail of biomass distribution between different compartments. Hence computation of leaf area index (LAI) or harvest index (HI), which

depend on biomass partitioning (Marcelis et al., 1998; Vos et al., 2007), can lose efficiency when environmental conditions change.

In comparison, FSPMs simulate well individual plant biomass production and partitioning based on plant structure, using more mechanistic rules at the organ level (e.g. source-sink processes) (Marcelis and Heuvelink, 2007; Vos et al., 2007). Organ abortion, which largely determines the number of organs and the subsequent biomass partition (Marcelis et al., 1998), can be well addressed in FSPMs (Wernecke et al., 2007). In addition, the operating level of FSPMs is the individual plant, where population interactions such as competition take place. Nevertheless, despite their better efficiency for internal plant process simulation, FSPMs remain insufficiently adapted to address the stand level. For one thing, the external interactions between a plant and the environment or competitors have seldom been sufficiently addressed. For another, to implement organ-level functions and allocation (e.g. light interception, transport resistance) generally requires heavy computation resources, which could be a technical difficulty to apply FSPMs to field studies. On the other hand, as crop models have generally been submitted to large scale field validation, they are considered as sufficiently accurate for yield computation, and combining relevant features of crop models may provide global prospect to upscale FSPM simulations to the field level.

In this work, we have studied these two levels with two models which are based on similar processes for light interception and biomass computation. The empirical crop model PILOTE (Mailhol et al., 1997; Khaledian et al., 2009) was developed for modelling plant growth under water stress. However we have restricted this preliminary study to a maize field with neither water stress nor nutrition stress. The individual plant model GreenLab (de Reffye et al., 1997a; Yan et al., 2004), is a FSPM specialized in solving the source and sink functions involved in plant growth. Guo et al. (2006) have fitted the GreenLab parameters by inverse method for modelling maize growth in the field in order to capture organ expansion kinetics. After a parameter sensitivity test, Ma et al. (2007) showed that the sink related parameters were stable at different seasons and densities, which can largely explain inter-seasonal variability, and they modelled plant plasticity at different densities (Ma et al. 2008). Cournède et al. (2008) suggested that the parameters which represent light competition among individuals can potentially represent local effects, such as uneven space and emergence variability.

The following work is a preliminary study destined to solve individual variability in the field according to the variance of observations and the comparison between two models.

3.2 Materials and Methods

3.2.1 Field experiment

This experiment was conducted in 2009 at the Irstea experimental station in Montpellier, France (43°40'N, 3°50'E) on a loamy soil (18% clay, 47% silt, 35% sand) in the frame of a study dealing with the impact of irrigation systems and irrigation strategies on water productivity (Mailhol et al., 2011). Meteorological data including precipitation, global radiation and air temperature were fully recorded at the station. Maize (*Zea mays L.*, Pioneer PR35Y65) was sown on April 23 at 75000 plants ha^{-1}. Regarding the present work, the irrigation protocol involved surface drip irrigation, irrigation dates were adjusted on the basis of tensiometer monitoring and neutron probe measurements to avoid drainage risk and to supply a water amount of 350 mm (for further details see Mailhol et al., 2011).

LAI was monitored weekly during the cropping cycle, using a LAI2000 (LI-COR). Plants were collected after maturity for evaluating total above ground dry matter and grain yield according to the protocol described by Mailhol et al. (1997).

Organ-level observations were made at 5 dates throughout crop development, each time 6 plants were harvested. Fresh weight of aboveground organs (blade, petiole, internode, ear and tassel) were measured phytomer by phytomer in order to characterize organogenesis and organ expansion.

3.2.2 Model description: PILOTE and GreenLab

PILOTE has been described in detail by Mailhol et al. (1997) and Khaledian et al. (2009); GreenLab has been described by Yan et al. (2004) and Guo et al (2006). In the present work, only relevant descriptions centred on the connections between the two models are described.

Common points between PILOTE and GreenLab

PILOTE and GreenLab share the same theory based on Beer-Lambert's law to take into account light interception and biomass computation (Eq.3-1 and 3-2 in Table 3-1). Differences between the two models come from their different computing scales. PILOTE deals with population growth at a given density, based on a unit area of soil at a daily time step, while GreenLab operates on individual plants at the organ level by Growth Cycle (GC), which corresponds to the thermal time required to generate a new blade (the "phyllochron") on maize.

Table 3-1. Comparison of biomass equations of PILOTE and GreenLab

PILOTE	GreenLab
$Q = RUE \cdot \sum_{t_1}^{t_2} PAR_{(i)} \cdot \left(1 - \exp\left(-k \cdot LAI_{(i,WSI)}\right)\right)$ (3-1)	$q_n = \frac{RUE_n \cdot PAR_n \cdot S_p}{r}\left(1 - \exp\left(-k \cdot \frac{S_{b,n}}{S_p}\right)\right)$ (3-2)
	RUE: radiation use efficiency (g MJ^{-1})
	PAR: photosynthetically active radiation (MJ m^{-2})
	k: extinction coefficient
Q: final total dry matter (t ha^{-1})	*q*: total biomass of individual plant at GC *n* (g)
LAI: daily *LAI* according to water stress (m^2 m^{-2})	S_b: total area of living leaves (cm^2)
t_1, t_2: sowing date and harvest date of year	S_p: theoretic projection surface (cm^2)
WSI: water stress index calculated from soil water balance	*r*: growth resistance coefficient, equivalent to a conversion efficiency, cf. Cournède et al. (2009)
i: date *i*	*n*: current growth cycle (GC)

- Parameters *RUE*, *PAR* and *k* in bold type are shared the same concepts by PILOTE and GreenLab.
- Eq.1 represents the accumulated biomass from t_1 to t_2.
- Eq.2 indicates current biomass production at GC *n*.

The two models account for *LAI* in different ways. In PILOTE, *LAI* is simulated according to thermal time and is corrected by water stress.

$$LAI_{(i)} = LAI_{\max}\left[\left(\frac{\sum_{k=1}^{i} TT - T_s}{T_f}\right)^{\beta} \cdot \exp\left\{\frac{\beta}{\alpha}\left[1 - \left(\frac{\sum_{k=1}^{i} TT - T_s}{T_f}\right)^{\alpha}\right]\right\} - \left(1 - stress^{\lambda}\right)\right] \text{(Eq.3-3)}$$

When there is no water stress (and if other conditions are optimal), *LAI* evolves according to the sum of temperatures ($\sum TT$) from plant emergence (T_s) to reach the maximum value LAI_{max}; but if there is a stress (*stress*<1) computed from the soil water module (Mailhol et al., 1997), the value of *LAI* will decrease. Other variables in the equation are T_f, the temperature sum required to reach LAI_{max}; α and β, parameters to be calibrated; λ, an empirical parameter to characterize the response of a plant type to water stress.

In GreenLab, LAI is adapted from the classical definition at the individual plant level. It is written as the current (at GC *n*) living leaf area (S_b) per plant divided by a theoretic projective surface (S_p) (Eq.3-2), in order to keep the same water use efficiency (WUE) that is available at soil area level. The total living leaf area S_b is the result of source and sink processes, following Eq.3-4:

$$S_b(n) = \frac{1}{e} \cdot \sum_{i=n-t_b+1}^{n} N_b(i) \sum_{j=i}^{n} \frac{p_b(i,j)}{D(j)} \cdot Q(j-1) \quad \text{(Eq.3-4)}$$

Current (n) living leaf area is accumulated (first summation) by different initial dates (i), and biomass of each leaf is accumulated (second summation) GC by GC (j) since its initiation. While the incremental biomass at each GC is distributed from previous biomass production ($Q(j\text{-}1)$ = "source") by the ratio of the leaf sink strength (p_b = "sink") to the total demand of all growing organs ($D(j)$). Other variables in the equation are e, specific leaf weight, a measurable parameter for converting leaf biomass to area; t_b, the longevity (by GCs) of the current oldest leaf and $N_b(i)$, the number of leaves expanding since GC i.

Parameter S_p (Eq.3-2, Table 3-1) has been shown to be linked to ecological effects (Guo et al. 2006). Ma et al. (2008) calculated S_p by inverse method (following Zhan et al., 2003), and found for fertile fields at high plant densities that, when the canopy closes, S_p tends towards $S_d=1/d$, the inverse of density d. Parameter S_p can be considered as the average space per plant available for light interception. At low densities, S_p characterizes the self-shading effect per plant as plants become isolated and spatial competition decreases. Cournède et al. (2008) have shown that for tree growth, where individuals have a more complex architecture development and a much longer growth period, S_p increases during growth according to Eq.3-2 and indicates the evolution of crown size.

We applied PILOTE and GreenLab on the same unstressed maize field, with full irrigation (stress = 1 in PILOTE), and sufficiently fertilized. As they have a common basis for biomass computation, it was expected they could run consistently with each other.

Crop parameters and parameter estimations

In GreenLab, there are two kinds of parameters: visible and hidden (see Appendix I). Visible parameters are generally relevant to architecture definition, allometric relationships between organ fresh weight and their size, expansion and function duration of organs, which are observed directly. Hidden parameters generally include a resistance parameter (r), organ sink related parameters (sink factor p_o and sink variation parameter b_o, where o= b, p, i, f, m denote blade, petiole, internode, ear and tassel) and theoretic projective area (S_p), which were calibrated for maize by Guo et al. (2006). For simplification, in this study, most allometric parameters and blade symbols were applied from past measurements carried out by Ma et al. (2008). In addition, although ears were produced on several metamers, the last one was always the biggest contributing by more than 90% to the "ear" compartment, therefore a single ear at the average phytomer rank of 13 was considered. Organ fresh biomass by phytomer rank was measured at five successive dates, to generate a "target file" for GreenLab. Hidden parameters were fitted by generalized least square method according to source-sink processes following Zhan et al. (2003).

For PILOTE, crop parameters were provided by Khaledian et al. (2009), they were either measured or drawn from literature (T_s,T_f, ,LAI_{max}, *RUE*) and calibrated (α,β) for the Pioneer variety of corn in 2007 with conventional tillage.

3.3 Results

3.3.1 Model calibration

The evolution of *LAI*, was simulated by PILOTE (Fig.3-1a). Two weeks after sowing (day 113), *LAI* appeared and began to increase with time. It reached the maximum value of 3.5 around day 200, and then began to decrease. Measurements were distributed closely along the simulated *LAI* curve. In Fig.3-1b, simulated and measured dry mass of aerial parts and grain yield (at 15% humidity), for rain fed and irrigated treatments in 2009, were very close to the line *x=y* , highlighting the ability of the model to predict the irrigation water productivity (Mailhol et al., 2011).

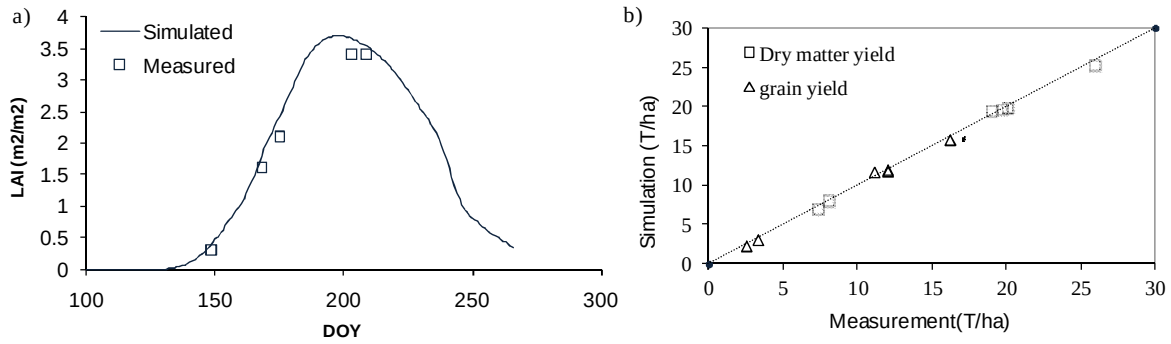

Fig.3- 1 Comparison between measurements and simulation of PILOTE a) Measured (squares) and simulated (solid line) evolution of LAI; b) Simulated / measured dry mass of maize aerial part (square) and grain yield (triangle) for the different irrigation treatments . Diagonal dotted line shows the1:1 ratio.

GreenLab hidden parameters were estimated by multi-fitting (see Appendix III and Table AIII.1). Fig.3-2 shows organ expansion: dashed lines illustrate the GreenLab simulation and dots represent organ weight measured at five dates. Blade expansion was drawn according to phytomer rank (Fig.3-2a). Each dashed line can be regarded as the pattern of maize morphology at a given GC. From these patterns, it can be seen that the blades at low phytomer ranks had a shorter expansion duration, whereas the blades at higher phytomer ranks had longer expansion duration. The biggest blades appeared at phytomer rank 11, which corresponds with the measured data. The simulated ear expanded from GC 13 onwards, and increased at high speed after the first GCs (Fig.3-2b), which agrees with the observations. The growth of individual plants could be visualized as in Fig.3-3.

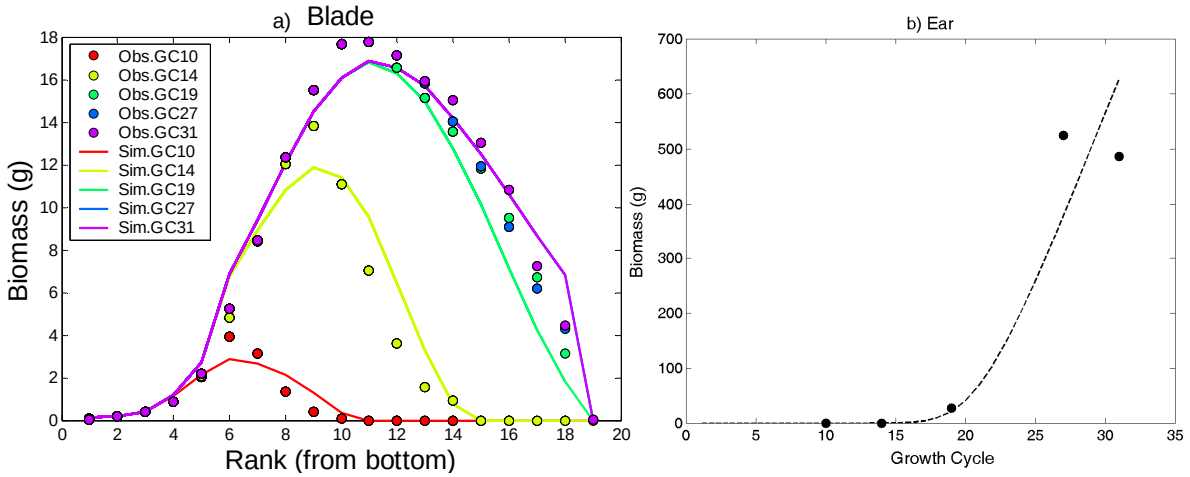

Fig.3- 2 Organ Measurements (solid circle) in 5 stages (GC 10, 14, 19, 27, 31) and the corresponding simulations (dash line) by GreenLab. a) Measured and simulated blades by phytomer rank. Different values of measurements or simulation noted the historical evolution of the blade. b) Ear measurements and the simulated expansion.

Fig.3- 3 Maize architectures simulation by the calibrated GreenLab model. Blades symbol came from the 3D-digitizition in Ma et al. (2008)

3.3.2 Simulation comparison and combinational computation

To study the simulation results of the two models, their common outputs of total dry biomass (*TQ*) and *LAI* were compared (Fig.3-4). *TQ* from PILOTE was converted to the individual scale at the time step of a GC, since the same starting date as GreenLab. Fresh mass simulated by GreenLab was converted into dry matter by an average ratio of 18.9 % (based on field observations). Although the shapes and magnitudes of *TQ* and *LAI* dynamics simulated by the two models were similar, they exhibited a clear difference. In both figures, simulations from PILOTE had a smoother and delayed trend occurring at the beginning of the

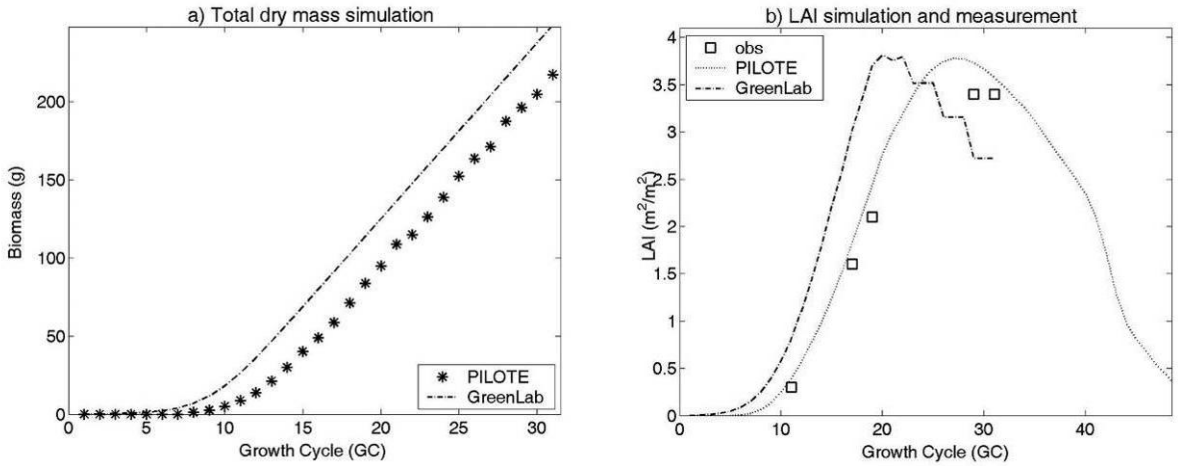

Fig.3- 4 Comparison of simulations between PILOTE and GreenLab a) Dry mass growth b) LAI development. Stars and dotted lines represented PILOTE, dash lines represented GreenLab, and squares represented measured LAI. Dry mass of PILOTE are converted to individual level by plant density, whereas dry mass of GreenLab are converted from fresh biomass by the mean of measured water contents.

simulation compared with simulations from GreenLab. In fact, during our field observations, we noticed that the number of metamers varied from plant to plant especially at the vegetative stages (Fig.3-5a), which could signify non-synchronous growth among individuals. By comparison between the two models, we speculate that there is an individual variability in plant emergence or growth rate, which could render simulations at different levels (i.e. stand and individual level) different.

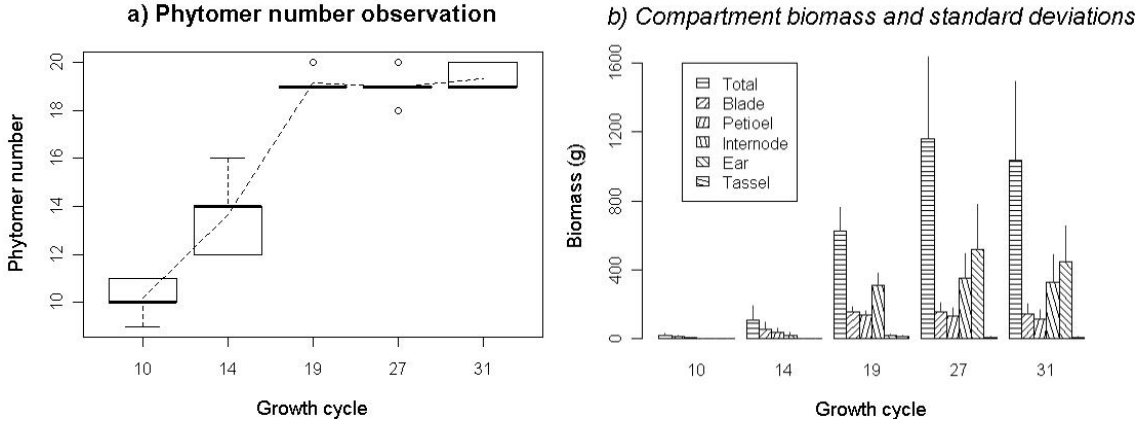

Fig.3- 5 Observed variability at GC 10, 14, 19, 27, 31, in a) phytomer number and b) compartment weight. Bars indicate means of compartment (of total aerial part, blade, petiole, internode, ear and tassel). Segments equal to 2 times of the standard deviation.

On the basis of this speculation we considered that there was a distribution of emergence variability, with which individual growth simulated by GreenLab could be composed to obtain the same stand level result as that simulated by PILOTE. Fig.3-6 shows a solution of discrete distribution captured by a negative binomial distribution function. In this

distribution, most emerging events (about 98%) were concentrated in four GCs (1, 2, 3, 4), where the average emerging date was GC 2.7 with a standard deviation of 2.1 GC. By considering this distribution, GreenLab produced an almost identical *TQ* curve and a closer *LAI* curve to that of PILOTE (Fig.3-7).

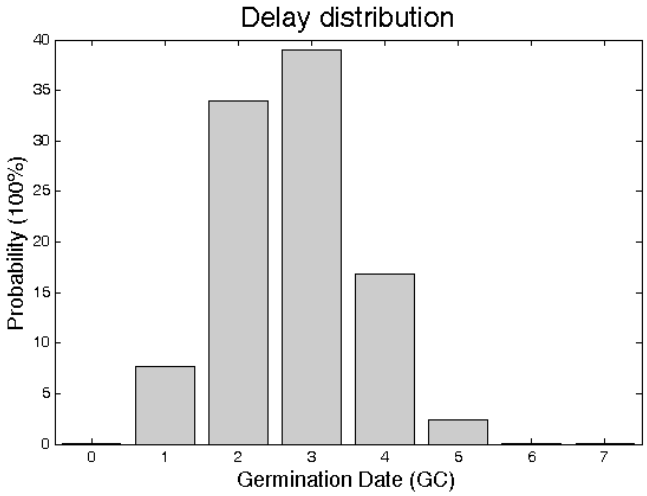

Fig.3- 6 An estimated distribution of plant emergence date by GC, fitted by a negative binomial law.

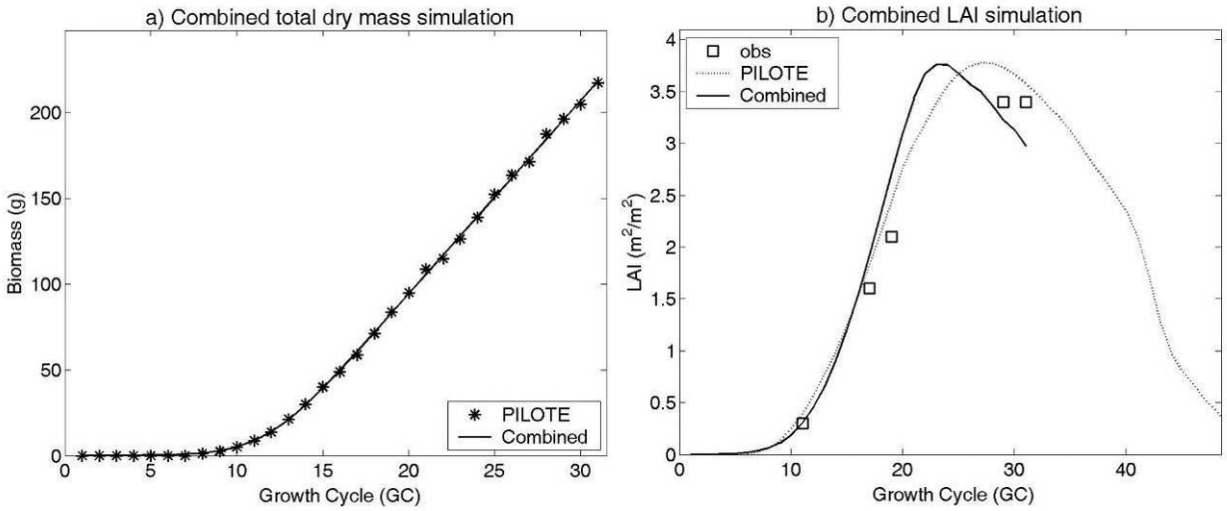

Fig.3- 7 Simulated population growth by integrating GreenLab with the estimated emergence distribution compared with stand level simulation by PILOTE. a) Dry mass growth; b) LAI development. Stars and dotted lines represented PILOTE, solid lines represented GreenLab, and squares represented measured LAI. For comparison, biomasses simulated from both GreenLab and PILOTE were formalized as average individual dry mass

3.3.3 Simulation of individual variability

Individual variability was observed for the biomass compartment (Fig.3-5b). As GreenLab equations can represent compartment increment (*Q*) and total biomass (*TQ*) and their variances (i.e. v_Q and v_{TQF}), it can attribute individual variability to certain parameters (see Appendix III). Therefore, assuming S_p is the major determinant attributed to individual

growth performance, the variance of incremental biomass for compartment ($v(Q)$) can be represented by the variance of S_p (v_{Sp}) and the correlation of S_p and simulated biomass production (r_{Sp,Q_i}) as in Eq.3-5, where *G'* is the first-order partial derivative of biomass production (Eq.3-2), *v* is the variance, *Q* is biomass production at each GC, and *i* and *j* are the indices of GC ($\leq n$).

$$v(Q(n)) = \left(G'_{Sp}\right)^2 v_{Sp} + \sum \left(G'_{Qi}\right)^2 v_{Q_i} + 2\sum G'_{Sp} \cdot r_{SpQ_i} \sqrt{v_{Sp}.v_{Q_i}} + 2\sum\sum G'_{Qi} G'_{Qj} . r_{Q_iQ_j} \sqrt{v_{Q_i}.v_{Q_j}} \quad \text{(Eq.3-5)}$$

The correlation coefficients $r_{Sp,Q}$ and $r_{Qi,Qj}$, calculated according to de Reffye et al. (2010), are here equal to 1 because only one parameter (S_p) is at the origin of the variance. Thus, the variance of the total biomass compartment ($v(TQ)$), which was accumulated by biomass production (Q) GC by GC, can be represented by v_{Sp} as well (Appendix Eq.A III.5 and A III.6). In this way, the variance of S_p (v_{Sp}) can be solved as S_p by inverse method (Zhan et al., 2003).

Compartment mean and variance of blade (Fig.3-8a), internode (Fig.3-8b), petiole (Fig.3-8c) and ear (Fig.3-8d), simulated by GreenLab with the parameter $\overline{S_p}$ (1379 cm^2) and standard deviation σS_p (290.42 cm^2) were compared with the corresponding measurements on maize plants. Standard deviations of all compartments increased with means, reaching 1/8 of respective means.

3.3.4 Field simulation

A maize field was simulated to integrate the emergence delay and plant growth variability caculated following 3.2. For this stand simulation, a module was developed under the software "Simeo" (de Coligny, 2009) to implement the GreenLab individual-based modelling. "Simeo" is specifically designed for 3D scene edition, which incorporates functions as planting plot design, individual implantation, voronoi tessellation (Cournède et al., 2010; de Coligny, 2009). Plants were sown in a virtual field according to row spacing, within-row spacing, rate of germination and displacement range (deviation from regular spacing). Each sowing point corresponded to a plant. A Voronoi tessellation was applied to allocate the soil area to each plant (Fig.3-9a), which was used as S_p, the indicator of individual variability.

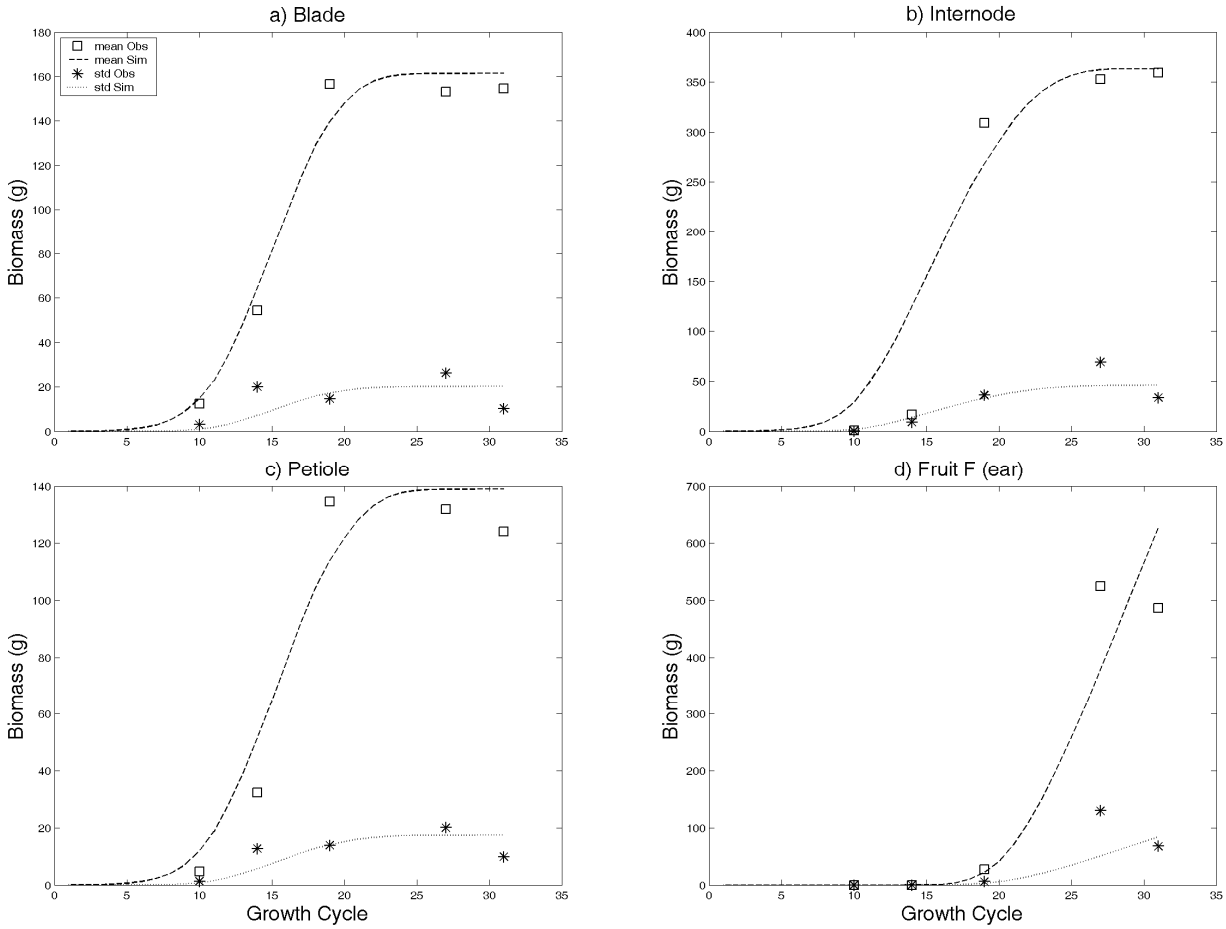

Fig.3- 8 Measured and simulated evolution of standard deviation of compartment fresh biomass, comparing with the mean of a) Blade; b) Internode; c) Petiole; d) Ear. Squares: mean of observed organ weight; dash lines: mean of simulated organ weight; stars: standard deviation of observed organ weight; dotted lines: standard deviation of simulated organ weight.

Row spacing and within-row spacing regulated the average S_p, while random effects such as rate of germination, and displacement range generated S_p variability. By adjusting them, we obtained an implantation plot having the same S_p distribution caracteristics as computed by GreenLab. Individual plant emergence dates were generated and distributed plant by plant according to the distribution of emergence delay as in Fig.3-7. Finally, stand level maize growth was simulated GC by GC, inside the virtual field, where each individual plant was obtained by the GreenLab simulator. In this way, asychronous emergence (Fig.3-9b) and plant-to-plant variability (Fig.3-9c) were represented during growth.

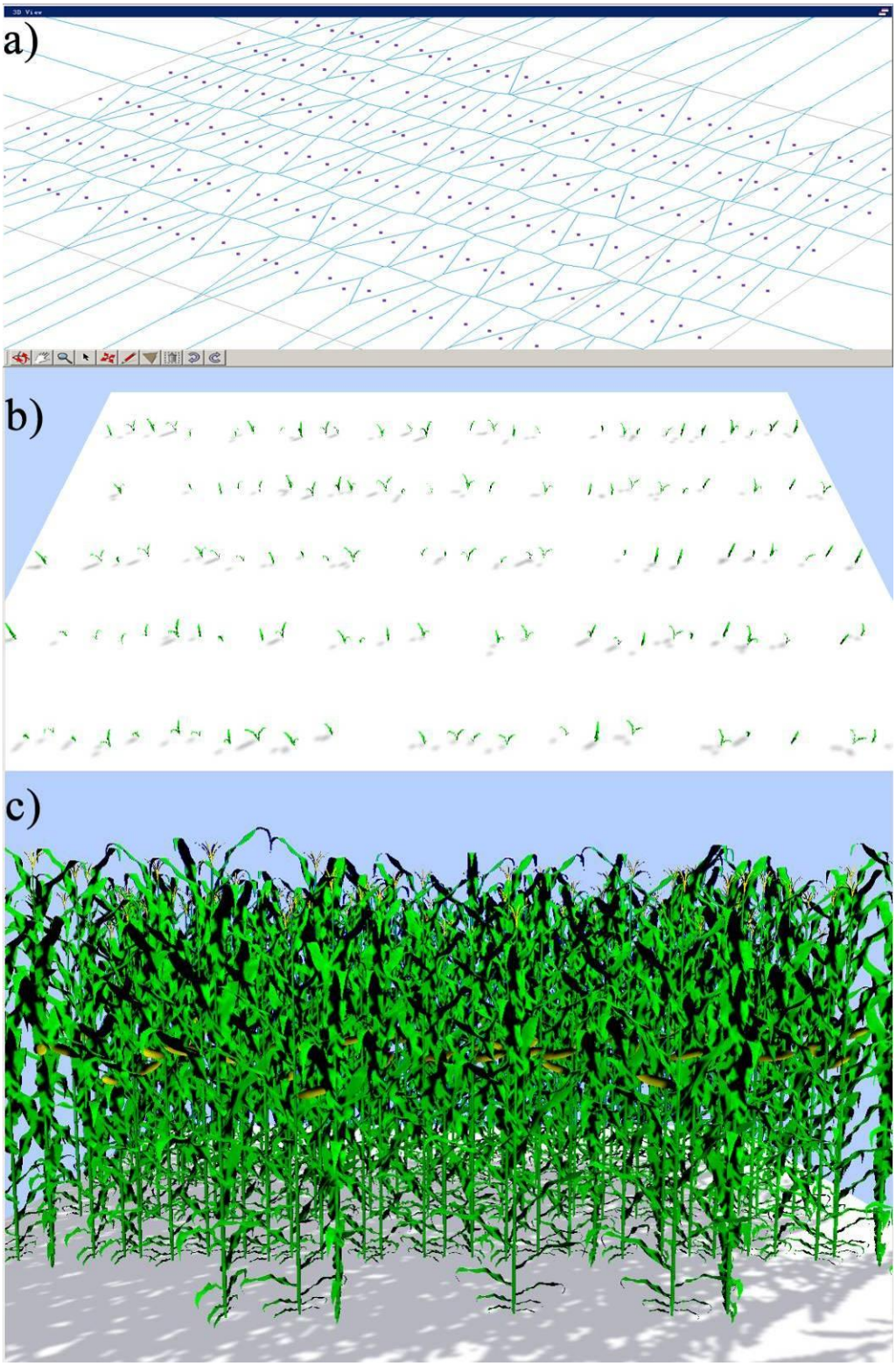

Fig.3- 5 Visualization of maize stand growth, simulated by GreenLab with variance of Sp. a) Virtual sowing plot and the voronoi tessellation; b) Emerging situation of the maize stand; c) matured maize stand. Individual variability were characterized by variance of Sp

.

3.4 Discussion

3.4.1 Combination between the crop model and the FSPM

In this work, PILOTE and GreenLab were use independently, so their respective hypotheses for plant growth modelling were retained in the result. By simulating a distribution of plant emergence date, the results of both models were very close. Variation of plant emergence in the field has been commonly accepted, since most researchers use a ratio of emergence to determine the stand level emergence date (Gesch and Archer, 2005), but the distribution of this event has seldom been studied. Through matching PILOTE and GreenLab on the same maize field, we obtained a distribution of emergence delay (Fig.3-6). The standard deviation of the computed distribution was about 2 GCs, which indicates the average difference between individuals, corresponding to 7~10 days in this experiment. This variation extent was slightly smaller than the treatment of two-leaf emergence delay (12 days) of Liu et al. (2004a) and Tollenaar et al. (2006), who observed a yield reduction of 40% and 4% respectively for the late individuals and the local stand. Accordingly, we can speculate that the reduction of yield should be somewhat less in our field for individuals and for the stand, but the individual variability could still be greatly influenced.

Plant emergence does not behave uniformly in the field, and this has an effect on individual growth and final yield. Most studies on individual variability concern factors such as uneven space distribution (Nafziger, 1996; Pommel and Bonhomme, 1998), or resource stress (Edmeades and Daynard, 1979; Ipsilandis and Vafias, 2005; Maddonni and Otegui, 2004; Rossini et al., 2011; Sangoi, 2000), but they rarely mention the emergence situation of plants in the field. The variability effect these authors have observed could be mixed with the effect of non-uniform emergence. We suggest that future studies should better account for such non-uniform emergence.

In the present simulations, it can be noticed that the matching of *LAI* curves was not improved as much as for *TQ* by accounting for the emergence delay distribution. The primary cause may be that PILOTE and GreenLab apply different methods to estimate blade surface for computing LAI. In GreenLab blade surface is computed from source-sink processes. In this work, we considered a value of specific leaf weight (*e*) measured by Ma et al. (2008), but it was not a measured on our sample, which could introduce an error. In PILOTE the blade surface was estimated, based on LAI2000 measurements under the assumption that the crop canopy is evenly distributed in the field. However most fields are not evenly distributed,

especially during the early stages. When LAI becomes saturated (>3.5), the sensitivity of the optic device decreases, which can be another cause of such discrepancy, however at saturation this has little influence on biomass production.

3.4.2 Computation of plant-to-plant variability by FSPM

As GreenLab is an individual based mathematical plant growth model, we could derive a solution from its equations to compute individual variability and we attributed this variability to the parameter S_p . Therefore we could generate growth dynamics of the whole maize field. Such variability is often attributed to seed biomass, space occupancy (S_p), local environment (Cournède et al., 2008), but we suggest here that S_p is an appropriate choice from a view point of FSPMs. S_p was introduced in GreenLab for adpating Beer Lambert's law to individual plants, to represent the corresponding projected area. In this sense, S_p is associated with plant architecture and therefore radiation interception (Cournède et al., 2008). Thus S_p may be regarded as a result of iterated growth and partition functions of plant architecture dynamics. S_p is an intermediate parameter between model and real plants, and has been used here as a driver of individual variability.

S_p was considered to have a constant value for each plant during growth, because the canopy of individual plants can be overcovered in the field for a short time due to fast plant expansion. A constant value of S_p during plant architecture development corresponds to the maximal projective area when the maximum crown size is reached (Cournède et al., 2008).

In the simulations of different compartments (Fig.3-8) there was a high variability as soon as the early stages for blade and petiole. This can be related to the non-uniform emergence. The six plants we harvested randomly each time from the field could represent a mixture of different emergence dates. The virtual maize field (Fig.3-9) demonstrated non-uniform emergence as well as individual variability, but the relationship between the two phenomenons could not be studied here. This relationship would be interesting to study in a next step, in particular to check our assumption that S_p can be used as the main parameter causing individual variability.

The scatter at later stages of the simulation (Fig.3-8) can be attributed not only to variations in emergence and in S_p, but also to the fact that we used fresh biomass to calibrate GreenLab, as the allometric relations provided by Ma et al. (2008) were estimated on this basis. At the final stages of the growth simulation, the real plants had probably begun to lose water, and the fresh biomass was no longer a good indicator of biomass growth. This can also

explain the decrease for ear and petiole (Fig.3-8c and 3-8d) at the last observation points (GC 31). A way to avoid such discrepancy between fresh biomass and dry biomass would be to integrate a description of the variation of water content, which can be observed directly, into the growth simulation.

3.5 Conclusion

The combination of a crop model and an FSPM showed a discrepancy which could be explained by the variability due to non-uniform emergence. Such variability could not be studied by one single model, but was expressed by their combination. This individual variability was evidenced by solving the variance of one model parameter of GreenLab, which integrated the effect of non-uniform emergence. For a further step, we suggest that the quantitative relationship between non-uniform emergence and individual variability should be studied. This could be undertaken with GreenLab, by making use of the theoretic projective area parameter (S_p) to quantify the response of individual variability on emergence dates.

As crop models are well adapted for simulating stress conditions at the population level, they can be used to improve the carbon assimilative function of FSPMs, and conversely, FSPMs can provide more accurate simulation of *LAI* and *HI* (Vos et al., 2007) to guarantee the prediction of crop models available in a more extensive environment.

Acknowledgements

This study was part of the PhD project of the first author, which was funded by the China Scholarship Council with the support of CIRAD. We thank F. de Coligny and P. Borianne for Simeo software development. We also thank Y. Ma, Prof. Y. Guo and other colleagues from the China Agricultural University who contributed in the long-term experiment and modelling study on maize.

4. Model combination to visualize evolution of Black pine stand

4. Model combination to visualize evolution of Black pine stand

Based on an article published in Annals of Forest Science

Title: Connecting an architectural plant model to a forest stand dynamics model – application to Austrian black pine stand visualization

Lu FENG[1] , Philippe DE REFFYE[1] , Philippe DREYFUS[2], Daniel AUCLAIR[3]

1. CIRAD, UMR AMAP, F-34398 Montpellier, France.

2. INRA, URFM, F-84914 Avignon, France

3. INRA, UMR AMAP, F-34398 Montpellier, France.

Annals of Forest Science
DOI 10.1007/s13595-011-0144-5

ORIGINAL PAPER

Connecting an architectural plant model to a forest stand dynamics model—application to Austrian black pine stand visualization

Lu Feng · Philippe de Reffye · Philippe Dreyfus · Daniel Auclair

Received: 10 March 2011 / Accepted: 22 September 2011

Abstract
• ***Context*** Forest stand dynamics models simulate the growth of trees in stands; based on field measurements and system knowledge, they provide a relatively precise representation of forest growth and are well adapted for forest management purposes. Architectural models describe the structure of plants according to ontogenetic development processes; as a support of biomass production and partitioning at organ scale, they simulate individual tree development.
• ***Aims*** The aim of this study was to link a stand dynamics model and an architectural model to simulate stand dynamics, in which the ecological or silvicultural modelling from the stand model and the architecture representation could be integrated, to provide individual tree details at the stand level.
• ***Methods*** Stand-level simulations of Austrian black pine dynamics provided global results on tree growth from the empirical forest growth model PNN, and branching details for individual trees were provided by the functional–structural plant model (FSPM) GreenLab.
• ***Results*** Individual tree dynamics were computed, and the simulated trees were integrated at the stand level for visualizing two different management scenarios.
• ***Conclusion*** By combining a stand dynamics model adapted to forest management with an FSPM with detailed tree architecture, it is possible to simulate individual tree structure with consistent dimensions, adapted to ecological and silvicultural modelling for decision support in forest management.

Keywords Empirical forest growth model · Architectural model · GreenLab · *Pinus nigra nigra* · Visualization

Handling Editor: Gérard Nepveu

L. Feng (✉) · P. de Reffye
UMR AMAP (botAnique et bioinforMatique de l'Architecture des Plantes), CIRAD,
TA A-51/PS2, Bd. de la Lironde,
34398 Montpellier cedex 5, France
e-mail: fyafeng@gmail.com

P. Dreyfus
URFM, INRA,
84914 Avignon, France

D. Auclair
UMR AMAP, INRA,
34398 Montpellier, France

1 Introduction

Forest growth and yield simulators are commonly used for decision support in forest management (Pretzsch 2009). Many different types of models have been developed, and several ways of classifying forest models can be found in the literature (e.g. Vanclay 1994; Pretzsch et al. 2008). Schematically, for predicting the effects of silvicultural management, forest stand models can be subdivided into empirical forest models (EFMs) and process-based models (PBMs). EFMs are mostly devoted to stand level production and tree size distribution, and are extensively used for forest management purposes. They are established on system knowledge, by which various ecological factors such as site conditions, stand structure, inter-plant competition or management scenarios can be taken into consideration. PBMs account for the major eco-physiological components of the system and the rates of transfer between

Published online: 14 October 2011

4.1 Introduction

Forest growth and yield simulators are commonly used for decision support in forest management (Pretzsch 2009). Many different types of models have been developed, and several ways of classifying forest models can be found in the literature (e.g. Vanclay 1994; Pretzsch et al. 2008). Schematically, for predicting the effects of silvicultural management, forest stand models can be subdivided into empirical forest models (EFMs) and process-based models (PBMs). EFMs are mostly devoted to stand level production and tree size distribution, and are extensively used for forest management purposes. They are established on system knowledge, by which various ecological factors such as site conditions, stand structure, inter-plant competition, or management scenarios can be taken into consideration. PBMs account for the major eco-physiological components of the system and the rates of transfer between components (photosynthesis; water balance, nutrient cycling). According to Kimmins et al. (2008), EFMs make "excellent" predictors under unchanging environmental conditions, whereas PBMs exhibit high flexibility under changing environment. The pros and cons of each have been addressed for example by Mäkelä et al. (2000) and Kimmins et al. (2008), who suggest combining these in "hybrid simulation models". With improvements in computer technology and progress in scientific knowledge concerning plant morphology, tree dynamics, and competition within forest stands, new generations of models are being developed (Pretzsch et al. 2008, Muys et al. 2010). With increasing concern of forest managers, as well as other stakeholders, about sustainable ecosystem management and ecosystem services, it has become necessary to address a large scope of spatio-temporal scales. These extend upwards from forest stands to ecosystem or landscape level (Auclair 2010), and downwards to individual trees (King 2005), and such up- and down-scaling entails increased complexity and uncertainty (Brugnach et al. 2008).

It is becoming increasingly important to take in account individual tree structure in forest management, for different objectives including for example carbon allocation and sequestration (Melson et al. 2011), fuel description for fire risk assessment (Parsons et al. 2011), stand or landscape visualization (Griffon et al. 2011), or for calibrating models for remote sensing applications (Castel et al. 2001; Biliouris et al. 2009).

The organization of individual plant components in space consists of topology (the physical connections between plant components) and geometry (the shape, size, orientation and spatial location of the components), which change during the development of the plants. Modelling individual trees requires accounting for their structure, and can (but does not

necessarily) involve physiological processes, leading to “functional-structural plant models” (FSPMs). Such models are usually built on recursive equations with more or less detailed organ-level computation, depending on the needs for simulation of tree development (de Reffye and Houllier 1997; Perttunen et al. 1998; Yan et al. 2004, Vos et al. 2010). The description of tree structure commonly involves empirical geometric models (Collin et al. 2011; Côté et al. 2011), and seldom includes details of the ontogenetic developmental processes (Sterck and Schieving 2007). The latter are based on the concept of plant architecture, which was initiated in the 1970’s by Hallé and co-workers (Hallé et al. 1978) and followed by many in-depth studies reviewed by Barthélémy and Caraglio (2007). Architectural analysis addresses both endogenous processes inherent to each species, and exogenous constraints exerted by the environment.

FSPMs are considered as very relevant for modelling physiological processes, individual tree level biomass production and carbon partitioning into different compartments (Pretzsch et al. 2008), but the extension from individual tree to stand level can be extremely demanding on computing capacity and time. Despite the importance of detailed canopy description for many applications, forest stand simulators very rarely address individual tree structural details (Sievänen et al. 2008), mainly due to the high computing time required. Maintaining a high degree of structural detail when scaling up from organ level to stand (or landscape) remains an important challenge, as in general the limitations of computer capacity require many simplifications in individual tree structure modelling (Kohyama et al. 2005). To address this challenge, tree structure can be simply represented by crown envelope shape (Rautiainen et al. 2008), or by using allometric relations (King 2005; West et al. 2009), fractals (Collin et al. 2011; Parsons et al. 2011), “numerical tree modelling” (Collin et al. 2011) or other geometric representations of tree architecture (Cescatti 1997; Perttunen et al. 1998; Biliouris et al. 2009). However, these simplifications can greatly affect the uncertainty of estimations, as has been shown by Melson et al. (2011) who cite differences up to 50% in volume and biomass according to differences in tree form.

To address the dilemma posed by the requirement for accurate, detailed estimations, at the stand or ecosystem level, with limited computer capacity, several authors have suggested coupling models at different scales, using a hierarchical approach (Mäkelä 2003). Jallas et al. (2009) added a 3-D architecture component to a plant simulation model for cotton, a “simple” plant; Renton et al. (2005) introduced architectural analysis in an L-system based model, coupled with a canonical model of tree resource allocation, to simulate individual plant form

and function for birch; and Wang et al. (2006) used static computer-designed 3-D tree images together with an empirical growth model based on inventory data, for forest landscape visualization purposes. However, to our knowledge, the only example of coupling a detailed tree architectural model (*sensu* Hallé et al. 1978) with a forest stand dynamics model was that of Meredieu et al. (2004) who constrained AMAPsim architectural model parameters by outputs from a stand growth and yield model for *Pinus pinaster*.

The present work is a further attempt to benefit both from the high reliability and the high computing speed of an Empirical Forest Model and from the high degree of detail of an Architectural Model, by combining two such models. As an example, two realistic silvicultural scenarios (thinned stand or unthinned control) were applied to Austrian black pine, simulated with the Empirical Forest Model "PNN" (Dreyfus 1993). The results obtained through the simulator were then used to calibrate the Architectural component of the Functional-Structural Plant Model "GreenLab" (Yan et al. 2004), which in turn provided detailed individual tree architecture data. Among the various outputs of decision support tools, forest stand visualization is becoming increasingly important for stakeholder involvement and negotiation (Pretzsch et al. 2008; Muys et al. 2010). An application to visualization of the forest stands resulting from the two simulated scenarios is presented here.

4.2 Materials and Methods

4.2.1 Austrian black pine architecture

According to Barthélémy and Caraglio (2007), a plant can be seen as a hierarchical branched system in which the axes can be grouped into categories according to their morphological, anatomical or functional distinctive features. Austrian black pine (*Pinus nigra* Arn. subsp. *nigra*) has a rhythmic ramification and growth, all axes are monopodial and branches are orthotropic. It belongs to Rauh's architectural model as described by Hallé et al. (1978), presented in Fig.4-1a (from Barthélémy and Caraglio 2007). Black pine is monocyclic: the time step used to describe meristem development is one year, corresponding to one new growth unit (GU) that produces a whorl of branches along the stem (Fig.4-1b). In *Pinus*, GUs are composed of a large number of very small internodes, but for computing requirements (see 3. Model combination) we have considered the GU as the smallest entity to be represented, similarly to Wang et al. (2010). Barthélémy and Caraglio (2007) defined the "physiological age" (PA) of a meristem or of an elementary botanical entity, and in simple cases such as *Pinus nigra nigra* the physiological age corresponds to the branching order.

Black pine exhibits four branching orders, the stem being defined as order 1. The number of branches on a whorl can vary, both with the position and the order of the axis, generally from 1 to 5 on the stem, and from 1 to 3 on higher order axes (Castel et al. 2001).

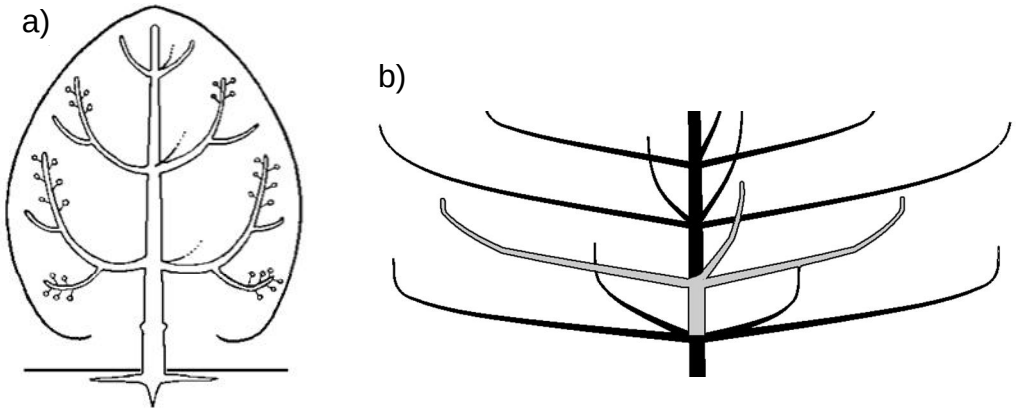

Fig.4-1 a) A simplified representation of Rauh's architectural model (from Barthélémy and Caraglio 2007); b) Detail of 4 successive growth units on the stem, showing branch whorls. The second stem GU with its whorl is presented in grey.

4.2.2 Field data

The dataset used for calibration of the PNN growth model (individual size and increments, mortality) came from a network of 76 plots (46 plots in 6 thinning or pre-commercial thinning experiments + 30 permanent yield plots), from regeneration stage to mature stands, within the Mediterranean range of this species in Southern France, and covering various site conditions, initial stand structures and thinning characteristics. It contained *ca*. 25750 diameter increments, 3750 height increments, on more than 13000 trees; the stem density ranged from 200 to 18000 stems ha^{-1}, and the basal area from 1 to 64 m^2 ha^{-1}, according to thinning treatments (from unthinned control to relative spacing values up to 100%). For the branching model, the data were obtained from stem analyses performed on four trees per stand (dominant, codominant, average and suppressed) in a subset of 8 stands from the above-mentioned network, with age ranging from 23 to 114 years, height from 5.3 to 27.0 m, *dbh* (stem diameter at 1.3 m height) from 7 to 45 cm. More than 3200 branches (dead/green) were measured for diameter, and 1300 for angle and extents. Additional botanical data on black pine came from the observations of Castel et al. (2001).

4.2.3. The empirical forest dynamics model PNN

For *Pinus nigra nigra*, a tree-level distance-independent growth model (Dreyfus 1993) including sub-models predicting height and stem diameter growth, competition-induced

mortality, stem volume, height to living crown, and an allometric branching sub-model was calibrated, connected and embedded in a module of the Capsis simulation platform (http://www.inra.fr/capsis, Dufour-Kowalski et al. accepted), named "PNN". This module enables simulation of the evolution of a black pine stand according to site index and to competition controlled by thinning scenarios, from young stage (trees a few metres high and around 10-15 years old) to age 100 or more, with a 5-year time step.

At each step, the outputs from PNN include usual stand characteristics (number of stems, basal area …) and individual information (age, *dbh*, total height *H*, and height to crown base *Hcb*) for each tree. After validation, the growth model predictions have served for example to define management guidelines in a new technical guide for forest managers (Ladier and Rey 2011).

Virtual tree coordinates were computed in the present study for visualization purposes (not used by the distance-independent growth model). The branching sub-model provided additional individual tree outputs calculated at each time step for the trees remaining in the stand after thinning or natural mortality, concerning each whorl (whorl order from the bottom

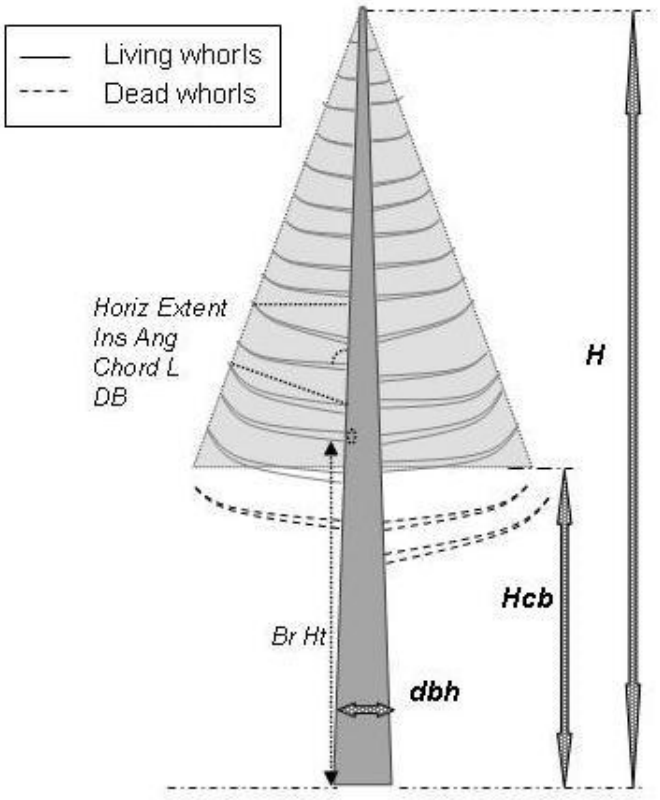

Fig.4-2 Detail of individual tree variables from PNN: global tree variables (diameter at breast height *dbh*, height of crown basis *Hcb*, total tree height *H*) and variables for each living whorl, corresponding to Table 1 (height of insertion *Br Ht*, base diameter *DB*, chord length *Chord L*, insertion angle *Ins Ang* and horizontal extent *Horiz Extent*).

to the top of the tree, number of branches in the whorl). Within each whorl the following characteristics of the main axis of each green branch were computed: height of insertion from the ground (*Br Ht*), basal diameter (*DB*), angle of insertion (*Ins Ang*), horizontal extent (*Horiz Extent*) and distance between origin and tip (*Chord L*, see Fig. 4-2, an example is shown in Table 4-1). As the branching model in each whorl and the characteristics of the corresponding branches were simulated at each simulation step and there is no direct link between a branch at one step and a branch in the same whorl at the previous step.

Table 4-1 : An example of output related to branching from PNN for one individual tree. Four whorls are presented here.

Tree Id	Whorl number from bottom	*Br Ht* (m)	*DB* (mm)	*Horiz Extent* (cm)	*Chord L* (cm)	*Ins Ang* (grade)
4689	9	2.28	8	17	20	52
4689	9	2.28	8	17	20	52
4689	9	2.28	7	15	18	52
4689	9	2.28	6	14	16	52
4689	8	2.03	11	26	31	56
4689	7	1.77	5	16	17	63
4689	7	1.77	11	31	36	61
4689	7	1.77	5	16	17	63
4689	7	1.77	16	40	53	59
4689	7	1.77	16	40	53	59
4689	6	1.52	10	31	34	66
4689	6	1.52	8	27	29	66

4.2.4. The functional-structural plant model GreenLab

GreenLab provides a generic mathematical framework for functional-structural plant modelling, based on the botanical concepts of plant architecture (de Reffye et al. 1988); it has been described in detail by Yan et al. (2004). Organogenetic rules provide the plant structure, which can be defined as an interconnected network of organs, whereas source–sink relationships among these organs determine biomass production and allocation. A consistent time unit for architectural development and ecophysiological functioning is defined. This allows the discrete dynamic system of growth to be derived, and its state variables are

sufficient to deduce the whole-plant architecture (Mathieu et al., 2009). The FSPM GreenLab has been validated for a large number of small cultivated plants (de Reffye 2009). A complete validation (for both structure and function) for mature trees is still under way, but the architectural component and particularly the visual aspects have been evaluated, mainly by expert knowledge, and are currently used for architecture and landscape planning purposes (http://www.bionatics.com/).

In the present study we restricted the use of the model to plant structure (topology and geometry), without considering the physiological processes, as the growth of individual plants was driven by the outputs of PNN. Following Barthélémy and Caraglio (2007), each axis is composed of a succession of growth units, and the different categories of axes are characterized by the notion of physiological age (PA). For black pine, four PAs are defined, each characterizing one of the four axis orders. As *Pinus nigra* is monocyclic, the number of growth units on the stem, N_1, equals to the age of the tree, whereas the number of growth units ($N_{2,3,4}$) on branches depends on the location, age, and life span of the axes.

4.2.5. Simulation scenarios

To illustrate the model combination, we simulated a 1-ha initial stand with a density of 6000 stems ha^{-1} and height 2.5 m at age 10, which is a common situation for black pine natural regeneration in south-eastern France. Two different management options were compared: the first, named “thinning treatment”, consisted in one pre-commercial thinning at age 15, followed by three thinnings at ages 45, 60, and 75, which is close to management recommendations for this species in such relatively good site conditions (Ladier and Rey 2011); the second scenario was a control without any thinning, but with natural mortality (Table 4-2).

4.3 Model combination

The outputs from PNN are less detailed than those from GreenLab for individual trees, but some output variables are common for both models. GreenLab was constrained by these common variables. Two adaptations were necessary, the time step and the resolution scale. The time step of PNN simulations was 5 years, whereas it was one year for GreenLab: as a first approximation, a linear interpolation was applied. The finest resolution of PNN concerns the main branches (2^{nd} order axes) for each individual tree, whereas for GreenLab it is the organ level: the branching information for each whorl at each time step was computed by

PNN, and for GreenLab additional information was included by considering the botanical information on the development of axes described by Castel et al. (2001).

Table 4- 2 : Thinning scenarios and corresponding stand density

Age	stems ha^{-1}	
	Thinning	Unthinned
15	6000 – *1100* [a]	6000
20	1100	6000
25	1095	5960
30	1090	5900
35	1085	5795
40	1075	5650
45	1060 – *625* [a]	5495
50	623	5259
55	620	5085
60	620 – *400* [a]	4750
65	400	4260
70	395	3715
75	395 – *275* [a]	3185
80	275	2695

a: in italics: after thinning

4.3.1. Branch mortality

Branch mortality was estimated from *Hcb*, as shown in Fig.4-3 a, b for two management scenarios ("thinning treatment" or "unthinned control", see 4. Simulation). At each time step, the highest branch below *Hcb* was the last dead one, whose life span could then be determined by its position (whorl order). By interpolation, the life span of the main branches was computed until the last dead one (Fig.4-3c). The life span of higher order branches was determined empirically as half of the life span of its parent axis, based on botanical observations reported by Castel et al. (2001).

4.3.2. Branch number

The number of main branches (2^{nd} order axes) along the stem was an output of PNN. The branch number for higher order axes was generated randomly, with a maximum branch number of 3 and 2 respectively for the 3^{rd} and 4^{th} order axes, based on Castel et al. (2001).

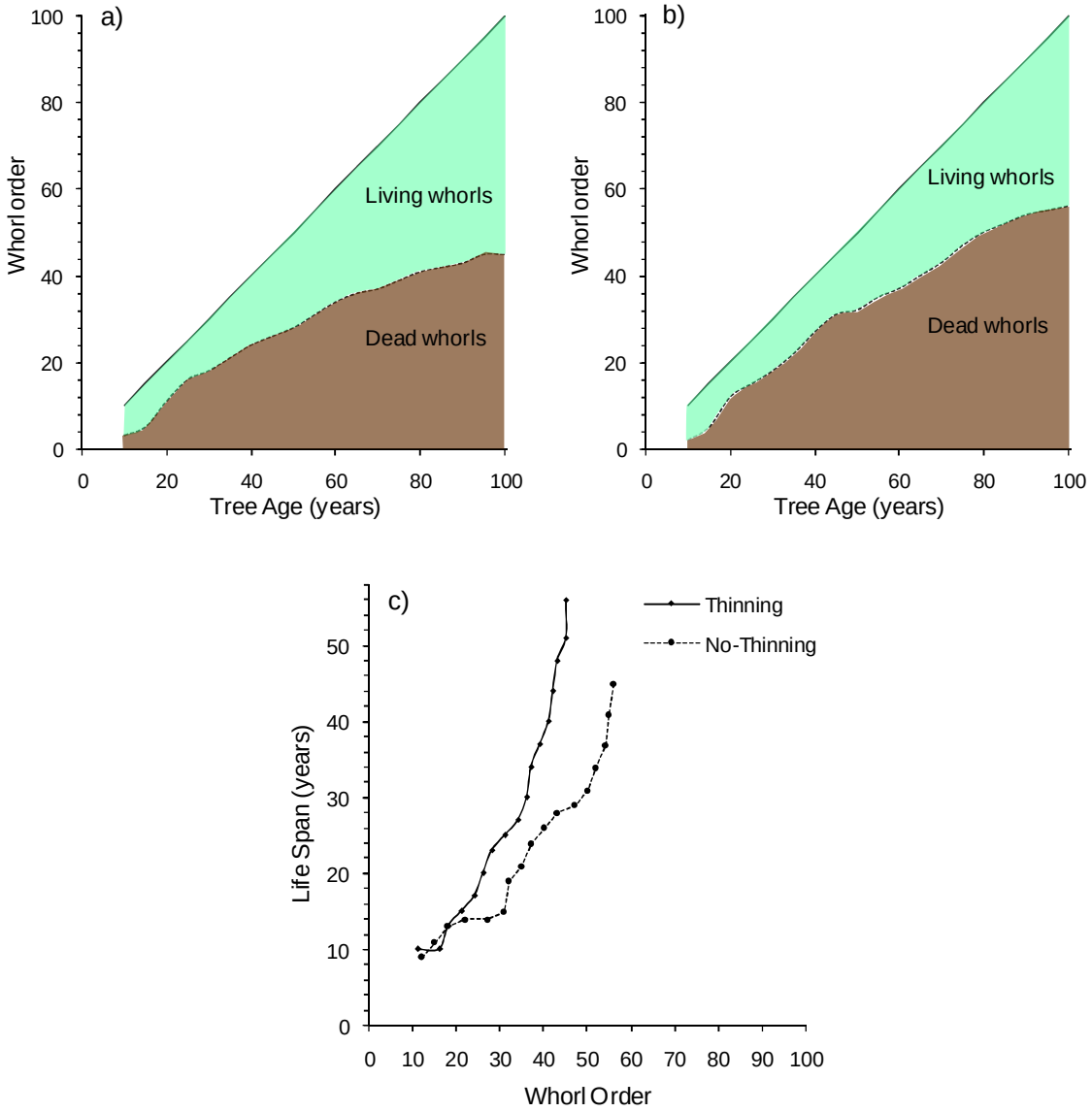

Fig.4-3 Dynamics of crown height for the thinning treatment (a) and the unthinned control (b), showing dead and living whorls. (c) Life span of the main branches for each whorl from the bottom to the top of the stem: the full line represents the thinning treatment and the dashed line the unthinned control.

4.3.3. Growth Unit length and diameter

The length of GUs (l) on the stem and on 2nd order axes, related to the increment of tree height and of branch length (L), was calculated directly by differential equation (4-1):

$$l_{(i)} = \frac{L_{(i+1)} - L_{(i)}}{t_{(i+1)} - t_{(i)}} \qquad \text{(Eq.4-1)}$$

Diameter growth of GUs was simulated by a cone frustum, for which the aperture was estimated from tree height and dbh for the stem (considering no butt swell), and for branches

from total branch length (*L*) and branch base diameter (*DB*). This way, the diameter of each GU composing the stem or the branches could be estimated by *dbh* or *DB* and its distance to the base (*s*). *dbh* and *DB* at different stages were outputs from PNN, whereas the length of GUs to calculate *s* was the result of equation (1). Length and diameter of GUs on 3rd or 4th order axes were outputs of GreenLab. They were set to be proportional to their corresponding GUs along the parent axes. A ratio 0.25 was used for diameter, whereas ratios 0.8 and 0.6 respectively were used for length of 3rd and 4th order axes, based on Castel et al. (2001).

4.3.4. Branch position and bending

The positions of branches were determined by both insertion angle (between the initial direction of branch and the direction of its parent GU) and phyllotaxy angle. For main branches, insertion angles were PNN outputs (in the branching sub-model of PNN, the insertion angle is related to branch age and branch diameter), whereas a counter-clockwise rotation angle of 112.45° was applied for the phyllotaxy, based on observations by Castel et al. (2001). Insertion angles between 45° and 60° were used for 3rd order axes, insertion angles between 30° and 45° were used for 4th order axes, while the phyllotaxy angle of 180° was taken for both.

Branch shape has been estimated in this study, mainly for visualization purposes, based on simple mechanical processes. An elastic curvature of Young's modulus was first used to simulate the bending effect under the weight of the branch in the basal part, as described by Jallas et al. (2009). Then, a re-orientation was calculated to account for the orthotropic growth at the end of the axis, based on the geometrical data (insertion angle and chord length) provided by PNN. The turning angle of each GU was linearly related to an appointed final angle from the vertical.

4.3.5. Leaf rendering for visualization purpose

Similarly to the foliage representation of Côté et al. (2011), a symbol representing a bunch of pine needles was applied as the leaves for one growth unit, and the scale was set according to growth unit length (see Fig.4-4c). A constant needle life span of 3 years was applied.

4.4 Simulation result

Fig.4-4 shows an example of simulated architecture of the crown of a 30-year old *Pinus nigra nigra*. On the left is the woody architecture with no leaves, showing the form and

position of branches. Below is a zoom on the symbol representing the needles for visualization purpose. On the right is the entire crown, including needles. The bottom part of the stem, with no living branches, is not presented here.

Fig.4-4 shows the architectural development of individual trees according to the two silvicultural scenarios, from age 10 to 80 years. The scenario for the thinned stand (Fig.4-5a) shows the wide

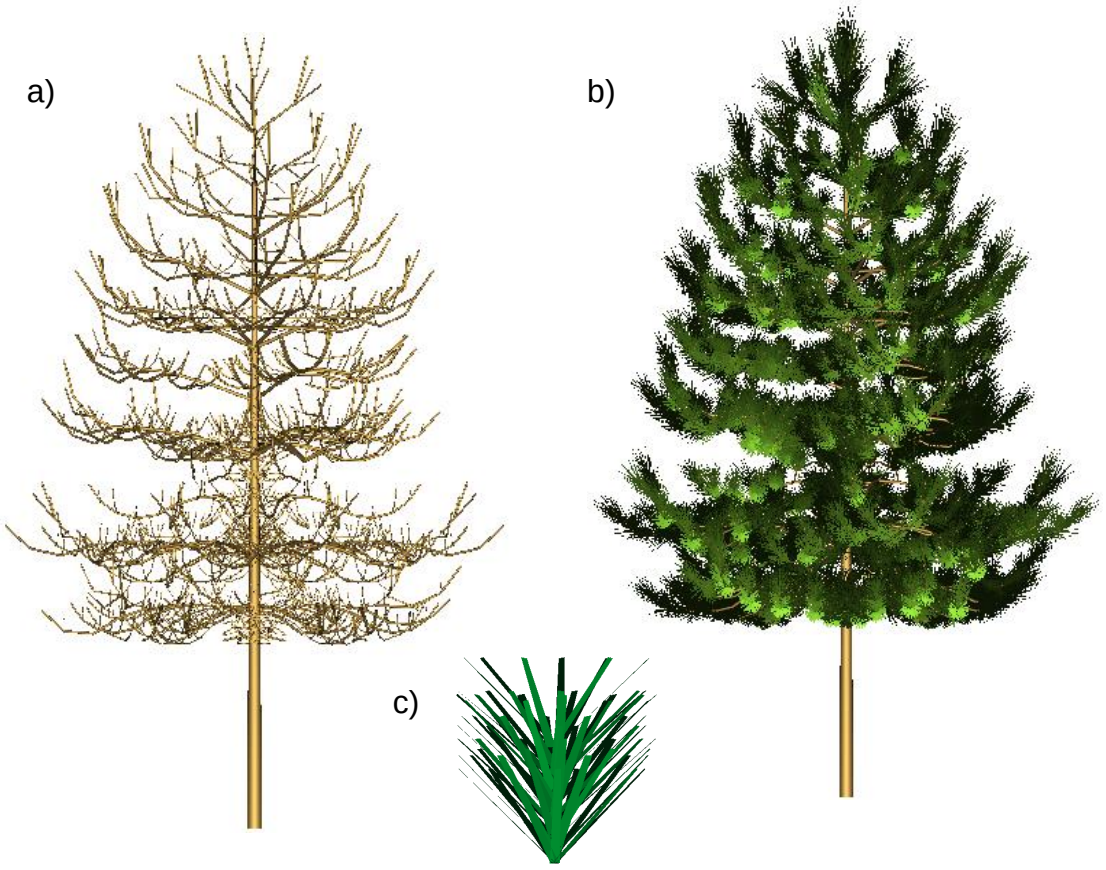

Fig.4-4 Simulated crown of a 30-year old Pinus nigra nigra. On the left (a) is the woody architecture with no leaves, on the right (b) is the entire crown, including leaves. The bottom part of the stem, with no living branches, is not presented. The symbol representing the needles for visualization purpose is shown below (c).

crown development and trees with large diameter, whereas the unthinned control scenario (Fig.4-5b) shows trees with smaller diameter, high crown base and a small crown, due to the high tree density leading to (tree and) branch mortality.

The simulated stands could then be visualized. The mean characteristics of the stands at age 50 are presented in Table 4-3. Fig.4-6 shows (top) the simple output generated by PNN through the Capsis stand visualizer for the thinned stand (left) and the unthinned control (right) at age 50, compared to the output from the present work coupling GreenLab to PNN for the

same scenarios: thinned stand (bottom left) and unthinned control (bottom right). The objective was not to represent the entire ecosystem, therefore no ground vegetation has been added for a more realistic visualization. Computation time to produce a HD (1920 x 1080 pixels) image of the unthinned 1-ha stand (5259 trees) was 25 minutes on a 32-bit classical computer, with Intel Core2 duo T9600 processor and 3G ram.

Table 4-3 : Characteristics of the stands at age 50 according to the thinning scenarios.

N = Stand Density (stems ha^{-1}); H_m = average tree height; Hcb = height of crown basis; G = stand basal area; D_g = quadratic mean diameter

	Thinned	Unthinned
N	623	5259
H_m	14.8 m	14.5 m
Hcb	9.6 m	11.4 m
G	22.7 m^2 ha^{-1}	50.8 m^2 ha^{-1}
D_g	21.5 cm	11.1 cm

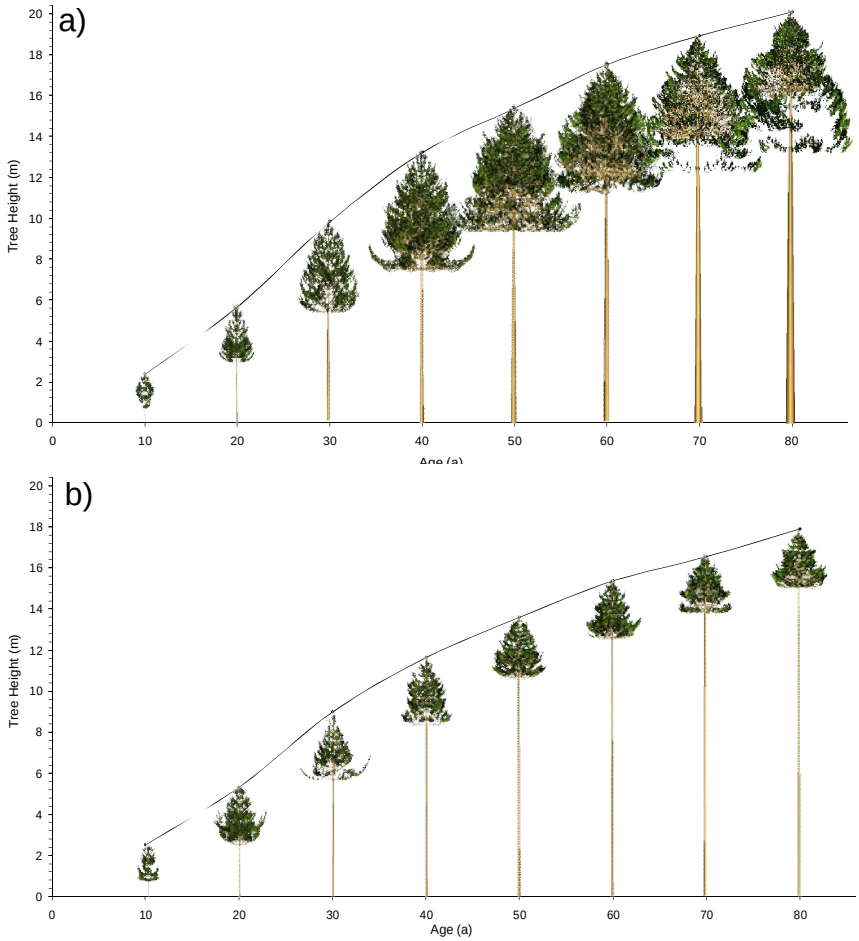

Fig.4-5 Visual representation of black pine dynamics, showing the crown development for the thinning treatment (a) and the unthinned control (b)

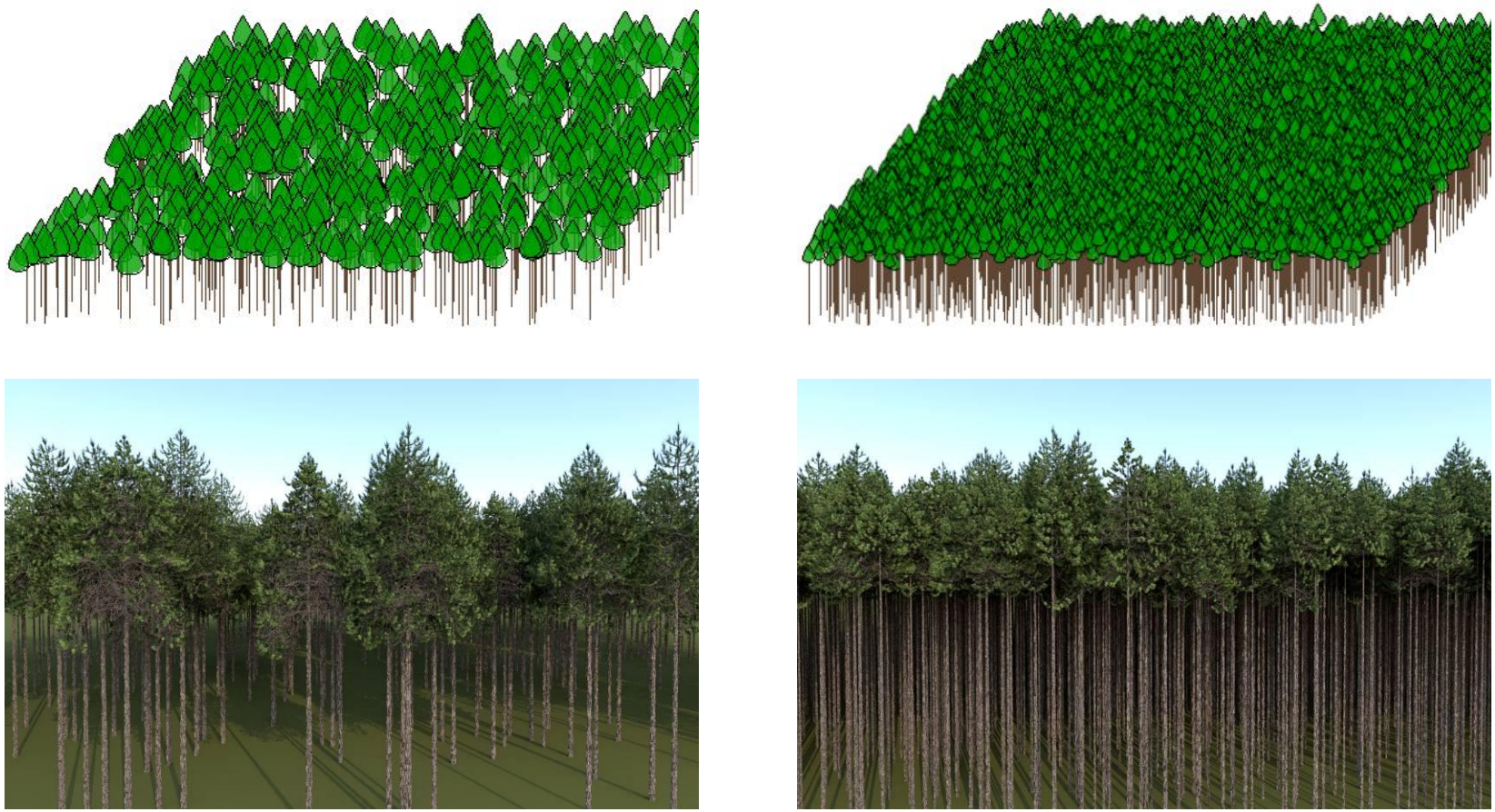

Fig.4-6 Visual representation of a black pine stand at age 50: output generated by PNN through the Capsis stand visualizer (top), and output from the present work (bottom). The thinned stands are presented at the left and the unthinned control at the right. Dead branches are not visualized. See Table 4-3 for tree and stand characteristics.

4.5 Discussion

In the present study, we combined the EFM simulation of tree and stand growth of black pine with a FSPM, in order to link the architectural development of individual trees to the information produced by the EFM. Therefore, individual trees were simulated not only with growth information in relation to silvicultural scenarios, but also with consistent botanical information.

This has been used in the present study to produce a data-driven forest visualization from the EFM simulation. Many different visualization approaches have been developed, as described by Pretzsch et al. (2008). Some can provide interactive real-time visualizations and free perspectives (Lim and Honjo 2003, Griffon et al. 2011). In most approaches, the individual tree development is poorly represented, if at all. Several individual plant simulators have been developed to obtain visually satisfactory tree shapes to be used for example in computer graphics, in which neither detailed botanical knowledge on tree architecture nor precise growth dynamics are necessary. Software like Xfrog (www.xfrog.com, Deussen and Lintermann 2005) and OnyxTree (www.onyxtree.com, Bosanac and Zanchi 2002) for example produce very realistic 3-D tree models, satisfactory for static visualization. Among the few examples which couple a forest stand simulation model with a visualization software in order to represent tree growth satisfactorily we can cite TREEVIEW and L-VIS (Pretzsch et al. 2008) or MONTE (Muys et al. 2010). With increasing stakeholders' requirements, it is important to represent individual trees as close as possible to their real architecture and dimensions. In the present work, combining an architectural model and a stand dynamics model produced simulations consistent both with forest growth and with detailed organ-level architecture, leading to a high degree of realism of the represented vegetation, as suggested by Lange (2001). For even better realism, ground vegetation could be added.

Besides visualization, detailed analyses of architecture can be undertaken. For example, Fig.4-3 shows the dynamics of crown depth for the thinning treatment (Fig.4-3a) and the unthinned control (Fig.4-3b). Based on these values, Fig.4-3c shows how the life span of main branches (2^{nd} order) increased from the bottom of the tree upwards. This is consistent with the "morphogenetic gradient" described by Barthélémy and Caraglio (2007).

Such coupling between an EFM and a FSPM could also be of great interest for estimating biomass production and carbon allocation in the various compartments of the ecosystem. However, for such applications additional data would be required, to better

calibrate the dimensions of various organs, in particular the 3rd and 4th order axes. The present data were not collected for such an objective, and further field work would be required.

Process-based models generally consider physiological processes, either at the stand level or (for FSPMs) at the individual plant level, but rarely consider the ontogenetic developmental processes which produce the structure of the plants. The objective of the present work was to up-scale individual tree ontogenetic processes at the stand level. A further step will be to integrate not only the architectural component of GreenLab into an EFM, but also the physiological processes. Several complementary approaches can be envisaged, such as the hierarchical treatment of multiscale processes suggested by Mäkelä (2003), and/or using Bayesian methods for combining empirical and process-based models as suggested by Radtke and Robinson (2006).

4.6 Conclusion

In this attempt to combine an architectural model with a stand dynamics model, we used the outputs of PNN to calibrate the first and second order axes of the architectural component of GreenLab. The PNN model simulated tree and stand growth, according to silvicultural treatment, while GreenLab provided details of the architectural development. In this example, the combined simulation could integrate both the ecological and silvicultural aspects from the stand dynamics model and the structure representation from the architectural model. As a result, tree architecture with a correct time scale was generated, in which it was possible to integrate a thinning scenario and forest growth function from the stand model into the FSPM. Since the two models are independent, the same method can be extended to linkage with other stand models. The first application presented here concerned stand visualization, but this work offers further perspectives for in-depth analyses at the organ level, including carbon allocation.

Acknowledgements

This work was funded as part of my PhD project by the China Scholarship Council with the support of CIRAD. The authors are greatly indebted to research technicians of INRA-URFM, non-permanent staff and students, involved in establishing and maintaining plots, measuring surveyed trees, performing stem and branch analyses in the field, and hence gathering the data necessary for calibrating the EFM. Thanks are also due to the French National Forest Service (ONF) for allowing us to establish experimental plots in managed stands and to fell trees for stem and branching analyses, to Sébastien Griffon and François de Coligny for their contribution to visualization software development, and to two anonymous reviewers for their constructive comments.

5. Conclusion and prospects

5. Conclusion and prospects

5.1 FSPMs in Agricultural studies

5.1.1 Architecture and individual variability studies

Crop growth in a field always exhibits variations in architectural construction and the final sizes of organs, including grain yield, which can in turn influence crop yield. The reasons for such variation may be the heterogeneous distribution of resources (i.e. space, light radiation, temperature, water and nutrients supply), stress, and may also have a genetic origin (i.e. plasticity of the phenotype). Researchers have been aware of this problem in agricultural productivity for a long time from field observation. Although our understanding of individual variability has improved in recent years, some conclusions on the same questions remain confused (Liu et al. 2004a). The reason may be that certain underlying processes have been overlooked. Modelling approaches may be able to provide clues.

However, by addressing plant growth as an output of a unit area, crop models have limited ability for doing this, except for characterizing whole crop productivity as an average yield.

Comparatively, models including architecture are specialized in such problems, since architecture is the medium for capturing resources as well as reflecting plant behaviour (response). An early attempt that can be cited is the work by Pommel et al. (2001). They used the ADEL-Maize model (Fournier and Andrieu, 1998, 1999) built with L-system formalism to reconstruct 3D plots for maize stands with different spatial arrangements. Based on this, they tried to calculate light interception to interpret the differences in yield. By virtual computation, the model found that stands with an irregular arrangement had less light interception overall than a constant plant density, which provided an explanation for their different yields from resource capture. However, this ADEL-Maize model did not have biomass-related functions as an executor; plant development and organ extension were described by simulated curves built according to temperature, and consequently the leaf sizes had to be corrected with observations for specific situations. This is a limitation for this application. A promising perspective can be foreseen using an FSPM with well-established relationships between plant functions and architecture dynamics, since variations essentially come from plant development and growth processes, as applied in this thesis (Chapter 3). By jointly studying with a crop model, PILOTE, and the mathematical FSPM GreenLab model on a maize field,

divergent emergences were revealed from the simulation comparison, which provided an explanation for individual variability from an ontogeny viewpoint.

Ultimately, a better mechanistic understanding can provide advice for agricultural management, while explicit cause and effect descriptions in plant development and growth can provide clear guidance for breeders.

5.1.2 Cooperation between crop models and FSPMs

An underlying consideration of this thesis was that through model combination, FSPM can introduce architectural support into traditional modelling simulations, and in the future can even provide crucial feedback, such as LAI, HI, etc. for crop models or EFMs for improving their predictive abilities.

Crop model bottlenecks. Crop models can provide accurate estimations of biomass production for most field or greenhouse conditions. The computation is mainly driven by changes in LAI, which is usually provided by an independent module depending on the sum of temperatures, and may therefore not be well predicted in the case of stress. Many efforts have been made to improve leaf area prediction accuracy for crop models. For instance, Lizaso et al. (2003) proposed a model which describes the life cycles of leaves as expansion, longevity and senescence, and it simulates in accordance with some genotypic attributes (e.g. area of largest leaf, longevity of most long-lived leaf). Later, in the new version of CSM-CERES-Maize (Lizaso et al. 2011), they added a water stress effect on leaf transformations. Although the physiological processes of leaf development have been integrated, which has improved the robustness of leaf area simulations, computation is found to be very sensitive to leaf number estimation. However, as there is no architectural consideration in a crop model, the total number of leaves is assigned by observation or by an empirical formula, which can change when conditions change. On the other hand, C partitioning, though introduced into the model (Lizaso et al. 2011), is separated from changes in leaf area.

Another crucial weakness in crop models is the simplification of carbohydrate allocation, which is also a challenge to almost all plant growth models. HI is usually used for grain yield estimation, but it varies with biomass production dynamics and depends on the growth strategy implemented by plants, which may also change with climate, plantation layout, irrigation scheme, and fertilization strategies. Moreover, organ abortion caused by stress is a more crucial factor for HI but is usually overlooked in crop models. All these indeterminate factors may lead to a loss of efficiency in HI. In a review of carbon allocation

modelling undertaken by Marcelis (2007), it was found that plant architecture information is more important for the more mechanistic approaches. Allocation takes place in all expanding organs, which depends on organ initiation, abortion and senescence, whilst for large vascular plants the carbohydrate transport pathway and phloem physiology can become important. For these considerations, knowledge of plant architecture is needed.

Neither do crop models take into account secondary stem growth, which is not important for herbaceous plants but significant for woody plants such as cotton.

Potential and limitations of FSPMs. The principal merits of FSPMs come from their emphasis on the interaction between plant development dynamics and plant physiological processes. Plant architectures provide a full view of a plant's history, for meristem functions as well as biomass production and partitioning, which reflects genetic regulation and environmental constraints (Barthélémy and Caraglio 2007). By tracing the evolution of plant architecture, it should provide us with a clue as to how morphogenesis, photosynthetic functions, carbohydrate allocation and resource acquisition mediate and cooperate with each other. Explicit descriptions in topological and geometric structures with interconnections between organs provide a means of looking into the underlying processes and functions, with which to regulate the carbohydrate allocation process, and it should be possible to estimate a more accurate “HI” for grain yield computation. As architecture development is greatly determined by genetic information, it is possible to find effective variables or parameters to be used for genotype studies. Lastly, 3D plants can be used for different applications, such as visualization, radiation interception simulation (reviewed by Chelle and Andrieu 2007), water transpiration (e.g. Dauzat and Rapidel 2001), biomechanical functions (e.g. Fourcaud et al. 2003; Sellier and Fourcaud 2006), and to aid the retrieval of vegetation properties (Casa et al. 2010).

However, at present, FSPMs commonly encounter difficulties in plant growth studies and yield computation. One problem arises from measurements. Plant architectures are laborious to record and manage, as the data are cumbersome and very frequently accompanied with great variability from one individual to another, since stochastic behaviours exist in meristems. How can this be dealt with?

Passage from the individual plant function to the plant population function is not clear and is still a challenge. Improving field productivity is not a simple question of having the best individual performance, but also importantly depends on the compound effects from populations. Individuals compete with each other for limited space, light, water and nutrients,

and conversely as a whole they can change the environment (e.g. temperature). Individual variability as a direct result of competition is an indispensable component for understanding compound effects. Several authors (Muldoon and Daynard 1981; Tollenaar and Wu 1999; Liu et al. 2004b) have suggested that field productivity is highly related to variability (or uniformity). High individual variability always takes place with a yield reduction.

Another serious problem comes from the general manipulation of the FSPM itself. Computation of parallel organ growth is time consuming and demanding in memory space. As light interception is taken into account in most FSPMs, building the plant architecture, carrying out Ray-Tracing or Radiosity for radiation computation at each step of growth is another crucial cost for computation. Moreover, continual construction of plant architecture based on biomass transportation and partitioning requires additional time. The heavy computation involved in all these processes may bar the method from some practical uses.

The last problem is parameter estimation and model calibration. A large proportion of FSPMs mainly use simulation techniques, so they do not have equations for direct reverse computation. Heuristic inverse algorithms such as Simulated Annealing and PSO would be required to search for solutions from the continuous repetition of simulations. Depending on the time needed for one simulation, calibration of the model may be practically impossible (Fourcaud et al. 2008). To help solve this problem, it can be advocated to build equations which underly the simulations. Staying in the domain of hypothesis testing using simulations may inspire researchers, but they could lack the ability for agricultural applications.

A solution from GreenLab. GreenLab has proposed a solution able to overcome the difficulties mentioned above. As a mathematical model, it takes into account assimilation and carbon allocation as the main growth functions, which is supported by architectural processes and can reversely supply architectural development. For growth processes, the GreenLab model is a close relative of PBM models (e.g. TOMSIM, Heuvelink 1996; 1999) and shares knowledge in:

- Assimilative biomass as a common pool shared by all organs. The compartments of organs are often used in PBMs. If they are detailed into leaves, internodes, fruits, roots, GreenLab has the equivalence for them, since in GreenLab the sum of the organs attached to the plant architecture gives the corresponding compartment.
- The light exposure model is adopted. Through an individual theoretical projective area (S_p), GreenLab adapts LAI into individual level computations, whereby the leaf area is

computed dynamically using the accumulative living leaf biomass and the *e*. In this way, production depends mainly on LAI and RUE.

- Biomass allocation is regulated by the source-sink processes, where assimilative production and partitioning are computed separately. Relative sink strengths are used for organs.

The philosophy shared by all FSPMs that plant functions interact with architecture development is kept in GreenLab, while efforts have been made to replace heavy simulations with equations.

- Substructure factorizations are used for topological structure analysis. Therefore, the number of organs can be obtained directly without constructing the architecture during plant development.
- A light exposure model is used in place of radiation interception simulation using plant architecture. As leaf areas are regulated by the source-sink process, precision has been better guaranteed compared with PBM. Particularly, the heavy computation of light distribution in 3D plants has been avoided. Light interception at individual level is determined by S_p, which is treated as a plant performance indicator and computed by inverse method.
- Organ production is computed from architectural development equations in GreenLab, which is rapid when compared with the simulation of organogenesis. Organs enter directly in the source-sink functions which compute their demand and manage biomass partitioning.
- Parameter identification, optimization and sensitivity analyses are available because the dynamic equations of the GreenLab model provide support for that.
- Specific stochastic and feed-back accounts are a promising bonus for advanced studies.
- Finally, as a result of this PhD thesis, it becomes possible to build a passage from individuals to plant populations. In particular, individual variability in emergence and plant architectural performances (S_p) are retrieved by the combination study with PILOTE and its own inverse method.

For the next step, focus should continue to be placed on individual variability, particularly the effects of stress or heterogeneity on individual plant behaviour, and it is important to take into account the supporting architectures, in order to answer some specific

agricultural questions. For instance, in this thesis, individual variability was found in emergence and plant performance. Are they interrelated with each other? While in terms of the model, questions on model abilities remain to be explored. Taking GreenLab as an example, if S_p is sufficient for indicating plant performance, how can it be used for further stress studies? At the same time, support for genetics studies is another topical task, as breeding is a substantial way of bringing about a revolution in crop production. In most genetic studies, plant architecture has not been considered, as emphasis has only been placed on specific physiological processes. Attempts by Letort and co-workers (2008) highlighted a new approach to studying more fundamental traits for QTL (quantitative trait loci) determination with FSPMs.

5.2 FSPMs for silvicultural studies

5.2.1 Architecture for trees

The significance of spatial structure has long been a concern in tree studies. Some classic theories have been established on the basis of structures, such as the famous pipe model (Shinozaki et al. 1964). Also the first FSPMs were proposed for trees (Perttunen et al. 1996; de Reffye et al. 1997a). Compared with herbaceous plants, trees usually have more complicated structures and development stages, and their functions are shown to have a more obvious dependence on them.

In the application to combine GreenLab with PNN (Chapter 4), the black pine used is a tree with a simple architecture, in which each GU (whorl) only has branching at the top of the GU. Consequently, deterministic architecture is quite efficient for representing it, whereas the number of branches is based on the output from the PNN model.

However, most trees display stochastic features in their architecture, which are essentially determined by meristem behaviour. Generally, meristem functions can be divided into three types with their probability features: growth, death and branching (de Reffye et al. 1988). Continuous development can be simulated using a Bernoulli process interacting with a mortality law. However, for trees with rhythmic growth the case can be more complicated, because the creation of GCs is also a stochastic event. In this case the number of phytomers inside a shoot follows a compound distribution. It is essential to take into account the stochastic structures of plants in functional studies, since the stochastic process determines the initiation of organs and then determines plant development and growth.

The implementation of simulation and reverse computation for stochastic plants is the second level of GreenLab (GL2), which was first developed in GreenScilab software but with great simplifications. All the phytomers generated in a GU, which are provided by stochastic simulation, are created at the beginning of the GC, so photosynthetic production and carbon allocations from and to these phytomers are treated identically. Trees such as pine or maple usually produce only one GU per year in a short period, so the simplification with regard to phytomers in a GU as a whole is acceptable. However, a large proportion of trees have preformation, neoformation and polycyclism, such as cherry, poplar, elm and walnut. For these trees, the detailed development and growth history is crucial for a correct simulation, thus a finer CU is needed to enter the GU sub-process. An upgraded GreenLab level (GL5) has been launched for that purpose and is under development in two software packages: Qing Yuan (Hu et al. 2003, at LIAMA) and GLOUPS (de Reffye, at CIRAD-AMAP). It is worth noting that AMAPsim software is already able to simulate the architectural development of various kinds of trees very correctly. That said, it should be noted that the architectural dynamics are only the visible parts. The phytomers distributed in a GU are simulated and delivered to reference axes without considering the meristem resting periods (pause in development) inside a GU or between GUs. However, both the resting and active meristem periods are made use of by organ growth processes (e.g. photosynthesis and carbon allocation), and the real growth durations are easily overlooked by modellers when simulating perennial trees as they are not visible directly.

5.2.2 Integration of FSPMs and EFMs

In order to have long-term economic productivity, achieving sustainable development is a substantial objective for forest management. However, a forest is a complex spatio-temporal system, in which trees, the environment and humans play key roles, and interact with each other. Consequently, models are highly significant for decision-support, since they can synthesize knowledge and information, and provide scenario simulations.

Abilities and limitations of EFMs. Through statistical methods, EFMs can integrate system knowledge including various ecological factors (e.g. site conditions, stand structure, inter-plant competition) and management scenarios in the prediction of forest stand growth, even without any understanding of the eco-physiological functions of trees. This approach played an irreplaceable role in the early stages of forest research. However, the major limitation of this empirical method is that the underlying processes and interactions have been overlooked in the analysis of final production based on system inputs. Thus, they are not very

reliable for changing conditions, which is a great challenge for them in terms of their advanced capabilities (Landsberg and Sands 2011).

Role of FSPMs. FSPMs can be difficult to apply directly in forest growth studies, since they are individual-based and involve high computing time and memory space requirements for trees. However, as they are built from mechanistic considerations, in which the physiological processes regulated together with the spatial-temporal organization of plant components, they can provide suitable knowledge or underlying support to serve other models or approaches for silvicultural studies.

Model coupling. From a methodology viewpoint, EFMs can be described as macro, system and direct (or so-called black box), whereas FSPMs can be described as relatively micro, process-based and detailed. They are opposite but also complementary. In the practice of coupling models for black pines (Chapter 4), the PNN EFM provided growth simulation for trees and for the stand according to thinning scenarios, whilst the GreenLab FSPM supplied the supporting structures from its architectural model. Although there has been no consideration of biomass, the development process of trees has been established.

Prospects. Development is the result of meristem activity, which is closely connected with the environment. For instance, self-thinning intensity and time largely depend on the planting density, which can express architectural plasticity (Cournède et al. 2008). From the interrelation between development and growth, the plasticity in building GUs is very important. Meristem death and branching patterns and the relevant distribution of phytomers can be greatly modified in competition for space (de Reffye et al. 1995).

Moreover, meristem activity also depends on genetic factors. If such variables can be retrieved from architectural information with the help of stochastic computation by software packages like GreenScilab, a comparison between species or cultivars becomes possible, with or without consideration of different treatments.

In order to make model coupling between an EFM and an FSPM a generalized method, the biggest problem can be missing architectural information. EFMs commonly consider dimensional (e.g. tree height, *dbh*, *Hcb*) and sometimes also geometric (e.g. height of branches, insertion angle) attributes of plant structure, whereas a structural unit such as a phytomer, GU and their topological connections are ignored. Except for some simple cases (e.g. pine tree), the creation time and the number of GUs can be processed from geometric variables (e.g. branch increments) and time durations. More frequently, additional

observations are needed. The cost of accurate measurements may not be extremely heavy if simplifications can be made using architectural concepts, such as PAs. As architectural models have provided general descriptions of almost all plants, the development of trees can directly benefit from them. In this way, additional measurement costs can be reduced to a large extent.

As wood production essentially comes from biomass production and partitioning, physiological processes can be integrated, but the accuracy in locating functioning organs and managing time information for organs largely depends on the architectural construction. Be that as it may, before a whole FSPM is available for application on a stand level, there will be plenty of preconditions that will have to be met, such as parameter calibration, and appropriate measures to upscale individual-based FSPMs into stand-level FSPMs, etc.

As trees can develop a very complicated structure over their long life-spans, available reverse computations are seldom available in FSPMs. GLOUPS software is dedicated to solving the source-sink processes with an explicit description of architectural development, which might provide an efficient tool for that purpose and is very much awaited.

Introducing biomass and the supporting structure into crop or forest growth studies is a promising way whereby the dynamic spatial-temporal distribution of mass and energy can open up new approaches to advanced agricultural or silvicultural/ecological problems.

References

References

Allen MT, Prusinkiewicz P, DeJong TM. 2005. Using L-systems for modeling source–sink interactions, architecture and physiology of growing trees: the L-PEACH model. *New Phytologist* 166: 869-880.

Auclair D (2010) Forest and natural ecosystem managers in the landscape – multiscale modelling, challenges and opportunities. In: Fabre JC, Jaeger M, Louchart X, Muller JP (eds) LandMod 2010: International Conference on Integrative Landscape Modelling, Montpellier, France. www.symposcience.org.

Barczi J-F, Reffye P de, Caraglio Y. 1997. Essai sur l'identification et la mise en oeuvre des paramètres nécessaires à la simulation d'une architecture végétale: le logiciel AMAPsim. In: J Bouchon, P de Reffye, D Barthélémy, eds. *Medélisation et Simulation de l'Architecture Des Végétaux*. Paris: Science Update, 205-254.

Barczi J-F, Rey H, Caraglio Y, Reffye P de, Barthélémy D, Dong Q, Fourcaud T. 2008. AmapSim: A Structural Whole-plant Simulator Based on Botanical Knowledge and Designed to Host External Functional Models. *Annals of Botany* 101: 1125-1138.

Barthélémy D, Caraglio Y (2007) Plant architecture: a dynamic, multilevel and comprehensive approach to plant form, structure and ontogeny. Ann Bot 99:375-407

Barthélémy D, Caraglio Y, Costes E. 1997. Architecture, gradients morphogénétiques et âge physiologique chez les végétaux. In: J Bouchon, P de Reffye, D Barthélémy, eds. *Modélisation et simulation de l'architecture des végétaux*. Paris: Sciences Update, 89-136.

Bernier G, Havelange A, Houssa C, Petitjean A, Lejeune P. 1993. Physiological Signals That Induce Flowering. *The Plant Cell Online* 5: 1147-1155.

Bernier G. 1988. The control of floral evocation and morphogenesis. *Annual review of plant physiology* 39: 175-219.

Biliouris D, Van der Zande D, Verstraeten WW, Muys B, Coppin P (2009) Assessing the impact of canopy structure simplification in common multilayer models on irradiance absorption estimates of measured and virtually created *Fagus silvatica* (L.) stands. Remote Sens 1:1009-1027

Booch G, Rumbaugh J, Jacobson I. 1998. *The Unified Modeling Language User Guide, the originaldevelopers of the UML* (JC Shanklin, Ed.). Addison Wesley.

Bosanac B, Zanchi P (2002) Onyx Tree Conifer User's Manual, version 5.1. Onyx Computing Inc, Cambridge, MA

Bouman BAM, Keulen H van, Laar HH van, Rabbinge R. 1996. The “School of de Wit” crop growth simulation models: A pedigree and historical overview. *Agricultural Systems* 52: 171-198.

Brisson N, Gary C, Justes E, Roche R, Mary B, Ripoche D, Zimmer D, Sierra J, Bertuzze P, Burger P, Bussiere F, Cabidoche YM, Cellier P, Debaeke P, Gaudillere JP, Henault C, Maraux F, Seguin B, Sinoquet H. 2003. An overview of the crop model STICS. *European journal of agronomy* 18: 309-332.

Brugnach M, Pahl-Wostl C, Lindenschmidt KE et al (2008) Complexity and uncertainty: rethinking the modelling activity. In: Jakeman AJ, Voinov AA, Rizzoli AE, Chen SH (eds) Environmental modelling, software and decision support, Elsevier, Amsterdam, NL, pp 49-68

Casa R, Baret F, Buis S, Lopez-Lozano R, Pascucci S, Palombo A, Jones H. 2010. Estimation of maize canopy properties from remote sensing by inversion of 1-D and 4-D models. *Precision Agriculture* 11: 319-334.

Castel T, Beaudoin A, Floury N, Le Toan T, Caraglio Y, Barczi JF (2001) Deriving forest canopy parameters for backscatter models using the AMAP architectural plant model. IEEE Trans Geosci Remote Sens 39:571-583

Cescatti A (1997) Modelling the radiative transfer in discontinuous canopies of asymmetric crowns. I. Model structure and algorithms. Ecol Mod 101:263-274

Cheeroo-Nayamuth B. 2000. Crop modelling/simulation: An overview. In: JA Lalouette, DY Bachraz, N Sukurdeep, eds. *Procedings of the Fourth Annual Meeting of Agricultural Scientists*. Reduit, Mauritius, 21-22 October 1999: THE FOOD AND AGRICULTURAL RESEARCH COUNCIL, 11-26.

Chelle M, Evers JB, Combes D, Varlet-Grancher C, Vos J, Andrieu B. 2007. Simulation of the three-dimensional distribution of the red:far-red ratio within crop canopies. *New Phytologist* 176: 223-234.

Cheng Z-L, Zhang X-P, Chen B-Q. 2007. Simple Reconstruction of Tree Branches from a Single Range Image. *Journal of Computer Science and Technology* 22: 846-858.

Cline MG. 1991. Apical dominance. *The Botanical review* 57: 318-358.

Collin A, Lamorlette A, Bernardin D, Séro-Guillaume O (2011) Modelling of tree crowns with realistic morphological features: new reconstruction methodology based on Iterated Function System tool. Ecol Mod 222:503-513

Cook ER. 1985. A time series analysis approach to tree ring standardization.

Côté JF, Fournier RA, Egli R (2011) An architectural model of trees to estimate forest structural attributes using terrestrial LiDAR. Environ Model Softw 26:761-777

Cournède PH, Guyard T, Bayol B, Griffon S, de Coligny F, Borianne P, Jaeger M, de Reffye P. 2009. A Forest Growth Simulator Based on Functional-Structural Modelling of Individual Trees. Third International Symposium on Plant Growth Modeling, Simulation, Visualization and Applications (PMA09), Beijing : Chine (2009)

Cournède P-H, Kang M, Mathieu A, Barczi J-F, Yan H, Hu B, Reffye P de. 2006. Structural Factorization of Plants to Compute Their Functional and Architectural Growth. *Simulation* 82: 427-438.

Cournède P-H, Mathieu A, Houllier F, Barthélémy D, Reffye P de. 2008. Computing competition for light in the GREENLAB model of plant growth: a contribution to the study of the effects of density on resource acquisition and architectural development. *Annals of botany* 101: 1207-1219.

Dauzat J, Clouvel P, Luquet D, Martin P. 2008. Using Virtual Plants to Analyse the Light-foraging Efficiency of a Low-density Cotton Crop. *Annals of Botany* 101: 1153-1166.

Dauzat J, Rapidel B. 2001. Simulation of leaf transpiration and sap flow in virtual plants: model description and application to a coffee plantation in Costa Rica. *Agricultural and forest meteorology* 109: 143-160.

de Coligny F. 2009. Wiki of simeo. http://amap-dev.cirad.fr/projects/simeo/wiki/Simeo. Checked in June, 2011

de Reffye P (2009) Production végétale et architecture des plantes. Comptes-rendus, Académie d'Agriculture de France, http://www.academie-agriculture.fr/mediatheque/seances/20090128 resume3integral.pdf

de Reffye P, Dinouard P, Barthélémy D. 1991. Modélisation et simulation de l'architecture de l'Orme du Japon Zelkova serrata (Thunb.) Makino (Ulmaceae): la notion d'axe de référence. *Comptes Rendus du 2ème Colloque International Sur l'Arbre*. Montpellier, 10-15, Septembre 1990: Naturalia Monspeliensia, 251–266.

de Reffye P, Edelin C, Françon J, Jaeger M, Puech C (1988) Plant models faithful to botanical structure and development. *Comput Graph* 22:151–158

de Reffye, Goursat M, Quadrat JP, Hu B. 2003. *The dynamic equations of the tree morphogenesis GreenLab model*.

de Reffye P, Heuvelink E, Barthélémy D, Cournède P-H. 2008. Plant Growth Models. In: SE Jorgensen, B Fath, eds. *Encyclopedia of Ecology*. Oxford: Academic Press, 2824-2837.

de Reffye P, Houllier F (1997 a) Modelling plant growth and architecture: some recent advances and applications to agronomy and forestry. *Curr Sci* 73:984-992

de Reffye P, Houllier F, Blaise F, Fourcaud T. (1997 b). Essai sur les relations entre l'architecture d'un arbre et la grosseur de ses axes végétatifs. In: Bouchon J, de Reffye P, Barthélémy D (eds) *Modélisation et simulation de l'architecture des végétaux*. Paris, France: INRA, 225-425.

de Reffye P, Hu B. 2003. Relevant qualitative and quantitative choices for building and efficient dynamic plant growth model: GreenLab case. In: B Hu, M Jaeger, eds. *International Symposium on Plant Growth Modeling, Simulation, Visualization and their Applications - PMA'03*. Beijing, China, 87-107.

Deleuze C, Houllier F. 2002. A flexible radial increment taper equation derived from a process-based carbon partitioning model. *Annals of forest science* 59: 141-154.

Deussen O, Lintermann B (2005) Digital design of nature: computer generated plants and organics. Springer, Berlin

Diggle PK. 2002. A developmental morphologist's perspective on plasticity. *Evolutionary Ecology* 16: 267-283.

Dingkuhn M, Luquet D, Quilot B, Reffye P de. 2005. Environmental and genetic control of morphogenesis in crops: towards models simulating phenotypic plasticity. *Australian Journal of Agricultural Research* 56: 1-14.

Dong Q, Louarn G, Wang Y, Barczi J-F, Reffye P De. 2008. Does the Structure–Function Model GreenLab Deal with Crop Phenotypic Plasticity Induced by Plant Spacing? A Case Study on Tomato. *Annals of Botany* 101: 1195-1206.

Dreyfus P (1993) Modelling Austrian black pine response to silvicultural practices in the South East of France. In: Burkhart HE, Gregoire TG, Smith JL (eds) Proc IUFRO S4.01 conf "Modelling stand response to silvicultural practices". Publ FWS-1-93, Virginia Polytech Inst and State Univ, Blacksburg, VA, pp 5-18

Dufour-Kowalski S, Courbaud B, Dreyfus P, Meredieu C, de Coligny F (200x) Capsis: an open software framework and community for forestry modelling. Ann For Sci, accepted

Dunbabin V, Diggle A, Rengel Z. 2003. Is there an optimal root architecture for nitrate capture in leaching environments? *Plant, cell and environment* 26: 835-844.

Edmeades GO, Daynard TB. 1979. The development of individual variability in maize at different planting densities. *Canadian Journal of Plant Science* 59: 561-576.

Evers JB, Vos J, Chelle M, Andrieu B, Fournier C, Struik PC. 2007. Simulating the effects of localized red:far-red ratio on tillering in spring wheat (Triticum aestivum) using a three-dimensional virtual plant model. *New Phytologist* 176: 325-36.

Ford JH, Hicks DR. 1992. Corn growth and yield in uneven emerging stands. *Journal of production agriculture* 5: 185-188.

Fourcaud T, Blaise F, Lac P, Castéra P, Reffye P de. 2003. Numerical modelling of shape regulation and growth stresses in trees. *Trees - Structure and Function* 17: 31-39.

Fourcaud T, Zhang X, Stokes A, Lambers H, Körner C. 2008. Plant growth modelling and applications: the increasing importance of plant architecture in growth models. *Annals of Botany* 101: 1053-63.

Fournier C, Andrieu B. 1998. A 3D Architectural and Process-based Model of Maize Development. *Annals of Botany* 81: 233-250.

Fournier C, Andrieu B. 1999. ADEL-maize: an L-system based model for the integration of growth processes from the organ to the canopy. Application to regulation of morphogenesis by light availability. *Agronomie* 19: 313-327.

Fritts HC. 1966. Growth-Rings of Trees: Their Correlation with Climate. *Science* 154: 973-979.

Geber MA, Watson MA, Kroon H de. 1997. Organ Preformation, Development, and Resource Allocation in Perennials. In: FA Bazzaz, J Grace, eds. *Plant Resource Allocation*. San Diego: Academic Press, 113-141.

Gesch RW, Archer DW. 2005. Influence of sowing date on emergence characteristics of maize seed coated with a temperature-activated polymer. *Agronomy journal* 97: 1543-1550.

Gifford RM, Evans LT. 1981. Photosynthesis, Carbon Partitioning, and Yield. *Annual Review of Plant Physiology* 32: 485-509.

Godin C, Caraglio Y. 1998. A Multiscale Model of Plant Topological Structures. *Journal of Theoretical Biology* 191: 1-46.

Green PJ. 1984. Iteratively reweighted least squares for maximum likelihood estimation, and some robust and resistant alternatives. *Journal of the Royal Statistical Society. Series B. Methodological* 46: 149-192.

Griffon S, Nespoulous A, Cheylan JP, Marty P, Auclair D (2011) Virtual reality for cultural landscape visualization. Virtual Reality, in press. doi: 0.1007/s10055-010-0160-z

Guedon Y, Puntieri JG, Sabatier S, Barthélémy D. 2006. Relative extents of preformation and neoformation in tree shoots: Analysis by a deconvolution method. *ANNALS OF BOTANY* 98: 835-844.

Guo Y, Ma Y, Zhan Z, Li B, Dingkuhn M, Luquet D, de Reffye P. 2006. Parameter Optimization and Field Validation of the Functional–Structural Model GreenLab for Maize. *Annals of Botany* 97: 217-230.

Hallé F, Oldeman R. 1970. *Essai sur l'architecture et la dynamique de croissance des arbres tropicaux*. Paris: Masson.

Hallé F, Oldeman RAA, Tomlinson PB. 1978. Tropical trees and forests. Springer, Berlin

Hammer GL, Oosterom E van, McLean G, Chapman SC, Broad I, Harland P, Muchow RC. 2010. Adapting APSIM to model the physiology and genetics of complex adaptive traits in field crops. *Journal of Experimental Botany* 61: 2185-2202.

Hemmerling R, Kniemeyer O, Lanwert D, Kurth W, Buck-Sorlin GH. 2008. The rule-based language XL and the modelling environment GroIMP illustrated with simulated tree competition. *Functional plant biology* 35: 739-750.

Heuvelink E. 1996. Dry matter partitioning in tomato: Validation of a dynamic simulation model. *Annals of botany* 77: 71-80.

Heuvelink E. 1999. Evaluation of a Dynamic Simulation Model for Tomato Crop Growth and Development. *Annals of Botany* 83: 413-422.

Hu B, de Reffye P, Zhao X. 2003. GreenLab: a new methodology towards plant functional-structural model-structural aspect. In: BG Hu, M Jaeger, eds. *Procedings of 1st International Symposium on Plant Growth Modeling, Simulation,Visualization and Applications (PMA03)*. Beijing, China: Tsing Hua University Press and Springer, 21-35.

Hughes MK. 2002. Dendrochronology in climatology - the state of the art. *Dendrochronologia* 20: 95-116.

Ipsilandis CG, Vafias BN. 2005. Plant density effects on grain yield per plant in maize: Breeding implications. *Asian Journal of Plant Sciences* 4: 31-39.

Ittersum MK van, Leffelaar PA, Keulen H Van, Kropff MJ, Bastiaans L, Goudriaan J. 2003. On approaches and applications of the Wageningen crop models. *European journal of agronomy* 18: 201-234.

Jacobson I, Christerson M, Jonsson P, Overgaard G. 1992. *Object-Oriented Software Engineering: A Use Case Driven Approach*. Addison-Wesley.

Jaeger M, de Reffye P. 1992. Basic concepts of computer simulation of plant growth. *Journal of Biosciences* 17: 275-291.

Jallas E, Sequeira R, Martin P, Turner S, Papajorgji P (2009) Mechanistic virtual modeling: coupling a plant simulation model with a three-dimensional plant architecture component. Environ Model Assess 14:29-45

Janssen JM, Lindenmayer A. 1987. Models for the control of branch positions and flowering sequences of Capitula in Mycelis muralis (L.) Dumont (Compositae). *New phytologist* 105: 191-220.

Jones JW, Hoogenboom G, Porter CH, Boote KJ, Batchelor WD, Hunt LA, Wilkens PW, Singh U, Gijsman AJ, F JTR. 2003. The DSSAT cropping system model. *European Journal of Agronomy* 18: 235-265.

Kang M, Cournède P-H, Reffye P de, Auclair D, Hu B. 2008. Analytical study of a stochastic plant growth model: Application to the GreenLab model. *Mathematics and Computers in Simulation* 78: 57-75.

Kang M, de Reffye, Barczi J-F. 2003. Fast algorithm for stochastic tree computation. *WSCG'2003.* Plzen, Czech Republic: Union agency-Science press, .

Kang M, de Reffye P, Cournède P-H. 2009. Modeling the Growth of Inflorescence. *Proceedings of 3rd International Symposium on Plant Growth Modeling, Simulation, Visualization and Applications (PMA09)*. Washington, DC, USA: IEEE Computer Society, 303-310.

Kang M, Evers JB, Vos J, de Reffye P. 2008b. The Derivation of Sink Functions of Wheat Organs using the GreenLab Model. *Annals of Botany* 101: 1099-1108.

Kang M, Heuvelink E, de Reffye P. 2006a. Building virtual chrysanthemum based on sink-source relationships: preliminary results. *Acta Hortic* 718: 129–136.

Kang M, Qi R, de REFFYE de, Hu B. 2006b. GreenScilab:A toolbox simulating plant growth in the Scilab environment, in : 8th Middle Eastern Simulation Multiconference, Alexandria, Egypt: 174-178

Kang M, Reffye P de, Hu B, Zhao X. 2004. Fast construction of geometrical structure of plant with substructures algorithm. *Journal of Image and Graphics2* 9: 79-86.

Kang M, Yang L, Zhang B, de Reffye P. 2011. Correlation between dynamic tomato fruit-set and source–sink ratio: a common relationship for different plant densities and seasons? *Annals of Botany* 107: 805-815.

Keating B, Carberry P, Hammer G, Probert M, Robertson M, Holzworth D, Huth N, Hargreaves J, Meinke H, Hochman Z, McLean G, Verburg K, Snow V, Dimes J, Silburn M, Wang E, Brown S, Bristow K, Asseng S, Chapman S, McCown R, Freebairn D, Smith C. 2003. An overview of

APSIM, a model designed for farming systems simulation. *European journal of agronomy* 18: 267-288.

Khaledian MR, Mailhol J-C, Ruelle P, Rosique P. 2009. Adapting PILOTE Model for Water and Yield Management under Direct Seeding System: The Case of Corn and Durum Wheat in a Mediterranean Context. *Agricultural Water Management* 96: 757-770.

Kimmins JP, Blanco JA, Seely B, Welham C, Scoullar K (2008) Complexity in modelling forest ecosystems: how much is enough? For Ecol Manage 256:1646–1658

King DA (2005) Linking tree form, allocation and growth with an allometrically explicit model. Ecol Mod 185:77–91

Kohyama T, Canadell J, Ojima DS, Pitelka LF (2005) Forest ecosystems and environments: scaling up from shoot module to watershed. Ecol Res 20:241-242

Lacointe A. 2000. Carbon allocation among tree organs: A review of basic processes and representation in functional-structural tree models. *Annals of Forest Science* 57: 521-533.

Ladier J, Rey F (eds) (2011) Guide des Sylvicultures de Montagne pour les Alpes du Sud françaises. ONF-Cemagref-INRA, Paris, in press

Lambers H, Shane MW, Cramer MD, Pearse SJ, Veneklaas EJ. 2006. Root Structure and Functioning for Efficient Acquisition of Phosphorus: Matching Morphological and Physiological Traits. *Annals of Botany* 98: 693-713.

Landsberg J, Sands P. 2011. The Carbon Balance of Trees and Stands. *Physiological Ecology of Forest Production*. US: ACADEMIC PRESS ,Elsevier, 115-149.

Lange E (2001) The limits of realism: perceptions of virtual landscapes. Landsc Urban Plan 54:163-182

Lauer JG, Rankin M. 2004. Corn Response to Within Row Plant Spacing Variation. *Agronomy Journal* 96: 1464-1468.

Letort V, Cournède P-H, Mathieu A, de Reffye P, Constant T. 2008. Parametric identification of a functional-structural tree growth model and application to beech trees (Fagus sylvatica). *Functional plant biology* 35: 951-963.

Li D, ZHAN Z, Guo Y. 2009. Improving the Calibration Process of GreenLab Model on the Cotton Plant. In: W Cao, JW White, E Wang, eds. *Crop Modeling and Decision Support*. Springer Berlin Heidelberg, 209-218.

Lim EM, Honjo T (2003) Three-dimensional visualization of forest landscapes by VRML. Landsc Urban Plan 63:175-186

Liu W, Tollenaar M, Stewart G, Deen W. 2004b. Impact of Planter Type, Planting Speed, and Tillage on Stand Uniformity and Yield of Corn. *Agronomy Journal* 96: 1668-1672.

Liu W, Tollenaar M, Stewart G. 2004a. Response of Corn Grain Yield to Spatial and Temporal Variability in Emergence. *Crop Science* 44: 847-854.

Lizaso JI, Boote KJ, Jones JW, Porter CH, Echarte L, Westgate ME, Sonohat G. 2011. CSM-IXIM: A New Maize Simulation Model for DSSAT Version 4.5. *Agronomy journal* 103: 766-779.

Ma Y, Li B, Zhan Z, Guo Y, Luquet D, Reffye P de, Dingkuhn M. 2007. Parameter stability of the functional-structural plant model GREENLAB as affected by variation within populations, among seasons and among growth stages. *Annals of Botany* 99: 61-73.

Ma Y, Wen M, Guo Y, Li B, Cournède P-H, Reffye P de. 2008. Parameter optimization and field validation of the functional-structural model GREENLAB for maize at different population densities. *Annals of botany* 101: 1185-94.

Ma Y, Wubs AM, Mathieu A, Heuvelink E, Zhu JY, Hu B, Cournède P-H, Reffye P de. 2011. Simulation of fruit-set and trophic competition and optimization of yield advantages in six Capsicum cultivars using functional–structural plant modelling. *Annals of Botany* 107: 793-803.

Maddonni GA, Otegui ME. 2004. Intra-specific competition in maize: early establishment of hierarchies among plants affects final kernel set. *Field Crops Research* 85: 1-13.

Mailhol J-C, Olufayo AA, Ruelle P. 1997. Sorghum and Sunflower Evapotranspiration and Yield from Simulated Leaf Area Index. *Agricultural Water Management* 35: 167-182.

Mäkelä A (2003) Process-based modelling of tree and stand growth: towards a hierarchical treatment of multiscale processes. Can J For Res 33:398–409

Mäkelä A, Landsberg J, Ek AR et al (2000) Process-based models for forest ecosystem management: current state of the art and challenges for practical implementation. Tree Physiol 20:289-298

Marcelis LFM, Heuvelink E, Goudriaan J. 1998. Modelling biomass production and yield of horticultural crops: a review. *Scientia Horticulturae* 74: 83-111.

Marcelis LFM, Heuvelink E. 2007. Concepts of modelling carbon allocation among plant organs. In: J Vos, LFM Marcelis, PHB de Visser, SP C, JB Evers, eds. *Functional-Structural Plant Modelling in Crop Production.* Dordrech: Springer, 103-111.

Mathieu A, Cournède PH, Letort V, Barthélémy D, de Reffye P (2009) A dynamic model of plant growth with interactions between development and functional mechanisms to study plant structural plasticity related to trophic competition. Ann Bot 103:1173-1186

Mathieu A, Zhang B, Heuvelink E, Liu S, Cournède P-H, Reffye P De. 2007. Calibration of Fruit Cyclic Patterns in Cucumber Plants as a Function of Source-Sink Ratio with the GreenLab Model. In: P Prusinkiewicz, J Hanan, B Lane, eds. *Proceedings of the 5th international workshop on Functional-Structural Plant Models (FSPM07)*. Napier, New Zealand: HortResearch, 5-1~4.

Měch R, Prusinkiewicz P. 1996. Visual Models of Plants Interacting with Their Environment Visual Models of Plants. *SIGGRAPH 96*. New Orleans, Louisiana, US, 397−410.

Melson SL, Harmon ME, Fried JS, Domingo JB (2011) Estimates of live-tree carbon stores in the Pacific Northwest are sensitive to model selection. Carbon Balance Manage 6:2

Meredieu C, Caraglio Y, Saint-André L, de Coligny F, Barczi JF (2004) The advantages of coupling stand description from growth models to tree description from architectural models. In: Godin C, Hanan J, Kurth W et al (eds) 4th international workshop on functional-structural plant models, 7-11 june 2004, Montpellier, France, pp 243-247

Muldoon JF, Daynard TB. 1981. Effects of within-row plant uniformity on grain yield of maize. *Canadian Journal of Plant Science* 61: 887-894.

Muys B, Hynynen J, Palahí M et al (2010) Simulation tools for decision support to adaptive forest management in Europe. For Syst 19:86-99

Nafziger ED, Carter PR, Graham EE. 1991. Response of corn to uneven emergence. *Crop science* 31: 811-815.

Nafziger ED. 1996. Effects of missing and two-plant hills on corn grain yield. *Journal of production agriculture* 9: 238-240.

Oppenheimer PE. 1986. Real time design and animation of fractal plants and trees. *Proceedings of the 13th annual conference on Computer graphics and interactive techniques*. New York, NY, USA: ACM, 55-64.

Parsons RA, Mell WE, McCauley P (2011) Linking 3D spatial models of fuels and fire: effects of spatial heterogeneity on fire behavior. Ecol Model 222:679-691

Pearcy RW, Muraoka H, Valladares F. 2005. Crown architecture in sun and shade environments: assessing function and trade-offs with a three-dimensional simulation model. *New Phytologist* 166: 791-800.

Perttunen J, Sievänen R, Nikinmaa E (1998) LIGNUM: a model combining the structure and the functioning of trees. Ecol Model 108:189-198

Perttunen J, Sievänen R, Nikinmaa E, Salminen H, Saarenmaa H, Väkevä J. 1996. LIGNUM: A Tree Model Based on Simple Structural Units. *Annals of Botany* 77: 87-98.

Pommel B, Bonhomme R. 1998. Variations in the vegetative and reproductive systems in individual plants of an heterogeneous maize crop. *European Journal of Agronomy* 8: 39-49.

Pretzsch H, Grote R, Reineking B, Rötzer T, Seifert S. 2008. Models for Forest Ecosystem Management: A European Perspective. *Annals of Botany* 101: 1065-1087.

Pretzsch H. 2009. *Forest Dynamics, Growth and Yield*. Berlin: Springer.

Prusinkiewicz P, Lindenmayer A, Hanan J. 1988. Development models of herbaceous plants for computer imagery purposes. *Computer Graphics* 22: 141-150.

Prusinkiewicz P, Lindenmayer A. 1990. *The Algorithmic Beauty of Plants*. New York: Springer-Verlag.

Prusinkiewicz P, Smith RS, Ottoline L. 2007. Apical dominance models can generate basipetal patterns of bud activation. In: P Prusinkiewicz, J Hanan, B Lane, eds. *Proc. of the 5 th international workshop on FSPM*. Napier, New Zealand, 10-1-5.

Prusinkiewicz P. 2004. Art and science for life: designing and growing virtual plants with L-systems. *Acta Horticulturae* 630: 15-28.

Puntieri JG, Stecconi M, Barthélémy D. 2002. Preformation and Neoformation in Shoots of Nothofagus antarctica (G. Forster) Oerst. (Nothofagaceae) Shrubs from Northern Patagonia. *Annals of Botany* 89: 665-673.

Radtke PJ, Robinson AP (2006) A Bayesian strategy for combining predictions from empirical and process-based models. Ecol Model 190:287-298

Rautiainen M, Mõttus M, Stenberg P, Ervasti S (2008) Crown envelope shape measurements and models. Silva Fennica 42:19-33

Reeves PH, Coupland G. 2000. Response of plant development to environment: control of flowering by daylength and temperature. *Current opinion in plant biology* 3: 37-42.

Reffye P de, Elguero E, Costes E. 1991b. Growth units construction in trees: a stochastic approach. *Acta biotheoretica* 39: 325-342.

Renton M, Kaitaniemi P, Hanan J (2005) Functional–structural plant modelling using a combination of architectural analysis, L-systems and a canonical model of function. Ecol Model 184:277-298

Rey H, Dauzat J, Chenu K, Barczi J-F, Dosio GAA, Lecoeur J. 2008. Using a 3-D Virtual Sunflower to Simulate Light Capture at Organ, Plant and Plot Levels: Contribution of Organ Interception, Impact of Heliotropism and Analysis of Genotypic Differences. *Annals of Botany* 101: 1139-1151.

Rossini MA, Maddonni GA, Otegui ME. 2011. Inter-plant competition for resources in maize crops grown under contrasting nitrogen supply and density: Variability in plant and ear growth. *Field Crops Research* 121: 373-380.

Sabatier S, Barthélémy D, Ducousso I. 2003. Periods of Organogenesis in Mono- and Bicyclic Annual Shoots of Juglans regia L. (Juglandaceae). *Annals of Botany* 92: 231-238.

Sangoi L. 2000. Understanding plant density effects on maize growth and development: An important issue to maximize grain yield. *Ciencia Rural* 31: 159-168.

Sellier D, Fourcaud T. 2005. A mechanical analysis of the relationship between free oscillations of Pinus pinaster Ait. saplings and their aerial architecture. *Journal of experimental botany* 56: 1563-1573.

Shinozaki K, Yoda K, Hozumi K, Kira T. 1964. A quantitative analysis of plant form—the pipe model theory I.Basic Analyses. *Japanese Journal of Ecology* 14: 97-105.

Sievänen R, Perttunen J, Nikinmaa E, Kaitaniemi P (2008) Toward extension of a single tree functional–structural model of Scots pine to stand level: effect of the canopy of randomly distributed, identical trees on development of tree structure. Funct Plant Biol 35:964–975

Sinoquet H, Roux X Le, Adam B, Ameglio T, Daudet FA. 2001. RATP: a model for simulating the spatial distribution of radiation absorption, transpiration and photosynthesis within canopies: application to an isolated tree crown. *Plant, Cell & Environment* 24: 395-406.

Soler C, Sillion FX, Blaise F, Reffye P de. 2003. An efficient instantiation algorithm for simulating radiant energy transfer in plant models. *ACM Transactions on Graphics* 22: 203-233.

Sterck FJ, Schieving F (2007) 3-D growth patterns of trees: effects of carbon economy, meristem activity, and selection. Ecol Monogr 77:405-420

Teale WD, Paponov IA, Palme K. 2006. Auxin in action: signalling, transport and the control of plant growth and development. *Nat Rev Mol Cell Biol* 7: 847-859.

Tollenaar M, Deen W, Echarte L, Liu W. 2006. Effect of Crowding Stress on Dry Matter Accumulation and Harvest Index in Maize. *Agronomy Journal* 98: 930-937.

Tollenaar M, Wu J. 1999. Yield improvement in temperate maize is attributable to greater stress tolerance. *Crop Science* 39: 1597-1604.

Vanclay JK (1994) Modelling forest growth and yield, applications to mixed tropical forests. CAB, Wallingford, UK.

Vos J, Evers JB, Buck-Sorlin GH, Andrieu B, Chelle M, de Visser PHB (2010) Functional-structural plant modelling: a new versatile tool in crop science. J Exp Bot 61:2101-2115

Vos J, Marcelis LFM, Evers JB. 2007. Functional-structural Plant Modelling in Crop Production. In: J Vos, LFM Marcelis, PHB de Visser, PC Struik, JB Evers, eds. *Functional-Structural Plant Modelling in Crop Production.* Netherlands: Springer, 1-12.

Wang F, Kang MZ, Lu Q, Han H, Letort V, Guo Y, de Reffye P, Li B (2010) Calibration of topological development in the procedure of parametric identification: application to the stochastic GreenLab model for *Pinus Sylvestris* var. *Mongolica*. In: Li B, Jaeger M, Gui Y (eds) Plant growth modelling, simulation, visualization and applications. IEEE Comput Soc, Los Alamitos, CA, pp 26-33

Wang X, Song B, Chen J, Zheng D, Crow TR (2006) Visualizing forest landscapes using public data sources. Landsc Urban Plan 75:111-124

Wernecke P, Muller J, Dornbusch T, Wernecke A, Diepenbrock W. 2007. The virtual crop-modelling system "VICA"specified for barley. *FUNCTIONAL-STRUCTURAL PLANT MODELLING IN CROP PRODUCTION*. Citeseer, 53-64.

West GB, Enquist BJ, Brown JH (2009) A general quantitative theory of forest structure and dynamics. PNAS 106:7040-7045

Yan H, Kang MZ, de Reffye P, Dingkuhn M (2004) A dynamic, architectural plant model simulating resource-dependent growth. Ann Bot 93:591-602

Zhan Z, de Reffye P, Houllier F, Hu B. 2003. Fitting a Functional-Structural growth model with plant architectural data. In: BG Hu, M Jaeger, eds. *Procedings of 1st International Symposium on Plant Growth Modeling, Simulation,Visualization and Applications (PMA03)*. Beijing, China: Springer and Tsinghua University Press, 108-117.

Zhan Z. Wang Y, de Reffye P, Wang B, Xiong Y. 2002. Architectural modeling of wheat growth and validation study. 2000 ASAE Annual International Meeting, July 2000.

Zhao X, de Reffye P, Xiong F, Hu B, Kang M. 2003. Simulation of Inflorescences Using Dual-Scale Automaton Model. *Chinese Journal of Computers* 26: 116-124.

Zhao X, de Reffye P, Xiong F, Hu B, Zhan Z. 2001. Dual-scale automaton model for virtual plant development. *The Chinese Journal of Computers* 24: 608-617.

Appendix I. GreenLab parameter file

Appendix I. GreenLab parameter file

List of the key parameters for executing a GreenLab simulation. They are grouped by scale, such as plant, axis, leaf, and functional organ (blade, petiole, internode, fruit female, fruit male, cambium and root). Cambium is used independently to represent secondary growth, so it is treated as an organ, which is also a part of internode.

Level	Parameter	Significance
Plant	plantName	Plant name, user determine, e.g.: maize_etm_09
	maxCUNb	Maximum computing units (age) to simulate plant growth, e.g.: 31
	temperateMode	If value=0, then “tropic” mode with continuous growth; otherwise (value=1) “annual” mode
	cuInYear	When terperateMode=1, cuInYear is the number of computing units in one year for the specific plant
	maxPhyAge	The number of physiological age in plant, usually corresponding to branch orders
	visuMode	If value=1, then visualize empty phytomer, corresponding pause during growth
	biomassMode	If value=0, then biomass computation is not realized; only topology and geometry are computed
	infloMode	If value=1, specific inflorescence development mode are activated
	infloMinimumPhyAge	Inflorescence mode only can be realised on the axis of physiological age ≥ infoMinimumPhyAge
	seedBiomass	Biomass of seed, the initial source of plant growth
	Resistance*	Indicates system resistance for biomass production
	projectiveSurface*	Theoretic projective area of plant,
	extinctionFactor	Extinction coefficient for radiation interception
Axis	rhythmMacrostate	Rhythms of each macro-state, ≤1
	macropause	The number of micro pause in macro pause
	reiterationOrder	The order of reiteration can happen for each order of axes (physiological age of axes)
	macroCycleNumberInYear	The number of macro-state (growth unit) in one year
	macroStateNbBeforeMutation	The number of macro-state before mutation occurs. The form of mutation is axis physiological age change.
	mutation	Axes/ macro-state physiological age after mutation
	microStatesNb	Sequence of microstate for each macro-state
	microBranchNumber	The number of lateral buds/ branches for each microstate
	mixedBranchNumber	The number of different lateral buds/ branches for each microstate
	phyAgeMixedBud	Different physiological age of lateral bud/ branches for each microstate

	organAppearanceDate	To mark the beginning date (computing unit) to appear for each type of organ
	organDisappearanceDate	To mark the terminated date (computing unit) to appear for each type of organ
	insertionAngleParameter	Control points characterizing piecewise insertion angle function of axes age, for each physiological age of axes
	phyllotaxyAngleParameter	Phyllotaxy angle for each physiological age of axes
	msk	Notations of actual positions of organ (leaf, internode, fruit female, fruit male) on each physiological age of axes
	delayAxisDev	Delay of the number of computing unit before lateral axes expanding
	delayBetaExpansion	Delay of the number of computing unit before the organ (leaf, internode, fruit female, fruit male, root) expanding
Leaf	organNbInPhytomer	The number of leaf on each phytomer
	insertionAngleParameter	Insertion angle between leaf and its porter internode
	phyllotaxyAngleParameter	Phyllotaxy angle of leaves on a axis
Blade	functionDuration	Control points of piecewise functional duration function of different genesis date (computing unit) of blades
	expansionDuration	Control points of piecewise expansion duration function of different genesis date (computing unit) of blades different
	sinkFactorByPhyAge	Sink factors of blades according to their physiological age. Default blade sink factor of physiological age 1 is 1.
	betaLawA *	Parameter a of beta law function to characterize variation of blade sink strength
	betaLawB	Parameter b of beta law function to characterize variation of blade sink strength
	specificLeafWeight	Ratio between biomass and blade surface, = 1/*SLA* (Specific leaf area)
	sizeDefault	Default size of blade surface
Petiole	functionDuration	Control points of piecewise functional duration function of different genesis date (computing unit) of petioles
	expansionDuration	Control points of piecewise expansion duration function of different genesis date (computing unit) of petioles
	sinkFactorByPhyAge *	Sink factors of petioles according to their physiological age
	betaLawA *	Parameter a of beta law function to characterize variation of petiole sink strength
	betaLawB	Parameter b of beta law function to characterize variation of petiole sink strength
	sizeDefault	Default length and diameter of petiole
Internode	organNbInPhytomer	The number of Internode on each phytomer =1

	functionDuration	Control points of piecewise functional duration function of different genesis date (computing unit) of internodes
	expansionDuration	Control points of piecewise expansion duration function of different genesis date (computing unit) of internodes
	sinkFactorByPhyAge *	Sink factors of internodes according to their physiological age
	betaLawA *	Parameter a of beta law function to characterize variation of internode sink strength
	betaLawB	Parameter b of beta law function to characterize variation of internode sink strength
	Allometry	Parameter a and b of Allometric relationship between height and diameter of internode
	sizeDefault	Default length and diameter of internode
Fruit Female	organNbInPhytomer	The number of fruit female on each phytomer
	functionDuration	Control points of piecewise functional duration function of different genesis date (computing unit) of fruit females
	expansionDuration	Control points of piecewise expansion duration function of different genesis date (computing unit) of fruit females
	sinkFactorByPhyAge *	Sink factors of fruit females according to their physiological age
	betaLawA *	Parameter a of beta law function to characterize variation of fruit female sink strength
	betaLawB	Parameter b of beta law function to characterize variation of fruit female sink strength
	insertionAngleParameter	Insertion angle between fruit female and its porter internode
	phyllotaxyAngleParameter	Phyllotaxy angle of fruit females on a axis
	sizeDefault	Default diameter of fruit (default form is a sphere)
Fruit Male	organNbInPhytomer	The number of fruit male on each phytomer
	functionDuration	Control points of piecewise functional duration function of different genesis date (computing unit) of fruit males
	expansionDuration	Control points of piecewise expansion duration function of different genesis date (computing unit) of fruit males
	sinkFactorByPhyAge *	Sink factors of fruit males according to their physiological age
	betaLawA *	Parameter a of beta law function to characterize variation of fruit male sink strength
	betaLawB	Parameter b of beta law function to characterize variation of fruit male sink strength
	insertionAngleParameter	Insertion angle between fruit male and its porter internode
	phyllotaxyAngleParameter	Phyllotaxy angle of fruit males on a axis

	sizeDefault	Default diameter of fruit (default form is a sphere)
Cambium	expansionDuration	Control points of piecewise expansion duration function of cambium
	sinkFactorByPhyAge *	Sink factors of cambium according to their physiological age
	betaLawA	Parameter a of beta law function to characterize variation of cambium sink strength
	betaLawB	Parameter b of beta law function to characterize variation of cambium sink strength
	lamdaCambium *	Parameter to regulate ratio between local mode determined by over leave surface and common pool mode to form cambium
Root	expansionDuration	Control points of piecewise expansion duration function of root
	sinkFactorByPhyAge *	Sink factors of root
	betaLawA *	Parameter a of beta law function to characterize variation of root sink strength
	betaLawB	Parameter b of beta law function to characterize variation of root sink strength
	allometry	Ratio between radium and height (default form is cone)
	sizeDefault	Default volume of root (default form is cone)

*: parameters need to be calibrated

Appendix II. An example of maize target file

Appendix II. An example of maize target file

```
Information
        Age_max_period_rank_tip # maximum age, nubmer of measurement, temporal rank from tip
        31      5       31
date_of_measurements # GCs of measurement
        10      14      19      27      31
        blade__petiol_internode_fruitF_fruitM_layer__root # flag of presence 1: yes; 0: no
        1       1       1       1       1       0       0
Organ_production/CU    # number of organs in the measurements
        Age_Nb_Bld__Nb_Int_Nb_FrF_Nb_FrM

        10      10      10      0       0
        14      14      14      0       0
        19      18      19      1       1
        27      18      19      1       1
        31      18      19      1       1
Global_Biomass_production/compartment/CU # organ compartments weight
        Age___TQ___TQb1_TQp1___TQL1_TQf1__TQm__TQr

        10      17.9    12.4    4.7     0.825   0       0       0
        14      103.7   54.3    32.3    16.9    0       0       0
        19      627.1   156.6   134.5   309.1   26.9    10.0    0
        27      1162.7  153     131.9   352.6   525.1   11.59   0
        31      1124.1  154.5   124.1   359.3   486.1   11.59   0
StDev_Global_production/compartment/CU/     # standard variation of organ compartments weight
        Age___TQ___TQb1__TQp1__TQL1__TQf1__TQm__TQr

        10      4.7     3.01    1.3     0.5     0       0       0
        14      41.9    20.1    12.7    9.2     0       0       0
        19      68.64   14.7    13.9    36.2    6       0       0
        27      236.9   26.2    20.1    69.2    130     0       0
        31      92.7    10.2    9.9     33.6    68      0       0
 Blade-size/position PA1 # blades weight along axis of PA=1, rank of phytomer from the tip
        rank    10      14      19      27      31
        31      -1      -1      -1      -1      -0.0001
        30      -1      -1      -1      -1      -0.0001
        29      -1      -1      -1      -1      -0.0001
        28      -1      -1      -1      -1      -0.0001
        27      -1      -1      -1      -0.0001 -0.0001
        26      -1      -1      -1      -0.0001 -0.0001
        25      -1      -1      -1      -0.0001 -0.0001
        24      -1      -1      -1      -0.0001 -0.0001
        23      -1      -1      -1      -0.0001 -0.0001
        22      -1      -1      -1      -0.0001 -0.0001
        21      -1      -1      -1      -0.0001 -0.0001
        20      -1      -1      -1      -0.0001 -0.0001
        19      -1      -1      0.05    0.05    0.05
        18      -1      -1      0.21    0.21    0.21
        17      -1      -1      0.39    0.39    0.39
```

16	-1	-1	0.89	0.89	0.89
15	-1	-1	2.16	2.16	2.16
14	-1	0.08	5.24	5.24	5.24
13	-1	0.21	8.44	8.44	8.44
12	-1	0.39	12.35	12.35	12.35
11	-1	0.89	15.48	15.48	15.48
10	0.08	2.09	17.67	17.67	17.67
9	0.2	4.81	17.77	17.77	17.77
8	0.38	8.37	16.55	17.12	17.12
7	0.89	12.05	15.15	15.84	15.92
6	2.04	13.8	13.55	14.04	15.01
5	3.94	11.08	11.84	11.94	13.04
4	3.11	7.03	9.49	9.08	10.84
3	1.32	3.63	6.71	6.16	7.23
2	0.37	1.53	3.13	4.27	4.45
1	0.08	0.9	0.01	0.01	0.01

Petiol-size/position PA1 # petioles weight along axis of PA=1, rank of phytomer from the tip

rank	10	14	19	27	31
31	-1	-1	-1	-1	-0.0001
30	-1	-1	-1	-1	-0.0001
29	-1	-1	-1	-1	-0.0001
28	-1	-1	-1	-1	-0.0001
27	-1	-1	-1	-0.0001	-0.0001
26	-1	-1	-1	-0.0001	-0.0001
25	-1	-1	-1	-0.0001	-0.0001
24	-1	-1	-1	-0.0001	-0.0001
23	-1	-1	-1	-0.0001	-0.0001
22	-1	-1	-1	-0.0001	-0.0001
21	-1	-1	-1	-0.0001	-0.0001
20	-1	-1	-1	-0.0001	-0.0001
19	-1	-1	0.06	0.06	0.06
18	-1	-1	0.16	0.16	0.16
17	-1	-1	0.5	0.5	0.5
16	-1	-1	1.26	1.26	1.26
15	-1	-1	3.81	3.81	3.81
14	-1	0.06	7.92	7.92	7.92
13	-1	0.16	11.15	11.15	11.15
12	-1	0.5	14.35	14.35	14.35
11	-1	1.26	15.26	15.26	15.26
10	0.06	3.81	15.3	15.3	15.3
9	0.16	7.92	14.74	14.74	14.74
8	0.5	11.41	14.11	14.11	14.11
7	1.26	10.58	13.08	13.08	13.08
6	2.15	4.18	11.14	12.09	12.09
5	0.55	0.48	7.79	10.13	11.47
4	0.03	0.15	4.4	7.7	8.93
3	0.01	0.07	2.26	5.28	5.76
2	0.01	0.02	1.39	3.46	3.2
1	0.01	0.01	0.01	0.01	0.01

Internode-size/position PA1 # Internode weight along axis of PA=1, rank of phytomer from the tip

0	10	14	19	27	31
31	-1	-1	-1	-1	-0.0001
30	-1	-1	-1	-1	-0.0001
29	-1	-1	-1	-1	-0.0001
28	-1	-1	-1	-1	-0.0001
27	-1	-1	-1	-0.0001	-0.0001
26	-1	-1	-1	-0.0001	-0.0001
25	-1	-1	-1	-0.0001	-0.0001
24	-1	-1	-1	-0.0001	-0.0001
23	-1	-1	-1	-0.0001	-0.0001
22	-1	-1	-1	-0.0001	-0.0001
21	-1	-1	-1	-0.0001	-0.0001
20	-1	-1	-1	-0.0001	-0.0001
19	-1	-1	0.47	0.47	0.47
18	-1	-1	0.95	0.95	0.95
17	-1	-1	1.42	1.42	1.42
16	-1	-1	1.89	1.89	1.89
15	-1	-1	8.57	8.57	8.57
14	-1	0.23	14.08	15.5	15.5
13	-1	0.45	29.26	30.42	30.42
12	-1	0.68	39.35	40.43	40.43
11	-1	0.91	49.8	52	52
10	-0.0001	2.75	51.44	51.44	51.44
9	-0.0001	6.67	49.49	49.49	49.49
8	-0.0001	7.7	37.8	37.8	37.8
7	-0.0001	2.11	18.34	25.81	28.96
6	-0.0001	0.65	5.5	16.21	17.72
5	-0.0001	0.22	1.58	11.52	13.09
4	-0.0001	0.12	0.59	9.1	10.3
3	-0.0001	0.04	0.27	5.85	7.01
2	-0.0001	0.01	0.14	4.05	4.38
1	-0.0001	0.01	0.01	1.83	2.96

FruitF-size/position PA1 # fruits female weight along axis of PA=1, rank of phytomer from the tip

0	10	14	19	27	31
31	-1	-1	-1	-1	-0.0001
30	-1	-1	-1	-1	-0.0001
29	-1	-1	-1	-1	-0.0001
28	-1	-1	-1	-1	-0.0001
27	-1	-1	-1	-0.0001	-0.0001
26	-1	-1	-1	-0.0001	-0.0001
25	-1	-1	-1	-0.0001	-0.0001
24	-1	-1	-1	-0.0001	-0.0001
23	-1	-1	-1	-0.0001	-0.0001
22	-1	-1	-1	-0.0001	-0.0001
21	-1	-1	-1	-0.0001	-0.0001
20	-1	-1	-1	-0.0001	-0.0001
19	-1	-1	0.01	0.01	0.01
18	-1	-1	0.01	0.01	0.01
17	-1	-1	0.01	0.01	0.01
16	-1	-1	0.01	0.01	0.01
15	-1	-1	0.01	0.01	0.01

14	-1	0.01	0.01	0.01	0.01	
13	-1	0.01	0.01	0.01	0.01	
12	-1	0.01	0.01	0.01	0.01	
11	-1	0.01	0.01	0.01	0.01	
10	0.01	0.01	0.01	0.01	0.01	
9	0.01	0.01	0.01	0.01	0.01	
8	0.01	0.01	0.01	0.01	0.01	
7	0.01	0.01	15.297	517.744		517.744
6	0.01	0.01	0.01	0.01	0.01	
5	0.01	0.01	0.01	0.01	0.01	
4	0.01	0.01	0.01	0.01	0.01	
3	0.01	0.01	0.01	0.01	0.01	
2	0.01	0.01	0.01	0.01	0.01	
1	0.01	0.01	0.01	0.01	0.01	

FruitM-size/position PA1 # fruits male weight along axis of PA=1, rank of phytomer from the tip

0	10	14	19	27	31
31	-1	-1	-1	-1	-0.0001
30	-1	-1	-1	-1	-0.0001
29	-1	-1	-1	-1	-0.0001
28	-1	-1	-1	-1	-0.0001
27	-1	-1	-1	-0.0001	-0.0001
26	-1	-1	-1	-0.0001	-0.0001
25	-1	-1	-1	-0.0001	-0.0001
24	-1	-1	-1	-0.0001	-0.0001
23	-1	-1	-1	-0.0001	-0.0001
22	-1	-1	-1	-0.0001	-0.0001
21	-1	-1	-1	-0.0001	-0.0001
20	-1	-1	-1	-0.0001	-0.0001
19	-1	-1	0.01	0.01	0.01
18	-1	-1	0.01	0.01	0.01
17	-1	-1	0.01	0.01	0.01
16	-1	-1	0.01	0.01	0.01
15	-1	-1	0.01	0.01	0.01
14	-1	0.01	0.01	0.01	0.01
13	-1	0.01	0.01	0.01	0.01
12	-1	0.01	0.01	0.01	0.01
11	-1	0.01	0.01	0.01	0.01
10	0.01	0.01	0.01	0.01	0.01
9	0.01	0.01	0.01	0.01	0.01
8	0.01	0.01	0.01	0.01	0.01
7	0.01	0.01	0.01	0.01	0.01
6	0.01	0.01	0.01	0.01	0.01
5	0.01	0.01	0.01	0.01	0.01
4	0.01	0.01	0.01	0.01	0.01
3	0.01	0.01	0.01	0.01	0.01
2	0.01	0.01	0.01	0.01	0.01
1	0.01	0.01	11.59	11.59	11.59

Appendix III. GreenLab basic equation and variability computation

Appendix III. GreenLab basic equation and variability computation

Biomass increment is based on previous biomass production, following:

$$Q(n)=\frac{E.Sp}{r}\left(1-\exp\left(-\frac{k}{e.Sp}\sum_{i=n-t_b+1}^{n}N_b(j)\sum_{j=i}^{T_x(i)}\frac{P_b(j-i+1)Q(j-1)}{D(j)}\right)\right) \quad \text{(AIII.1)}$$

In this equation, green leaf area computation is detailed by the source-sink process presented previously (Eq.4). E is the driving parameter (the local environmental driver, for example *PET* or *WUE*…) , r is the calibration coefficient for the driving factor, S_p the projection surface, e the SLW. The plant age in GC is j. $N_b(j)$ is the number of leaves produced at GC j, ($N_b(j)$ =1 for a single stem as maize). The sink function is written as $p(j)=p_o*f(b_1,b_{2,j})$. Where p_o is the sink strength and $f(b_1,b_{2,j})$ a function whose maximum is 1 in the interval of the sink variation. Parameters b_1 and b_2 are coefficients of an empirical beta law. In our case b_2 is fixed to 5. So, $P_{b(j-i+1)}$ is the sink value of a leaf which appeared at the GC i. The demand $D(j)$ corresponds to the sum of the sinks of all organs according to their age, at plant age j. They are : p_b for leaf, p_p for sheath, p_i for internode, p_f for the cob, p_m for the tassel. Corresponding parameters b_b, b_p, b_i, b_f, are coefficients of the sink function that control the sink variation. These parameters are hidden and they are computed from plant measurements using the non linear least squares method. The value S_p that corresponds to the space available for a single plant is computed at the same time as the sink values.

Table AIII.1 Estimated hidden parameter values, standard deviation and coefficient of variation

Parameters	Value	s.d.	CV (%)
r	20.05	0.40	1.99
S_p	1379	47	3.42
b_b	3.16	0.18	5.69
p_p	0.91	0.03	3.30
b_p	2.76	0.13	4.71
p_i	2.59	0.09	3.48
b_i	3.19	0.16	5.02
b_f	5.56	0.07	1.26
p_m	5.20	0.22	4.23

The sink strength of blades (p_b) is set to 1 as reference value because all sink strength parameters carry relative values. As sink strength of ear (p_f) is several orders of magnitude greater than sink strength of other organs, it was set to 1000.

The general function of average current biomass increment can be written as:

$$\overline{Q(n)}=G\left(\overline{E},\overline{Sp},Q_{n-1},Q_{n-2},\ldots,\overline{Q_0}\right) \quad \text{(AIII.2)},$$

where the related variables E, S_p and Q_0 are respectively the local environmental effects, theoretical projective area and the seed biomass. The variance of the dependent variable $Q(n)$ can be approximately written by the first-order derivatives (G'), variances (v) and correlation (r) of and among them, as:

$$v(Q(n)) = \sum \left(G'_{X_l}\right)^2 vX_l + \sum \left(G'_{Qi}\right)^2 vQ_i + 2\sum\sum G'_{X_l} G'_{Q_i} . r_{X_l Q_i} \sqrt{vX_l . vQ_i} + 2\sum\sum G'_{X_l} G'_{X_m} . r_{X_l X_m} \sqrt{vX_l . vX_m} + 2\sum\sum G'_{Qi} G'_{Qj} . r_{Q_i Q_j} \sqrt{vQ_i . vQ_j} \quad \text{(AIII.3)},$$

where X represents the relevant variables such as E, S_p, Q_0. When the correlations between variables such as r_{SpQi} and r_{QiQj} are difficult to measure, they can be virtually computed based on the simulations of their values.

Due to plant weight (TQ) is the accumulation of biomass production, as:

$$TQ(n) = \sum_{i=1}^{n} Q_i \quad \text{(AIII.4)},$$

its variance can be represented as:

$$v(TQ(n)) = \sum v(Q_i) + 2r_{Q_i Q_j} \sum \sqrt{v(Q_i) \cdot v(Q_j)} \quad \text{(AIII.5)}$$

Or:

$$v(TQ(n)) = \left(\sum_{i=1}^{n} \sigma Q_i\right)^2 \quad \text{(AIII.6)}$$

It should be noticed that v_{Qi} can be calculated recursively according to variability of E, Q_0 or S_p. In this way, the relationship between variability of certain factors and the variability of plant growth is established. Therefore on the one hand the plant-to-plant variability can be simulated by the variable factors, on the other hand it provides a solution to solve the variability of factors by inverse calculation.

Connexion entre modèles dynamiques de communautés végétales et modèles architecture-fonction – cas du modèle GreenLab

RESUME L'architecture des plantes est le résultat combiné des développements des structures topologique et géométrique qui interviennent dans l'acquisition de la biomasse et sa répartition sous l'influence des processus physiologiques. Pourtant cet aspect a été longtemps négligé dans la communauté des modèles dynamiques. Récemment les modèles structures fonction se sont montrés pertinents pour prendre en compte des questions comme les interactions plantes environnement (l'interception de la lumière), les interactions entre croissance et développement (répartition de la biomasse) en se plaçant au niveau de l'organe. Cependant les couts en calcul de la simulation numérique de ces processus rendent les applications impraticables en agriculture. Cette thèse vise a combiner le modèle structure fonction Greenlab avec d'une part un modèle de culture et d'autre part un modèle forestier basés sur le peuplement afin d'y introduire le concept d'architecture des plantes. Le modèle de culture Pilote fournit des prédictions de récoltes basés sur les paramètres de l'environnement (radiation, précipitations) et l'indice foliaire et l'indice de récolte. Une étude sur Maïs conjointe entre Pilote et GreenLab a permis d'expliciter en détail les paramètres de la production. Les indices foliaires et de récolte dépendent directement des paramètres sources puits, et la variabilité individuelle entre plantes est explicitée directement par les variations des retards a la germination et celles des surfaces disponibles par plantes (compétition spatiale). Tous ces paramètres peuvent être calibré par méthodes inverses. Ainsi la jonction des deux types de modèles est réalisée au niveau du passage de la plante au peuplement.
Une autre étude conjointe a été effectuée avec le modèle forestier empirique PNN qui modélise la croissance des peuplements forestiers de Pins noirs. A partir des données statistiques classiques sur les mesures de troncs et de houppiers, combinées avec les connaissances architecturales du Pin issues d'AMAP, GreenLab peut restituer l'architecture de l'arbre et visualiser des scenarios de sylviculture incorporant des élagages. Le procédé va jusqu'à l'obtention d'images de synthèse réalistes des peuplements.
En conséquence il semble efficace de coupler les modèles de cultures et les modèles forestiers qui intègrent les connaissances écophysiologiques au niveau peuplement avec les modèles structures fonctions qui intègrent ces connaissances au niveau de l'architecture de la plante. Le modèle GreenLab par ses affinités avec ces deux types de modèles et ses performances en calcul, permet d'apporter un complément d'information essentiel sur la description du fonctionnement d'un peuplement tant du point de vue développement, que du point de vue des relations sources puits dans la plante. Enfin le modèle couplé a une plateforme comme Xplo (AMAP) permet en plus une simulation réaliste 3D du peuplement végétal aux divers stades de la croissance.

Connection between plant community dynamics models and architectural-functional plant models – the GreenLab case

ABSTRACT Plant architecture involves the development of both topological and geometric structures over time, which determines resource acquisition, which, in so doing, interacts with physiological processes. However, it has long been overlooked in traditional community dynamic models. Functional-structural plant models (FSPM), which are based on plant architecture, have shown their particular suitability for addressing issues such as interactions between plants and the environment (e.g. light interception), and between structural development and growth (e.g. carbon allocation), as they take into account morphogenesis with explicit organ-level descriptions. However, FSPMs are time consuming and require a lot of memory space, which prevents greater use of them in agricultural or silvicultural practices. This thesis attempts to combine a mathematical FSPM, GreenLab, and a crop model or an empirical forest model (EFM), in order to introduce individual-based architectural support for community growth studies. In the case of maize, disagreements between stand level growth stimulations (by the PILOTE crop model) and individual level growth stimulations (by GreenLab) implies different individual emergence times, which are used to quantify distribution. Assuming that the theoretical projective area (S_p) is determined by the growth situation and the final size of the individual architecture, the variance of S_p is reversely computed with the variance in organ compartment measurements, in order to characterize individual variability. In the case of Black Pine, the architecture dynamics built in GreenLab according to Rauh's model (architecture model for the pine tree) were adapted to the simulation of an EFM, PNN. As a consequence, thinning scenarios are well incorporated in the final stand visualization. From these preliminary applications, the following conclusions can be drawn: (i) FSPMs are able to provide individual performances (i.e. organ development and expansion) inside an area of a crop field for crop models. (ii) The crop model may regulate the combined form of individuals from an integral level. Both aspects are significant for a clearer understanding of stand growth. (iii) Architecture designs integrated into FSPMs can be adapted to EFM simulations for data-driven visualization. (iv) EFMs can guarantee ecological/silvicultural functions for 3D stand visualization. In order to take biomass processes into consideration, additional observations are needed. As models are independent in combinations, the same methods can be extended and linked to other stand models.

DISCIPLINE Biologie des Organismes

MOTS-CLES Modèle de culture, Modèle structure fonction, Architecture de plante, Visualisation, GreenLab, *Pinus nigra nigra*, *Zea maïs*

INTITULE ET ADRESSE DE L'U.F.R. OU DU LABORATOIRE :
CIRAD, UMR AMAP, Bd de la Lironde, TA A-51/PS2, 34398 Montpellier cedex 5